

MODELING AND OPTIMIZATION OF MULTI-SCALE MACHINING  
OPERATIONS

A THESIS  
SUBMITTED TO THE DEPARTMENT OF INDUSTRIAL  
ENGINEERING  
AND THE GRADUATE SCHOOL OF ENGINEERING AND SCIENCE OF  
BILKENT UNIVERSITY  
IN PARTIAL FULFILLMENT OF THE REQUIREMENTS  
FOR THE DEGREE OF  
MASTER OF SCIENCE

by  
Fevzi Yılmaz  
July, 2012

I certify that I have read this thesis and that in my opinion it is full adequate, in scope and in quality, as a dissertation for the degree of Master of Science.

---

Asst. Prof. Yiğit Karpat (Advisor)

I certify that I have read this thesis and that in my opinion it is full adequate, in scope and in quality, as a dissertation for the degree of Master of Science.

---

Prof. Selim Aktürk

I certify that I have read this thesis and that in my opinion it is full adequate, in scope and in quality, as a dissertation for the degree of Master of Science.

---

Asst. Prof. Melih Çakmakcı

Approved for the Graduate School of Engineering and Science

---

Prof. Levent Onural

Director of the Graduate School of Engineering and Science

# **ABSTRACT**

## **MODELING AND OPTIMIZATION OF MULTI-SCALE MACHINING OPERATIONS**

Fevzi Yılmaz

M.S. in Industrial Engineering

Supervisor: Asst. Prof. Yiğit Karpat

July, 2012

Minimization of production time, cost and energy while improving the part quality is the main goal in manufacturing. In order to be competitive in today's global markets, it is crucial to develop high precision machine tools and maintain high productive operation of the machine tools through intelligent and effective selection of machining parameters. A recent shift in manufacturing industry is towards the production of high value added micro parts which are mainly used in biomedical and electronics industries. However, the knowledge base for micro machining operations is quite limited compared to macro scale machining processes.

Metal cutting, which allows production of parts with complex shapes made from engineering materials, constitutes a large portion in all manufacturing activities and expected to remain so in upcoming years. In this thesis, modeling and optimization of macro scale turning and micro scale milling operations have been considered. A well known multi pass turning problem from the literature is used as a benchmark tool to test the performances of Particle Swarm Optimization (PSO) technique and nonlinear optimization algorithms. It is shown that acceptable results can be obtained through PSO in short time.

Micro scale milling operation is thoroughly investigated through experimental techniques where the influences of machining parameters on the process outputs (machining forces, surface quality, and tool life) have been investigated and factors affecting the process outputs are identified. A minimum unit cost optimization problem is formulated based on the pocketing operation and machining strategies are proposed for different machining scenarios using PSO technique.

**Keywords:** Turning, Micro milling, Process optimization, Design of experiments, Particle swarm optimization.

# ÖZET

## ÇOK ÖLÇEKLİ TALAŞLI İMALAT İŞLEMLERİNİN MODELLENMESİ VE ENİYİLEMESİ

Fevzi Yılmaz

Endüstri Mühendisliği, Yüksek Lisans

Tez Yöneticisi: Yrd. Doç. Dr. Yiğit Karpat

Temmuz, 2012

İmalat endüstrisinde, özellikle biyomedikal ve elektronik endüstrilerinde kullanılmak üzere yüksek katma değerli mikro parçaların üretimine olan eğilim artmaktadır. Mikro parçaların üretilmesinde yüksek hassasiyetli kesici takımların geliştirilmesi ve işleme parametrelerinin doğru seçilmesi işlemeden yüksek verim elde edilebilmesi açısından önem teşkil etmektedir. Fakat mikro ölçekli imalat işlemleri için mevcut olan bilgi altyapısı makro ölçekli imalat işlemlerine göre oldukça kısıtlı olup geliştirilmeye gereksinim duyulmaktadır. Bu çalışmada mikro frezeleme işlemleri ile üç boyutlu geometriye sahip mikro parçaların üretimi amaçlanmıştır.

Bu yüksek lisans tezinde makro ölçekli tornalama ve mikro ölçekli frezeleme işlemleri modellenmiş ve eniyilemesi yapılmıştır. Parçacık sürü eniyilemesi yönteminin performansının doğrusal olmayan eniyileme algoritmaları ile kıyaslanması amacıyla literatürde yer alan çok geçişli tornalama işlemlerinin eniyilemesi problemi kullanılmıştır. Bu çalışma sonucunda parçacık sürüsü eniyilemesi yöntemi ile kısa sürede kabul edilebilir sonuçlar elde edilebildiği sonucuna ulaşılmıştır. Daha sonra mikro ölçekli frezeleme işlemlerinde kesme parametrelerinin işleme çıktılarına (kesme kuvvetleri, yüzey kalitesi ve takım ömrü) etkisinin araştırılması amacıyla deneysel

alıřmalar yapılmıřtır. Deneysel alıřmalardan elde edilen sonular dikkate alınarak cep ama iřlemi iin bir minimum birim maliyet eniyileme problemi matematiksel olarak modellenmiř, paracık sr eniyilemesi yntemi kullanılarak farklı iřleme senaryoları iin stratejiler deęerlendirilmiřtir. İřlem eniyilemesi sonucunda iřleme zamanında ve birim maliyetlerde nemli lde kazanımlar elde edilebileceęi gsterilmiřtir.

**Anahtar Szckler:** Tornalama, Mikro frezeleme, İřleme eniyilemesi, Deneysel tasarım, Paracık sr eniyilemesi.

## ACKNOWLEDGEMENT

I would like to express my sincere gratitude to Asst. Prof. Yiğit Karpat for his invaluable guidance and support during my graduate study. He has supervised me with everlasting patience and encouragement throughout this thesis. I consider myself lucky to have a chance to work with him.

I am also grateful to Prof. M. Selim Aktürk and Asst. Prof. Melih Çakmakcı for accepting to read and review this thesis. Their comments and suggestions have been invaluable.

I would like to thank to my precious friends Fatih Harmankaya, Pelin Elaldı, Onur Uzunlar, Müge Muhafız, Hüsrev Aksüt and Nurcan Bozkaya for their endless support and motivation. I am also thankful to İsmail Erikçi, Ali Can Ergür, Bengisu Sert and all friends I failed to mention here for their friendship and support. Life and the graduate study would have not been bearable without them.

I also would like to thank Onur Uzunlar for his useful technical discussions to my work and my friends Pelin Elaldı and Müge Muhafız for their collaboration in the design of this study.

Finally, I would like to acknowledge financial support of the Scientific and Technological Research Council of Turkey (Tübitak), the State Planning Agency (DPT) of Turkey and Bilkent University.

Last but not least, I would like to thank to my family for their love and encouragement.

# TABLE OF CONTENTS

Chapter 1 .....	1
Introduction .....	1
1.1 Motivation.....	8
1.2 Organization of the Thesis .....	10
Chapter 2 .....	11
Modeling and Optimization of Macro-Scale Turning Operation.....	11
2.1 Literature Review on Multi Pass Turning Operation Problem.....	12
2.2 Mathematical Modeling .....	15
2.3 Particle Swarm Optimization (PSO).....	22
2.4 Numerical Study.....	25
2.4.1 Constraint Analysis of Mathematical Model.....	26
2.4.2 Parameter Analysis of Particle Swarm Optimization.....	34
2.4.3 Performance Evaluation of Particle Swarm Optimization .....	37
2.5 Conclusion .....	41
Chapter 3 .....	43
Experimental Investigation of Micro Milling .....	43
3.1 Micro Machining .....	44
3.2 Literature Review .....	46
3.3 Design of Experiment (DOE) Methods .....	49
3.4 Experimental Investigation .....	53
3.4.1 Experimental Setup.....	54
3.4.2 Slot Milling Experiments .....	57

3.4.3 Pocket Milling Experiments .....	67
3.5 Conclusion .....	93
Chapter 4 .....	94
Modeling and Optimization of Square Pocket Milling .....	94
4.1 Numerical Example for Square Pocket Milling .....	100
4.1.1 Comparison of Machining Costs .....	101
4.1.2 Unit Production Cost Minimization.....	102
4.2 Summary .....	103
Chapter 5 .....	105
Conclusion and Future Work .....	105
Bibliography .....	107
Appendix .....	111

## LIST OF FIGURES

Figure 1.1 Manufacturing as percent of GDP between 1980 – 2008 (Hunter, 2010) .....	3
Figure 1.2 Shift in manufacturing sectors ROA values in US (Moavenzadeh et al., 2012) .....	4
Figure 1.3 Enabling technologies for high performance manufacturing (Kappmeyer et al., 2012)5	
Figure 1.4 Material removal processes (Groover, 2012).....	6
Figure 1.5 Machining optimization for minimum cost and maximum productivity (Groover, 2012) .....	7
Figure 2.1 Machining Model Data (Chen, 2004).....	25
Figure 2.2 Effects of feed rate and depth of cut on cutting force (Constraints 5 and 13).....	26
Figure 2.3 Effects of cutting speed, depth of cut and feed rate on power (Constraints 6 and 14)	29
Figure 2.4 Effects of cutting speed, depth of cut and feed rate on stability (Constraints 7 and 15) .....	31
Figure 2.5 Effects of cutting speed, depth of cut and feed rate on chip – tool interface temperature (Constraints 8 and 16) .....	34
Figure 2.6 Unit production cost reduction with respect to the iteration number .....	39
Figure 3.1 The effect of minimum chip thickness ( $R_e$ denotes the cutting edge radius, $h_m$ denotes minimum chip thickness and $h$ denotes undeformed chip thickness) (Chae et al., 2006) .....	45
Figure 3.2 CCD for three factors .....	52
Figure 3.3 (a) Micro Tools DT-110 (b) Kistler 9256 C1 dynamometer (c) NI PXI-7854R data acquisition card and PC (d) SEM image of micro cutting tool .....	55
Figure 3.4 Cutting tool is plunged out of the workpiece and feed direction is given in (a) and (b). Cutting tool is plunged into the workpiece with small feed rate and feed direction is given in (c) and (d) .....	57
Figure 3.5 Surface roughness measurement of experiment #2: (a) Channel #1 (b) Channel #19	61
Figure 3.6 Micro channel milling force measurements in Exp #2: (a) Channel #1, (b) Channel #9, (c) Channel #19 .....	62

Figure 3.7 Change in cutting forces .....	63
Figure 3.8 Relationship between tool wear and surface roughness .....	66
Figure 3.9 (a) Linear cutting strategy (b) Spiral cutting strategy.....	68
Figure 3.10 (a) Tool path generated by Cimatron, (b) Actual tool path after machining .....	69
Figure 3.11 As the feed direction changes (a), direction of cutting forces changes (b) .....	72
Figure 3.12 Cutting Forces with respect to axial depth of cuts (a) 80, (b) 114, (c)160 micron ...	74
Figure 3.13 ANOVA result of $\varnothing$ 0.8 mm pocket milling experiments.....	75
Figure 3.14 Tool wears of different cutting conditions .....	77
Figure 3.15 Resultant force increase due to tool wear for axial depth of cuts (a) 80 $\mu$ m, (b) 114 $\mu$ m and (c) 160 $\mu$ m.....	79
Figure 3.16 Surface images of first pockets .....	81
Figure 3.17 Surface images of tenth pockets .....	82
Figure 3.18 The effect of cutting conditions in terms of burr formation.....	84
Figure 3.19 Experimental design of $\varnothing$ 0.4 mm cutting tool pocket milling experiments .....	87
Figure 3.20 Images of (a) fresh and (b) worn tools.....	89
Figure 3.21 Measured tool diameters values with respect to the number of passes for experiments # 1, #2 and #3 .....	90
Figure 3.22 ANOVA and regression analysis .....	92
Figure 4.1 Tool path from center to outwards .....	95
Figure 4.2 Pocket milling procedures cutting path .....	96

## LIST OF TABLES

Table 1.1 Guideline for design of experiments (Montgomery, 2004).....	8
Table 2.1 Particle swarm optimization parameter values.....	24
Table 2.2 Swarm size and iteration number analysis for PSO.....	36
Table 2.3 Acceleration parameter analysis for PSO .....	36
Table 2.4 Unit production cost values obtained in the literature .....	37
Table 2.5 Obtained cutting parameters and <i>UC</i> for a single rough cut and a single finish cut....	38
Table 2.6 Obtained cutting parameters and <i>UC</i> for two rough cuts and a single finish cut .....	39
Table 2.7 Obtained cutting parameters and <i>UC</i> for a single rough cut and a single finish cut....	40
Table 2.8 Obtained cutting parameters and <i>UC</i> for two rough cuts and single finish cut .....	40
Table 2.9 Obtained unit costs and CPU times for different initial solutions .....	41
Table 3.1 Controllable factors in experimental studies .....	54
Table 3.2 Slot milling experiment parameters .....	59
Table 3.3 Measurements of slot milling experiments for $\emptyset$ 0.8 mm cutting tool.....	60
Table 3.4 Tool life values of experiments 1,2,3 and 4 .....	64
Table 3.5 Slot milling parameters for $\emptyset$ 0.4 mm cutting tool .....	65
Table 3.6 Measurements of slot milling experiments for $\emptyset$ 0.4 mm cutting tool.....	65
Table 3.7 Spindle speed and feed parameters used in $\emptyset$ 0.8 mm cutting tool pocket milling experiments.....	70
Table 3.8 Axial and radial depth of cut parameters used in $\emptyset$ 0.8 mm cutting tool pocket milling experiments.....	70
Table 3.9 Tool wear rates of experiment parameters .....	79
Table 3.10 Cutting times of experimented parameters.....	80

Table 3.11 Determined tool lives for burr formation criteria .....	83
Table 3.12 Measured cutting tool diameter after the preliminary study.....	85
Table 3.13 Parameter ranges used in $\emptyset$ 0.4 mm cutting tool pocket milling experiments.....	86
Table 3.14 Experiment parameters .....	88
Table 3.15 Tool life values obtained in the experiments.....	91
Table 4.1 Tool return and plunge feed rates .....	100
Table 4.2 Obtained results due to tool manufacturer catalogue values .....	101
Table 4.3 Obtained cutting parameters obtained by PSO.....	102
Table 4.4 Obtained cutting parameters for unit production cost minimization problem.....	103

# Chapter 1

## Introduction

Manufacturing is defined as transformation of raw materials into finished goods through application of physical and chemical processes. Raw materials follow a sequence of manufacturing operations and as a result finished goods are obtained. The critical issue is to add value in each manufacturing step so that the finished product becomes more valuable than the starting raw material (Groover, 2012). Manufacturing requires machinery, power, labor, know-how and effective use of these is paramount for high value added manufacturing. Minimization of production time, cost and energy while improving the part quality is the main goal in manufacturing.

Globalization, which is defined as the integration and interdependency of world markets in producing consumer goods and services, has immensely impacted manufacturing industry worldwide. As a result of globalization, the rules of competition between developed and emerging nations have changed and consequently the gravity of

manufacturing industry has been shifted towards Asia. In a recent report, Moavenzadeh et al. (2012) laid out some predictions about the future of global manufacturing based on current economic developments in US and European countries. These can be summarized as:

- It is necessary to invest in infrastructure for high value added manufacturing
- Foreign direct investment is important for the growth of emerging countries and the competition will intensify in near future
- Demand for materials with superior properties (light and durable, rare earth materials, etc.) will grow which will possibly result in breakthroughs in materials sciences
- Affordable clean energy resources will differentiate the competition among developed countries
- Level of human talent will determine the prosperity of countries and companies

Figure 1.1 shows the percentage of manufacturing in gross domestic products (GDP) for various countries. It can be seen from the figure that the percentage of manufacturing has been decreasing for a long period of time whereas the percentage of service industries in the GDP has been rising. This is mainly due to the decrease in relative prices of goods, in conjunction with the simultaneous growth of the demand for services. (Moavenzadeh et al., 2012)

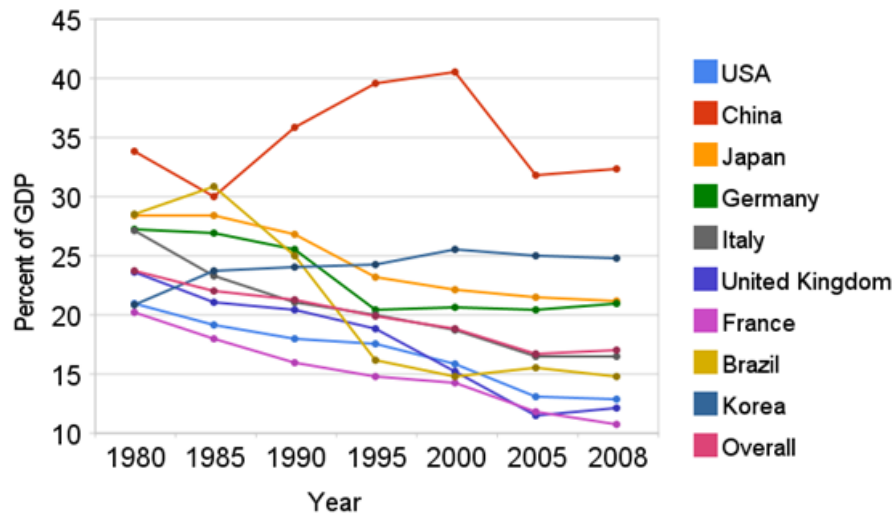


Figure 1.1 Manufacturing as percent of GDP between 1980 – 2008 (Hunter, 2010)

Figure 1.2 shows the historical data of return on assets (ROA) variation for different industries between 1965 and 2010 in USA. Based on the data, only the Aerospace and Defense (A&D) and Consumer Products sectors are on the rise, while the ROA of other manufacturing sectors have been declining since 1965. The most drastic decrease has been observed in labor intensive Automotive Industry which will cease adding value in near future based on the data given in Figure 1.2. It seems like the only way for developed countries to maintain their economic welfare is through innovation which explains their special interest in micro and nano technologies. It is believed that these new technologies will have profound effects on the development of future innovative consumer products.

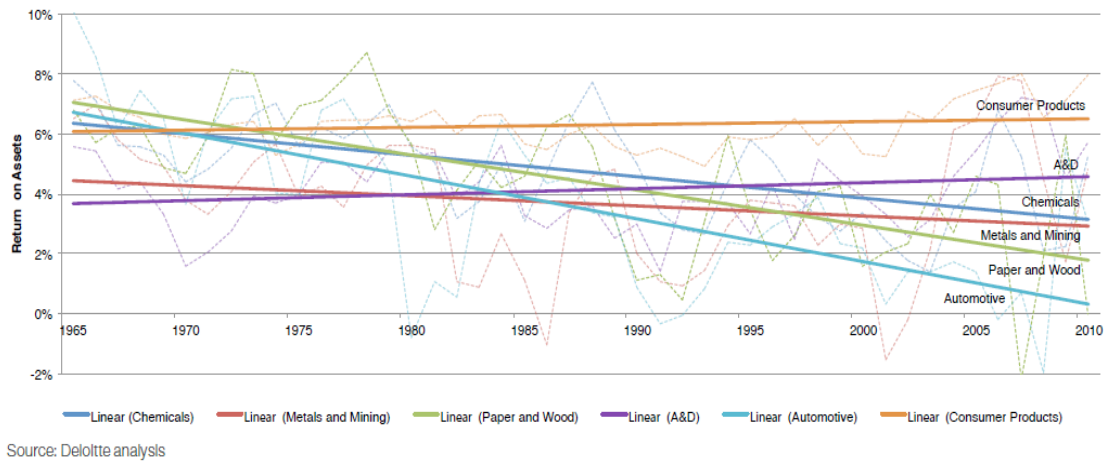


Figure 1.2 Shift in manufacturing sectors ROA values in US (Moavenzadeh et al., 2012)

As the manufacturing industry shifts to emerging countries, so does the technological know-how. With the help of existing digital infrastructure (internet, online data storage, etc.), engineers can easily collaborate using computer aided design, engineering, and manufacturing (CAD, CAE, CAM) software even they reside in different countries. This allows faster development products based on customer requirements and reduce the time it takes to introduce the product to the market. Design and manufacturing can be streamlined, if the gaps between CAx tools and computer numerical controlled (CNC) manufacturing processes can be filled within the framework of computer aided process planning (CAPP) systems. As a result, the general objectives of manufacturing can be satisfied.

Figure 1.3 summarizes such efforts in aerospace manufacturing, where the goal is to produce the first-part-correct with minimum trial and error. Computer aided engineering tools, high level automation, physics based process knowledge are integrated from manufacturing planning to quality control of finished parts within a systematic approach. This can only be made possible through a detail oriented investigation of manufacturing

processes. Similar examples can also be given for other industries such as the production of biomedical and electronics devices.

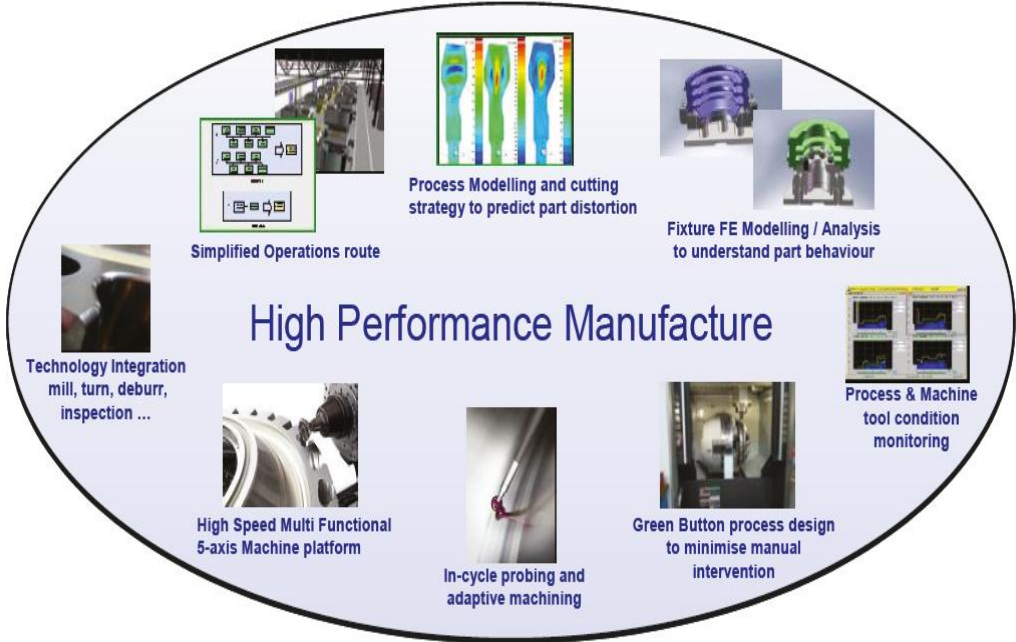


Figure 1.3 Enabling technologies for high performance manufacturing (Kappmeyer et al., 2012)

A major class in manufacturing processes is the material removal processes. The most important processes in this category are turning, drilling, and milling processes as shown in Figure 1.4.

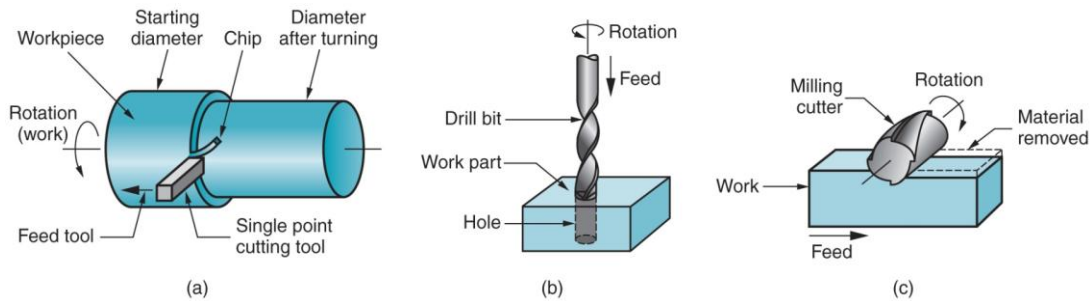


Figure 1.4 Material removal processes (Groover, 2012)

These processes use a cutting tool which is harder than the material being shaped in the process. The cutting tools shave off the material from the surface until the desired shape is obtained. A good surface quality can be obtained as a result of machining process. The cutting tool itself also wears out during the process based on the material properties of the tool and the part.

Machining process parameters must be set well in order to obtain an acceptable part quality considering the economics of the process. The cost of manufacturing, the speed of manufacturing and the produced part quality are conflicting objectives hence pose interesting optimization problems. In machining optimization problems, cutting speed, feed, depth of cut etc. are considered as process variables and the goal is to set these process variables to obtain minimum unit cost or maximum productivity (minimum processing time). Figure 1.5 shows the general machining optimization problems for minimum unit cost and maximum productivity cases. As cutting speed increases, machining time decreases which also decrease machining costs. However, tool life decreases as a result of faster processing which increases tooling cost which also means that machine will be idle due to tool change which will further increase total costs. Achieving optimum cutting conditions is important to minimize machining costs in aerospace industry or minimizing machining time in mold making industry.

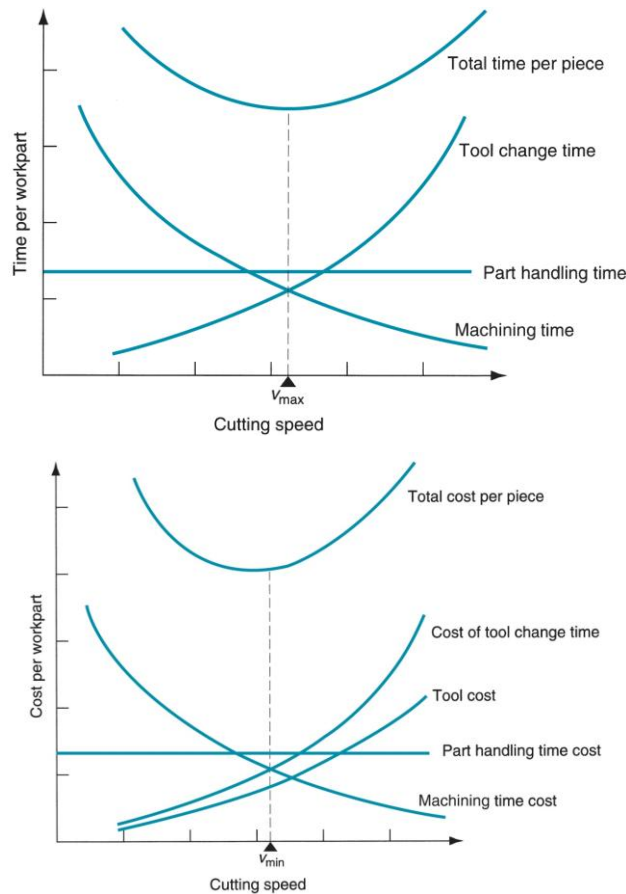


Figure 1.5 Machining optimization for minimum cost and maximum productivity (Groover, 2012)

Unfortunately these problems cannot be solved without any experimental data since reliable calculation of process outputs such as tool life and surface quality is not possible. These can only be calculated through experimental methods. Experimentation reveals influential factors that trigger variations in a process/system, to detect most influential factors on the output of a process/system or to find out the most suitable set of factors that minimizes the effect of uncontrollable factors such as noise and develop a robust process/system. Design of experiments (DOE) technique has an important role on generating model of the process/system correctly. In order to generate an accurate model

of the physical process, experiment parameters need to be well-chosen since the resulting model depends on the observed data. In manufacturing processes, DOE is widely used to improve the quality of a product, shorten the processing time and increase the life of cutting tool. Table 1.1 shows the outline of the DOE procedure.

Table 1.1 Guideline for design of experiments (Montgomery, 2004)

1. Statement of the problem
2. Selection of the response variable
3. Choice of factors, levels, and ranges
4. Choice of experimental design
5. Performing the experiment
6. Statistical analysis of the data
7. Conclusions and recommendations

It is possible to use regression techniques to represent the data obtained experimentally. Mathematical modeling techniques can be used to obtain the relationship between the objectives as a function of process parameters and various optimization techniques can be used to obtain optimum set of machining parameters. The objective functions in machining problems are usually nonlinear and constrained. As a result, evolutionary optimization algorithms are commonly employed to solve these optimization problems. The approach explained above is used in this thesis, to study macro and micro scale machining optimization problems.

**1.1 Motivation**

A recent trend in manufacturing industry is towards miniaturization, which has become more important in various industries such as biomedical, consumer products, electronics

in order to improve the quality of human life by producing more functional products which consume less energy. Micro power generators, fuel cells, lab-on-chip systems, stents, medical screening devices, micro robots and components of cell phones, miniature mold and dies for the mass production of plastic micro parts are some applications. It must be noted that, these are all high value added products and they can be produced in small factories with low energy requirements.

In order to produce miniature products, highly accurate micro components are required. Hence, different types of micromachining processes have been developed and used to produce micro components. Removal by mechanical force (micro milling, turning, drilling), removal by melting, vaporization, and ablation (micro electrical discharge machining, laser machining etc.) are some examples of these processes. Fabrication of micro components necessitates reliable, repeatable, cost effective and fast processes. Although lithography, laser, ion beam and micro EDM methods are available to manufacture good quality micro parts, they are not very preferable because of high costs, material and geometric limitations and time inefficiency. On the other hand, mechanical micromachining is a class of viable micro-manufacturing techniques for producing three dimensional (3D) features on various engineering materials such as metals, composite materials, ceramics and polymers. (Masuzawa, 2000)

Mechanical micromachining has advantages in manufacturing micro components. One of the advantages is that set up and tool costs are not expensive with regard to other techniques. Besides, it is possible to fabricate a broad range of materials with complex 3D geometries such as micro molds. Among mechanical micro manufacturing techniques, micro milling is considered as the most the flexible method. Unlike conventional milling process, the knowledge base for micro milling process is limited.

The general objective of this study is to contribute to the development of knowledge base for micro milling process. A particular application area is selected as the manufacturing of micro molds. Machining of micro molds can be divided into roughing and finishing processes where the roughing process can be considered as a series of pocketing operations. In this thesis, pocketing operation is investigated in detail and optimization of micro milling process is performed based on the pocketing model developed in this thesis. An evolutionary optimization technique called particle swarm optimization is used to obtain economical machining conditions. The performance of the PSO is also compared with conventional optimization algorithms.

## **1.2 Organization of the Thesis**

The organization of the thesis is detailed below:

In Chapter 2, modeling and optimization of macro scale turning problem is considered. This section is considered as a benchmark study to test the effectiveness of particle swarm optimization (PSO) method against the results given in the literature. In Chapter 3, experimental study conducted on micro milling is explained. Factors affecting micro milling forces, burr formation and surface roughness are explained and tool life expressions for micro milling is obtained. In Chapter 4, mathematical modeling of square pocket milling operation is developed and optimization of the pocketing operation is performed. In Chapter 5, conclusions are drawn and future research directions are given.

# Chapter 2

## Modeling and Optimization of Macro-Scale Turning Operation

Material removal processes are one of the most frequently used methods in manufacturing. Turning, milling and drilling are the most important operations among the material removal processes. This chapter focuses on the process parameter optimization for multi-pass macro-scale turning operation. Firstly, literature on multi-pass macro-scale turning operations is summarized. Secondly, the mathematical formulation of the multi-pass turning operation problem from the literature is explained. Thirdly, Particle Swarm Optimization algorithm is explained. And finally, a numerical example is given in order to test and compare the performance of PSO and nonlinear optimization algorithms with the results reported in the literature.

## **2.1 Literature Review on Multi Pass Turning Operation Problem**

The main objective of machining operations is fabricating high quality products with low costs in the shortest time. In order to achieve this objective, the selection of the machining parameters, such as cutting speed, depth of cut and feed rate, has become an important issue. Thus, many researchers studied the optimization of process parameter in turning operations.

Gilbert (1950) studied optimization of machining process for single-pass turning operation. Maximum production rate and minimum cost are considered as objective functions and gained different results from each objectives. Ermer (1971) added various operating constraints to the optimization model of single-pass turning operation and used geometric programming.

Shin and Joo (1992) presented an optimization model for multi-pass turning operations. In their study, cutting operations are divided into two parts as rough cutting and finishing cutting, and two sub-problems are solved separately using dynamic programming. Unit production cost is considered as objective function and consists of four main parts which are machining cost, machine idling cost, tool cost and tool replacement cost. Cutting speed, feed rate and axial depth of cut are determined as decision variables. Optimal solutions are obtained for both roughing and finishing operations in this study. Chen and Tsai (1996) modified the multi-pass turning optimization model of Shin and Joo (1992) by adding relation constraints for rough cutting and finishing cutting. Thus, the problem is solved considering both rough and finishing cutting simultaneously instead of solving two sub-problems. The objective of the model is minimizing unit production cost by using rough and finishing cutting speed, rough and finishing feed rate, finishing axial depth of cut and number of rough cutting as decision variables. Simulated Annealing (SA) Algorithm and Hooke-Jeeves Pattern

Search (SA/HJPS) based optimization algorithm is used to solve the nonlinear optimization problem. It is observed that the algorithm finds near optimal solution set within a reasonable computation time.

Chen (2004) applied scatter search (SS) algorithm to solve the multi-pass turning optimization problem stated by Chen and Tsai (1996). In this study, constrained nonlinear problem is converted into an unconstrained nonlinear problem by adding a penalty function to the objective function instead of defining constraints. An extremely large positive constant is given to the penalty function. Thus, objective function will be extremely large, if one of constraints is violated. The results indicated that scatter search algorithm found better solutions than FEGA and Hooke-Jeeves Pattern Search.

Onwubolu and Kumalo (2001) proposed a new optimization technique based on genetic algorithm (GA) to solve the same model proposed by Chen and Tsai (1996). While the objective function is same with the model constructed by Chen and Tsai (1996), the decision variables are set different from the previous work. Although Onwubolu and Kumalo (2001) obtained better results with respect to Chen and Tsai (1996), their result is invalid since they overlooked total depth of cut equality constraint which stated in the mathematical model of Chen and Tsai (1996). Chen and Chen (2003) realized the mistakes that Onwubolu and Kumalo (2001) made and published the correct results of their work.

Vijayakumar et al. (2003) applied ant colony algorithm (ACO) to solve the multi-pass turning optimization problem presented by Chen and Tsai (1996) and claimed that the proposed ACO algorithm provides better results than previously reported results. Machining parameters, number of passes and depth of cut are determined as decision variables and problem is solved as maximization of negative sign unit production cost. Wang (2007) stated that the solution achieved by Vijayakumar et al. (2003) is also not

valid. In order to check the validity of optimal solution, unit production cost is computed using the given values of parameters. Since optimal depth of cut information is not given in the study, Wang (2007) tried different number of pass values and revealed that minimum possible objective function value is larger than the result found in Vijayakumar et al (2003).

Yıldız (2009) proposed a hybrid method which combines immune algorithm and hill climbing local search algorithm (HIHC) to solve the nonlinear multi-pass turning optimization problem. The hybrid algorithm combines high exploration speed of immune algorithm with powerful ability of hill climbing local search algorithm to prevent being trapped in local minimum. The same objective function and constraint set of Chen and Tsai (1996) is used in the study. It is revealed that HIHC outperforms FEGA, SA/HJPS and SS. However, the values of parameters found in the achieved solution are not provided. Costa et al. (2011) presented a hybrid particle swarm optimization (HPSO) algorithm to minimize unit production cost in multi-pass turning optimization problem. The hybrid algorithm consists of simulated annealing algorithm to enhance the search mechanism and particle swarm optimization algorithm to move away from local optima. In this study, a similar method to Chen (2004) is used. A penalty function is defined and added to the objective function in order to construct unconstrained nonlinear model instead of solving constrained nonlinear model. Besides, a repair procedure is used to avoid violation in equality constraints. Algorithm is performed for different total depth of cuts. Besides, various comparison modules are done to benchmark with previous works. According to the obtained results, HPSO provides better solutions than the previous works.

## 2.2 Mathematical Modeling

The process parameter optimization is done for multiple rough cuts and a single finish cut. The mathematical formulation of multi-pass turning operation model stated in Chen and Tsai (1996) is adopted for the process optimization problem which aims to minimize unit production cost. Unit production cost consists of four basic cost elements. These cost elements are actual machining time cost, machine idling cost due to the loading/unloading operations and idle tool motions, tool replacement cost and tool cost. While searching near optimal machining conditions, technological and physical restrictions are considered. These restrictions are cutting parameter and tool life upper / lower limits, maximum cutting force, machine power and chip-tool interface temperature. Relationship between rough and finish cut, stable cutting region restriction and maximum allowable surface roughness are also considered. In this model, the effect of reduction in workpiece diameter is not taken into consideration. In order to consider the diameter reduction effect, a modified model is also introduced.

The notation used in the mathematical model of multi-pass conventional turning is as follows:

$V_r$  : cutting speed in rough machining (m/min)

$V_s$  : cutting speed in finish machining (m/min)

$f_r$  : feed rate in rough machining (mm/rev)

$f_s$  : feed rate in finish machining (mm/rev)

$d_s$  : depth of cut for each pass of finish machining (mm)

$n$  : number of rough passes

$UC$  : unit production cost except material cost (\$/piece)

$C_0$  : constant pertaining to tool life equation

$C_I$  : machine idle cost (\$/piece)

$C_M$  : cutting cost by actual time in cut (\$/piece)

$C_R$  : tool replacement cost (\$/piece)  
 $C_T$  : tool cost (\$/piece)  
 $d_r$  : depth of cut for each pass of rough machining (mm)  
 $d_t$  : total depth of metal to be cut (mm)  
 $d_{rL}, d_{rU}$  : lower and upper bounds of depth of rough cut (mm)  
 $d_{sL}, d_{sU}$  : lower and upper bounds of depth of finish cut (mm)  
 $D$  : diameter of workpiece (mm)  
 $f_{rL}, f_{rU}$  : lower and upper bounds of feed rate in rough cut (mm/rev)  
 $f_{sL}, f_{sU}$  : lower and upper bounds of feed rate in finish cut (mm/rev)  
 $V_{rL}, V_{rU}$  : lower and upper bounds of cutting speed in rough cut (m/min)  
 $V_{sL}, V_{sU}$  : lower and upper bounds of cutting speed in finish cut (m/min)  
 $F_r, F_s$  : cutting forces during rough and finish cutting (kg f)  
 $F_U$  : maximum allowable cutting force (kg f)  
 $h_1, h_2$  : constants pertaining to tool travel and approach, depart time (min)  
 $k_1, k_2, k_3$  : constants for roughing and finishing parameter relations  
 $k_f$  : coefficient pertaining to specific tool – workpiece combination  
 $k_0$  : direct labor overhead cost (\$/min)  
 $k_q$  : coefficient pertaining to equation of tool – chip interface temperature  
 $k_t$  : cutting edge cost (\$/edge)  
 $L$  : length of workpiece (mm)  
 $p, q, r$  : constants pertaining to the tool – life equation  
 $P_r, P_s$  : cutting powers during rough and finish cutting (kW)  
 $P_U$  : maximum allowable cutting power (kW)  
 $Q_r, Q_s$  : temperatures during rough and finish cutting (°C)  
 $Q_U$  : maximum allowable temperature (°C)  
 $R_a$  : maximum allowable surface roughness ( $\mu\text{m}$ )  
 $R_n$  : nose radius of cutting tool (mm)  
 $S_c$  : limit of stable cutting region  
 $t$  : tool life (min)  
 $t_c$  : constant term of machine idling time (min)

$t_e$  : tool exchange time (min)  
 $t_p$  : tool life (min) considering roughing and finishing  
 $t_r, t_s$  : tool lives (min) considering roughing and finishing  
 $t_v$  : variable term of machine idling time (min)  
 $T_I$  : machine idling time (min)  
 $T_L, T_U$  : lower and upper bound of tool life (min)  
 $T_M$  : cutting time by actual machining (min)  
 $T_{Mr}, T_{Ms}$  : cutting time by actual machining for roughing and finishing (min)  
 $T_R$  : tool replacement time (min)  
 $X$  : vector of cutting parameters  
 $\tau, \phi, \delta$  : constants pertaining to expression of chip tool interface temperature  
 $\eta$  : power efficiency  
 $\lambda, \nu$  : constants pertaining to expression of stable cutting region  
 $\mu, \nu$  : constants of cutting force equation  
 $\theta$  : a weight for  $t_p$  where  $0 < \theta < 1$

As a first case, the mathematical model formulated by Chen and Tsai (1996), which neglects the effect of workpiece diameter reduction on unit production cost, is solved. The mathematical model of the first case is given as following:

$$\min UC = C_M + C_I + C_R + C_T$$

subject to

$$d_{rL} \leq d_r \leq d_{rU} \quad (1)$$

$$f_{rL} \leq f_r \leq f_{rU} \quad (2)$$

$$V_{rL} \leq V_r \leq V_{rU} \quad (3)$$

$$T_L \leq t_r \leq T_U \quad (4)$$

$$k_f f_r^\mu d_r^\nu \leq F_U \quad (5)$$

$$\frac{k_f f_r^\mu d_r^v V_r}{6120\eta} \leq P_U \quad (6)$$

$$V_r^\lambda f_r d_r^v \geq S_c \quad (7)$$

$$k_q V_r^\tau f_r^\phi d_r^\delta \leq Q_U \quad (8)$$

$$d_{sL} \leq d_s \leq d_{sU} \quad (9)$$

$$f_{sL} \leq f_s \leq f_{sU} \quad (10)$$

$$V_{sL} \leq V_s \leq V_{sU} \quad (11)$$

$$T_L \leq t_s \leq T_U \quad (12)$$

$$k_f f_s^\mu d_s^v \leq F_U \quad (13)$$

$$\frac{k_f f_s^\mu d_s^v V_s}{6120\eta} \leq P_U \quad (14)$$

$$V_s^\lambda f_s d_s^v \geq S_c \quad (15)$$

$$k_q V_s^\tau f_s^\phi d_s^\delta \leq Q_U \quad (16)$$

$$\frac{f_s^2}{8R_n} \leq R_a \quad (17)$$

$$V_s \geq k_1 V_r \quad (18)$$

$$f_r \geq k_2 f_s \quad (19)$$

$$d_r \geq k_3 d_s \quad (20)$$

$$d_r = (d_t - d_s)/n \quad (21)$$

In the model,  $V_r, f_r, V_s, f_s, n$  and  $d_s$  are determined as the decision variables.

Unit production cost ( $UC$ ) is calculated as the sum of four basic cost elements which are  $C_M, C_I, C_R, C_T$ . The formulation of each cost element is as follows:

$$C_M = k_0 T_M \quad (22)$$

$$C_I = k_0 [t_c + (h_1 L + h_2)(n + 1)] \quad (23)$$

$$C_R = k_0 \frac{t_e}{t_p} T_M \quad (24)$$

$$C_T = \frac{k_t}{t_p} T_M \quad (25)$$

where

$$T_M = nT_{Mr} + T_{Ms} \quad (26)$$

$$T_{Mr} = \frac{\pi DL}{1000 V_r f_r} \quad (27)$$

$$T_{Ms} = \frac{\pi DL}{1000 V_s f_s} \quad (28)$$

Actual machining cost ( $C_M$ ) is divided into two components which are multiple roughing and single finishing costs. Machine idling cost ( $C_I$ ) has two constant terms, loading and unloading operation costs and a variable term idle motion time due to tool motions between passes and length of workpiece. In tool replacement cost ( $C_R$ ) calculation, it is assumed that a single tool can be used for both rough cut and finish cut operations. Thus, the tool life is calculated as following:

$$t_p = \theta t_r + (1 - \theta) t_s \quad (29)$$

where

$$t_r = \frac{C_0}{V_r^p f_r^q d_r^r} \quad (30)$$

$$t_s = \frac{C_0}{V_s^p f_s^q d_s^r} \quad (31)$$

In order to estimate tool replacement cost, required number of tools and tool changing time are used. Tool cost ( $C_T$ ) is calculated by considering number of used tools.

Constraints (1), (2) and (3) bound depth of cut, feed rate and cutting speed for roughing process respectively. Constraint (4) keeps roughing process tool life within an

acceptable range to manufacture economic and high quality products. Constraint (5), (6) and (8) restrict the cutting force, power and chip – tool interface temperatures in the course of roughing operations. Constraint (7) ensures the cutting conditions of roughing process stay in the stable region. Constraints (9), (10) and (11) guarantee that the depth of cut, feed rate and cutting speed bounds for finish cut are not terminated. Constraint (12) keeps finishing process tool life within the determined range. Constraint (13), (14) and (16) restricts the cutting force, power and chip – tool interface temperatures during the finishing operations respectively. Constraint (15) ensures the cutting conditions of finish cut stay in the stable region. Constraint (17) provides that the quality of machined surface is within the required range. Constraints (18) – (20) define the relations of cutting speed, feed rate and depth of cut in roughing and finishing processes. Constraint (21) ensures that total depth of cut is equal to the sum of finishing depth of cut and total depth of roughing cut.

It must be noted that the diameter of the workpiece is assumed to be fixed during the cutting process in the original formulation. This may be a valid assumption if the diameter reduction is assumed to be small. Cutting speed is kept constant during the turning process which means that the rotational speed of the spindle must be increased as diameter decreases which implies that feed rate must increase at each pass therefore machining time changes in every machining pass. Decrease in part diameter affects unit production cost. For analyzing the effect of decrease in part diameter, another case is created. A modification is applied to the objective function of Chen and Tsai (1996) as a second case in order to investigate the effect of decrease in workpiece diameter on unit cost by considering the same restrictions. The diameter information is updated at each pass. In the second case, actual machining time of rough cut ( $T_{Mr}$ ) and finish cut ( $T_{Ms}$ ) are reformulated with respect to the assumption. Machining time calculation method is as follows:

$$1^{st} \text{ rough pass} : \frac{\pi DL}{1000 V_r f_r} \quad (32)$$

$$2^{nd} \text{ rough pass} : \frac{\pi(D-2d_r)L}{1000 V_r f_r} \quad (33)$$

$$n^{th} \text{ rough pass} : \frac{\pi(D-2(n-1)d_r)L}{1000 V_r f_r} \quad (34)$$

$$\text{finish pass} : \frac{\pi(D-nd_r)L}{1000 V_s f_s} \quad (35)$$

Objective function of the second case is as follows:

$$\min UC = C_M + C_I + C_R + C_T$$

where

$$C_M = k_0 \left[ \sum_{i=0}^{n-1} \frac{\pi(D-2id_r)L}{1000 V_r f_r} + \frac{\pi(D-2nd_r)L}{1000 V_s f_s} \right] \quad (36)$$

$$C_I = k_0 [t_c + (h_1 L + h_2)(n + 1)] \quad (37)$$

$$C_R = k_0 \frac{t_e}{t_p} \left[ \sum_{i=0}^{n-1} \frac{\pi(D-2id_r)L}{1000 V_r f_r} + \frac{\pi(D-2nd_r)L}{1000 V_s f_s} \right] \quad (38)$$

$$C_T = \frac{k_t}{t_p} \left[ \sum_{i=0}^{n-1} \frac{\pi(D-2id_r)L}{1000 V_r f_r} + \frac{\pi(D-2nd_r)L}{1000 V_s f_s} \right] \quad (39)$$

$C_I$  is not affected from the modification since the terms in machine idling cost is not dependent on actual machining time. However, machining time formulation of  $C_M$ ,  $C_R$  and  $C_T$  are changed due to the new assumption. Decision variables and constraints remain same as the first case.

As mentioned earlier, PSO is used to solve the multi pass turning optimization problem. PSO technique is explained in the next section.

### 2.3 Particle Swarm Optimization (PSO)

Particle Swarm Optimization (PSO) algorithms have been used in various optimization problems ranging from simple problems to highly complex problems. It has become a popular method in handling machining process optimization problems due to its robustness and efficiency. PSO is developed by Kennedy and Eberhart (1995). It is a population based stochastic optimization method inspired from the social behaviors of animals or insects such as bird flocking and fish schooling.

In PSO, a population of particles is randomly scattered in the search space. Each particle in the swarm has its own path in the search space. The path is updated by using its previous position information and current velocity at each iteration. The dimensions of position and velocity vectors are determined due to the number of decision variables in the model. As the solution improved, search space is narrowed around the highest performing particle for detailed search. The process continues until reaching the termination criteria.

In the algorithm, the velocity of each particle is updated by considering best position found by the particle (*pbest*) and best position found by the entire population (*gbest*). The update procedure is done with respect to the following equations:

$$v_i^{k+1} = wv_i^k + c_1r_1(pbest_i - x_i^k) + c_2r_2(gbest - x_i^k) \quad (40)$$

$$x_i^{k+1} = x_i^k + v_i^{k+1} \quad (41)$$

where  $v_i^k$  denotes velocity of particle  $i$  at iteration  $k$ ,  $x_i^k$  denotes current position of particle  $i$  at iteration  $k$ ,  $pbest_i$  denotes personal best position of particle  $i$ ,  $gbest$  denotes the best position in the entire population,  $r_1$  and  $r_2$  denote random values

generated between 0 and 1,  $c_1$  and  $c_2$  denote acceleration coefficients and  $w$  denotes the inertia weight.

Equation (40) shows the update procedure of velocity. It consists of three different terms. The first term  $wv_i^k$  is the weighted ratio of particle velocity and is used to carry the particle in its previous direction. The second term  $c_1r_1(pb_{est_i} - x_i^k)$  is used to carry the information of particles best position. The last term  $c_2r_2(gbest - x_i^k)$  attracts the entire population to the particle which performs best in the swarm. Random numbers  $r_1$  and  $r_2$  are used to provide stochastic behavior to the algorithm. Inertia weight  $w$  is used to define the area of search space. The algorithm searches a wide space when the inertia weight is large. Large inertia weight is commonly used at the beginning of the algorithm. As the solution improved, inertia weight can be reduced in order to confine the search region near  $gbest$ .

Equation (41) shows the update procedure of particles' current position. The position of particle is updated by using the velocity update term. The procedure of PSO is summarized as follows:

**Step 1:** Generate initial population with its positions and velocities.

**Step 2:** Evaluate the objective function of all particles. Assign the current position of each particle and its objective function value as  $pb_{est}$ . Select the best solution within the entire population and assign as  $gbest$ .

**Step 3:** Generate new positions and velocities of particles. If a particle has a better objective function value than its personal best, update  $pb_{est}$  with the current value.

Evaluate each particles' *pbest* value and assign *gbest*. If the new *gbest* is better than the previous *gbest* value, update *gbest* value.

**Step 4:** Repeat step 2 and step 3 until reaching determined iteration number.

Karpat and Özel (2006) developed a neural network model to model the surface roughness and tool wear characteristics of CBN tools and used particle swarm optimization (PSO) to optimize cutting parameters of turning operations. Karpat and Özel (2007) used multi objective particle swarm optimization (MOPSO) method in order to optimize hard turning operation for the cases of tool life and material removal rate maximization and surface roughness and machining time minimization. A Pareto optimal set is obtained for multi objective optimization problem.

Parameter selection has an important role on the processing time and solution quality of the heuristic algorithms. Thus, an analysis is required in order to increase the speed of algorithm without losing the solution quality. Parameter analysis is performed for the particle swarm optimization algorithm and the determined parameter values are given in Table 2.1. The detailed analysis of parameter selection is given in the numerical study section.

Table 2.1 Particle swarm optimization parameter values

Parameter Type	
$c_1$	2
$c_2$	2
Range of $w$	0.99 – 0.05
Swarm size	100
Iteration number	500

## 2.4 Numerical Study

In this section, a numerical study is performed to analyze the effects of decision variables on the model, determine particle swarm optimization algorithm parameters, evaluate and compare the performance of PSO with the results given in the literature. All of the analyses are performed on a personal computer with 2.20 GHz Intel Core 2 Duo CPU and 2 GB of RAM.

The constraints of cutting force, power, stable region and chip-tool interface temperature are investigated in order to measure the effects of decision variables on the model. Parameters of PSO are fine tuned using the turning operation model of Chen and Tsai (1996) and the data which is presented in Figure 2.1. For algorithm evaluation, the results obtained through PSO are compared with the previous studies. Besides, Matlab Optimization Toolbox which uses trust region, active set or interior point algorithms is also included in the comparison. The data used in the computational study is given in Figure 2.1.

$D = 50 \text{ mm}$	$L = 300 \text{ mm}$	$d_t = 6.0 \text{ mm}$
$V_{rU} = 500 \text{ m/min}$	$V_{rL} = 50 \text{ m/min}$	$f_{rU} = 0.9 \text{ mm/rev}$
$f_{rL} = 0.1 \text{ mm/rev}$	$d_{rU} = 3.0 \text{ mm}$	$d_{rL} = 1.0 \text{ mm}$
$V_{sU} = 500 \text{ m/min}$	$V_{sL} = 50 \text{ m/min}$	$f_{sU} = 0.9 \text{ mm/rev}$
$f_{sL} = 0.1 \text{ mm/rev}$	$d_{sU} = 3.0 \text{ mm}$	$d_{sL} = 1.0 \text{ mm}$
$k_o = 0.5 \text{ \$/min}$	$k_t = 2.5 \text{ \$/edge}$	$h_1 = 7 \times 10^{-4}$
$h_2 = 0.3$	$t_c = 0.75 \text{ min/piece}$	$t_e = 1.5 \text{ min/edge}$
$p = 5$	$q = 1.75$	$r = 0.75$
$C_0 = 6 \times 10^{11}$	$T_U = 45 \text{ min}$	$T_L = 25 \text{ min}$
$k_f = 108$	$\mu = 0.75$	$v = 0.95$
$\eta = 0.85$	$F_U = 200 \text{ kgf}$	$P_U = 200 \text{ kW}$
$\lambda = 2$	$v = -1$	$S_c = 140$
$k_q = 132$	$\tau = 0.4$	$\phi = 0.2$
$\delta = 0.105$	$Q_U = 1000^\circ\text{C}$	$R_n = 1.2 \text{ mm}$
$R_a = 10 \mu$	$k_1 = 1.0$	$k_2 = 2.5$
$k_3 = 1.0$		

Figure 2.1 Machining Model Data (Chen, 2004)

### 2.4.1 Constraint Analysis of Mathematical Model

Prior to the evaluation of PSO performance, the effects of decision variables on cutting force, power, stability and chip-tool interface constraints are investigated. Since the bounds in both roughing and finishing operation parameters and the constraint equations are the same, analysis is done with respect to three decision variables which are cutting speed, feed rate and depth of cut. In order to visualize the effects, three dimensional surface plots are created.

In Figure 2.2, the effects of feed rate and depth of cut on cutting force are introduced. It is revealed from the figure that cutting force increases as the depth of cut and feed rate increases. High feed rate and depth of cut values induce infeasibility in the problem. The white area in part (b) represents the infeasible region for cutting force constraints.

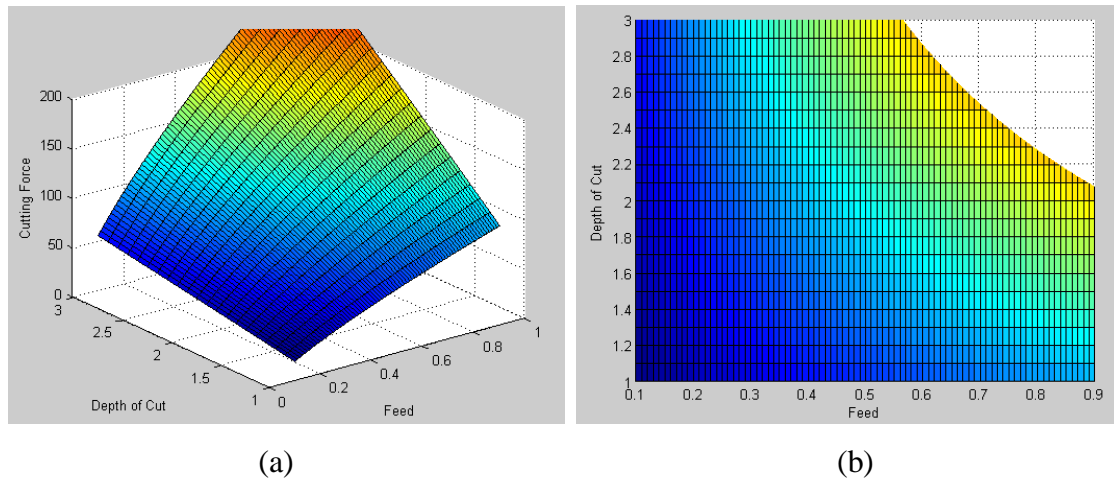
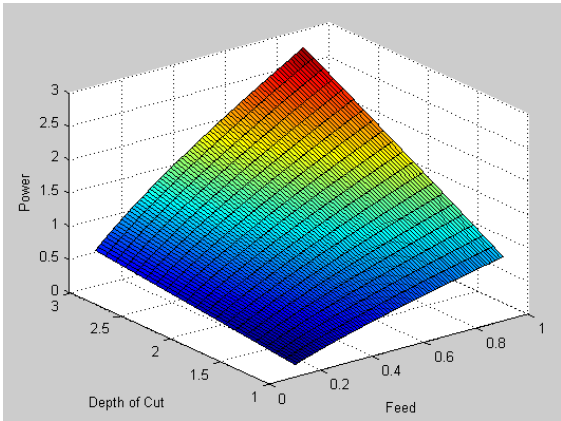


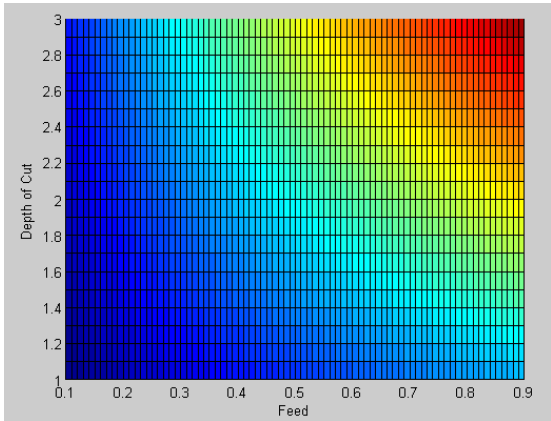
Figure 2.2 Effects of feed rate and depth of cut on cutting force (Constraints 5 and 13)

In Figure 2.3, the effects of feed rate, depth of cut and cutting speed on machine power are presented. Since there are three decision variables that affect power constraint, it is not possible to investigate the effect of all variables on power simultaneously. Thus,

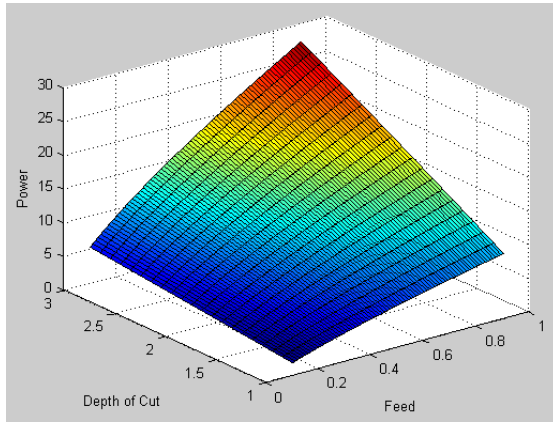
these variables are divided into groups of two and all possible combinations are analyzed. While constructing the groups, the remaining decision variable is fixed at its lower and upper bounds separately. In parts (a) – (b) and (c) – (d), the effects of depth of cut and feed rate are explored by fixing the cutting speed to its lower limit and upper limit respectively. In parts (e) – (f) and (g) – (h), the effects of cutting speed and feed rate are analyzed by fixing the depth of cut to its lower limit and upper limit respectively. In parts (i) – (j) and (k) – (l), the effects of depth of cut and cutting speed are searched by fixing the feed rate to its lower limit and upper limit respectively. Due to the surface plots, machine power increases by increasing depth of cut, feed rate and cutting speed. When the differences of highest obtained power values for lower and upper limits of the fixed decision variables are investigated, it is discovered that cutting speed changes the power value most. The second effective decision variable is feed rate and third effective is depth of cut.



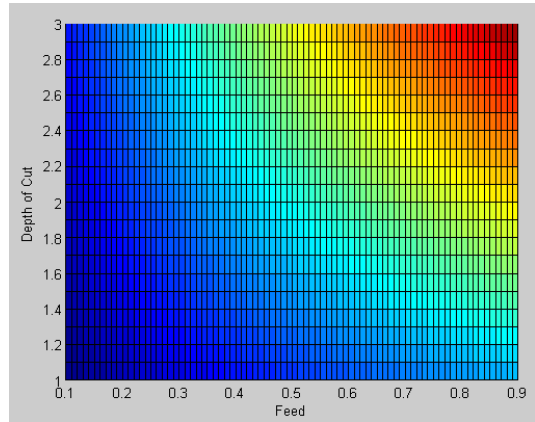
(a)



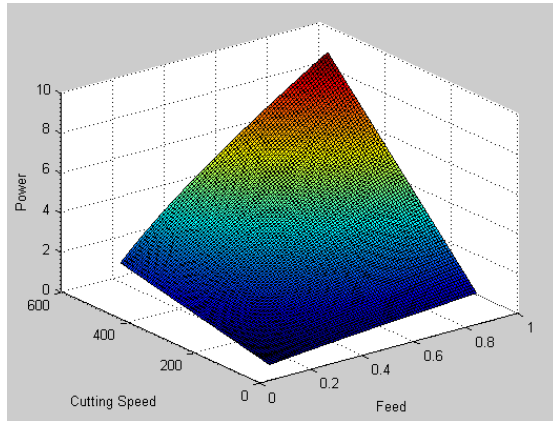
(b)



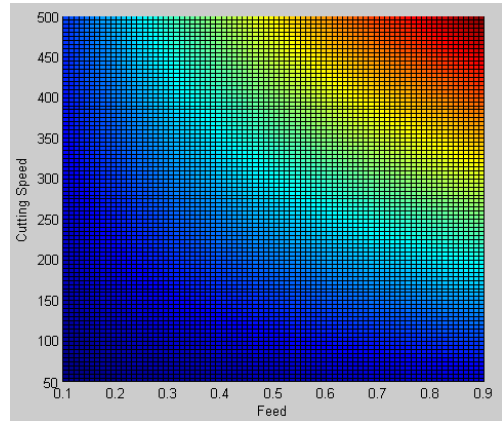
(c)



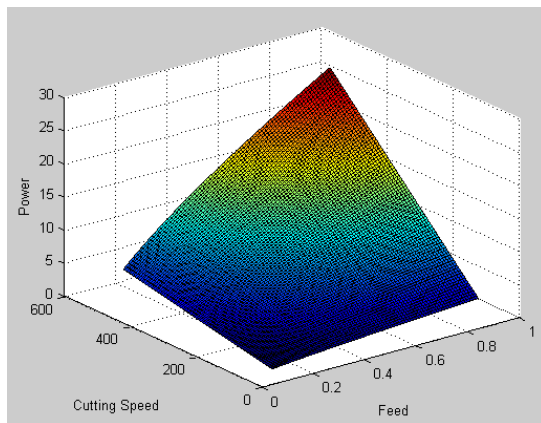
(d)



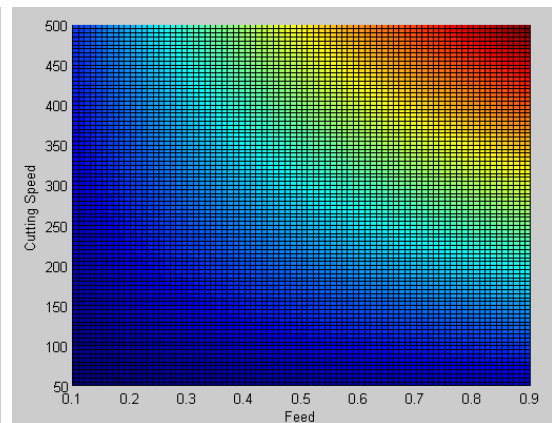
(e)



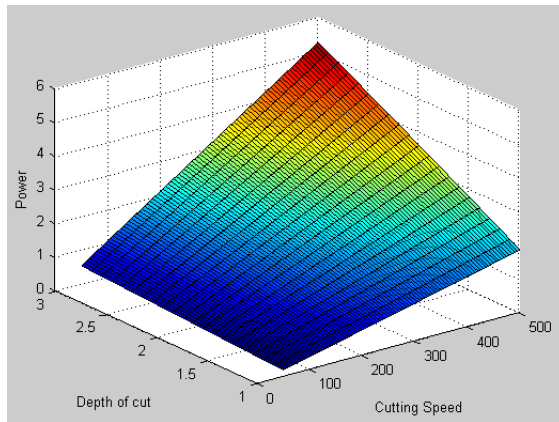
(f)



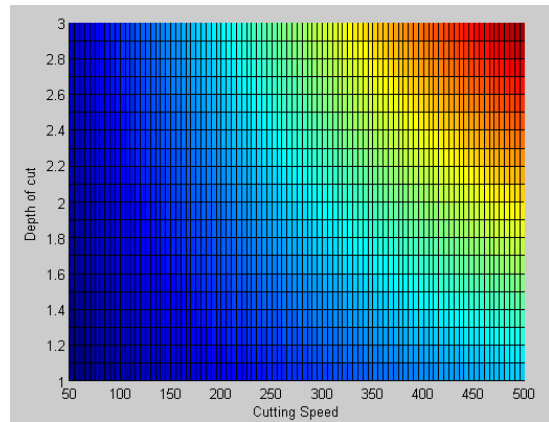
(g)



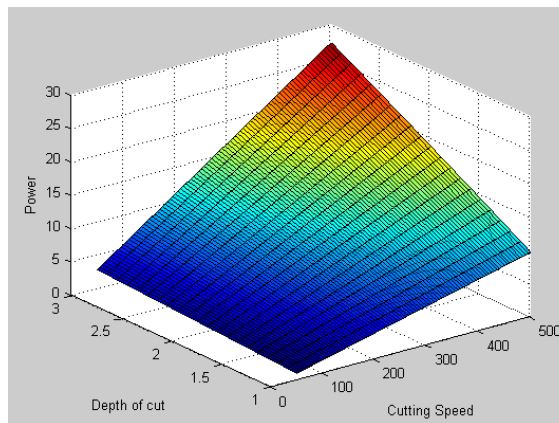
(h)



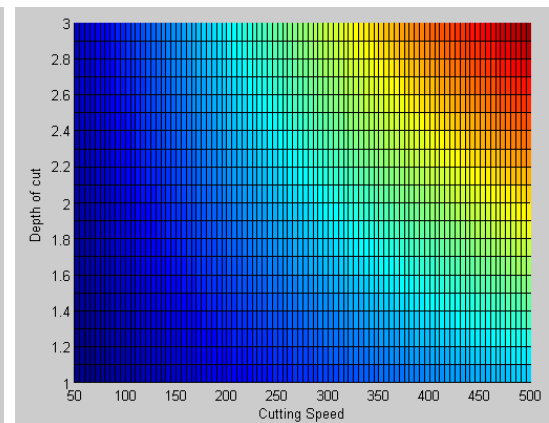
(i)



(j)



(k)



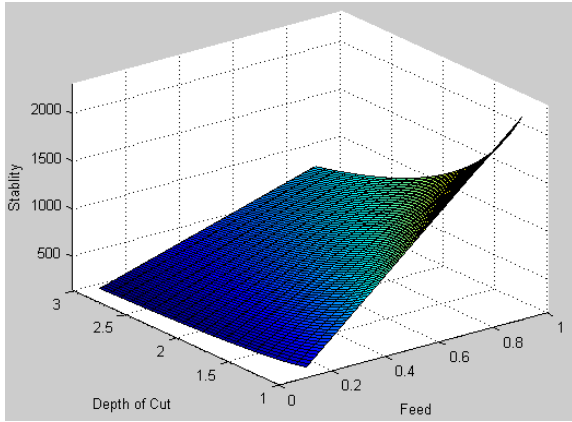
(l)

Figure 2.3 Effects of cutting speed, depth of cut and feed rate on power (Constraints 6 and 14)

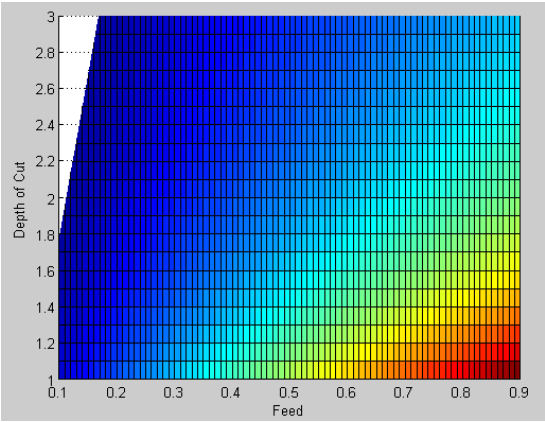
Besides, power constraint is never terminated within the given ranges of cutting speed, depth of cut and feed rate. Although the upper limit of power is 200 kW, the maximum obtained power is 27.24 kW.

In Figure 2.4, the effects of feed rate, depth of cut and cutting speed on stable region are shown. The same methodology with power constraint analysis is used in the course of the investigation of decision variables on stability constraint. In parts (a) – (b), the effects of depth of cut and feed rate are explored by fixing the cutting speed to its lower

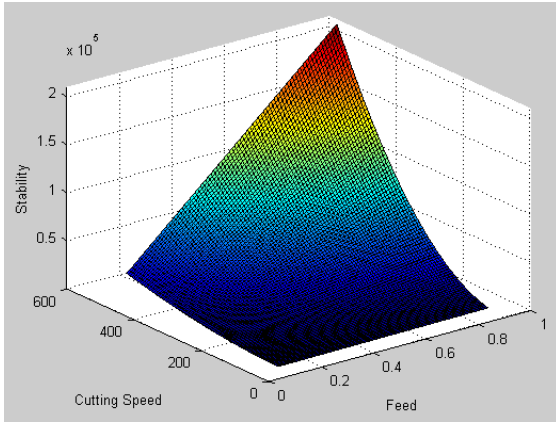
limit. The cutting speed is also fixed to the upper limit. However, feasible region for the fixed upper limit of cutting speed does not exist. In parts (c) – (d) and (e) – (f), the effects of cutting speed and feed rate are analyzed by fixing the depth of cut to its lower limit and upper limit respectively. In parts (g) – (h) and (i) – (j), the effects of depth of cut and cutting speed are searched by fixing the feed rate to its lower limit and upper limit respectively. It is revealed from the analysis that depth of cut should be small. If the depth of cut needs to be increased, feed rate and cutting speed should be increased in order to stay in the stable cutting region. Besides, stability cannot be achieved for the upper limit of cutting speed.



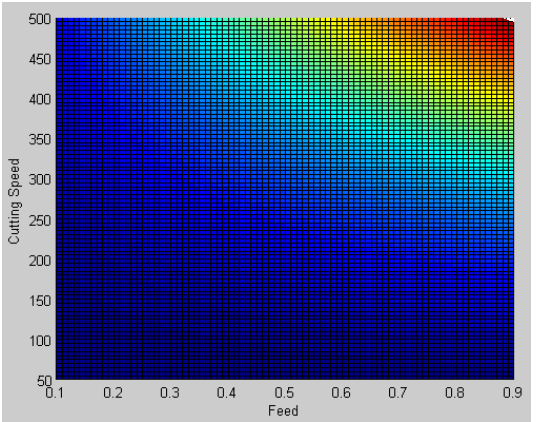
(a)



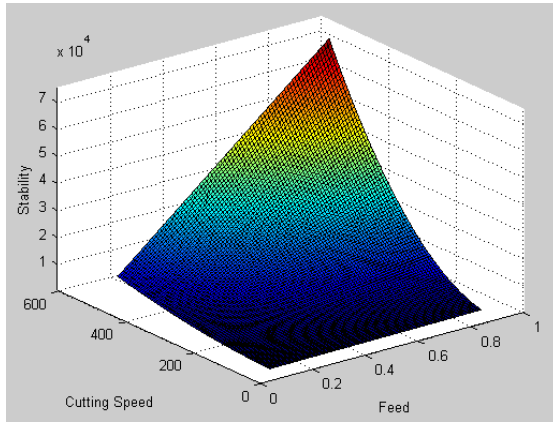
(b)



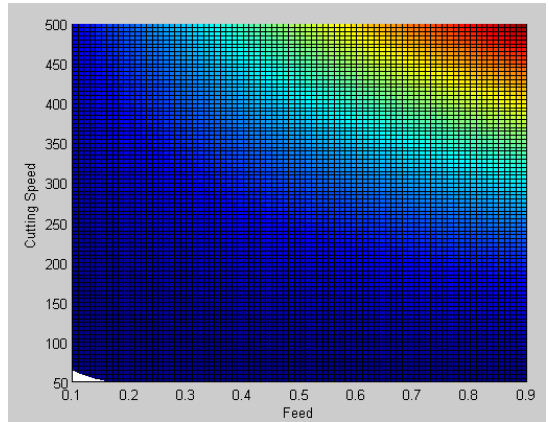
(c)



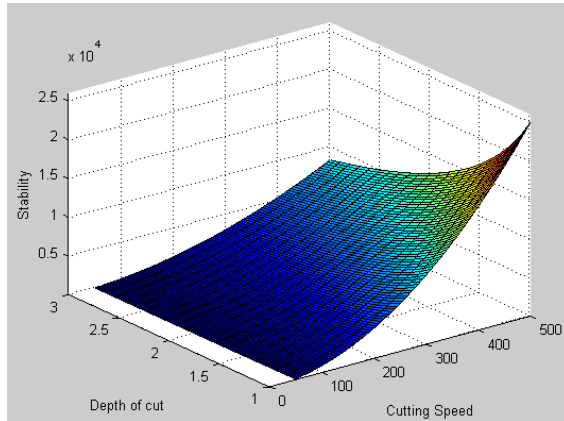
(d)



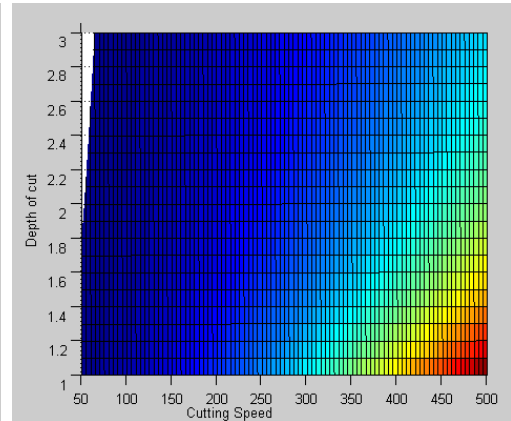
(e)



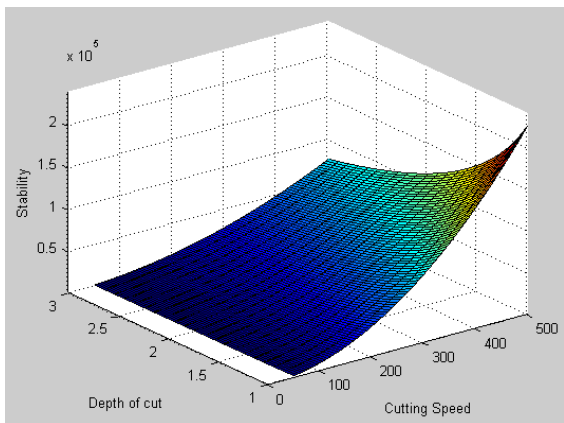
(f)



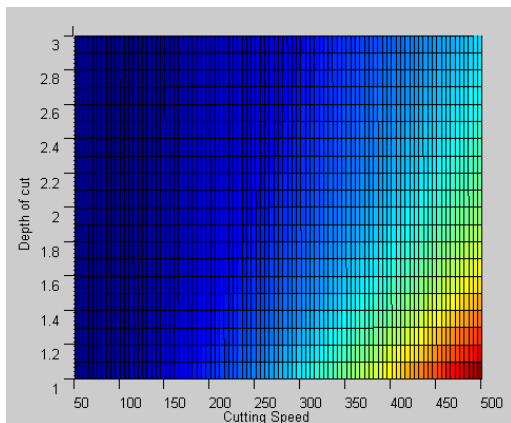
(g)



(h)



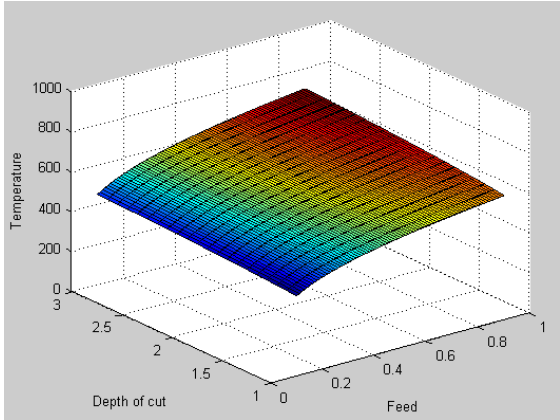
(i)



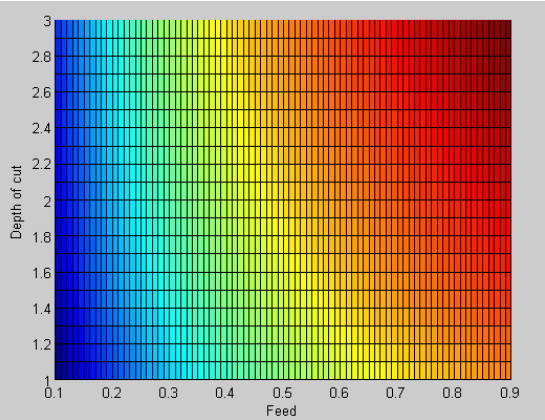
(j)

Figure 2.4 Effects of cutting speed, depth of cut and feed rate on stability (Constraints 7 and 15)

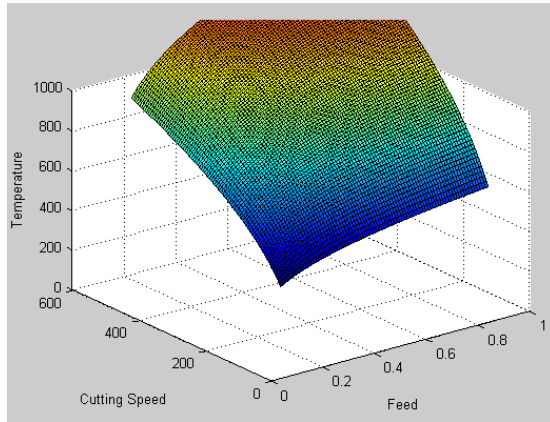
In Figure 2.5, the effects of feed rate, depth of cut and cutting speed on chip-tool interface temperature are presented. Since the effect of three decision variables on temperature cannot be visualized in one plot, the same approach with power and stable region analysis is used. In parts (a) – (b), the effects of depth of cut and feed rate are explored by fixing the cutting speed to its lower limit. Analysis is done for the upper limit, but feasible region cannot be found. In parts (c) – (d) and (e) – (f), the effects of cutting speed and feed rate are analyzed by fixing the depth of cut to its lower limit and upper limit respectively. In parts (g) – (h) and (i) – (j), the effects of depth of cut and cutting speed are searched by fixing the feed rate to its lower limit and upper limit respectively.



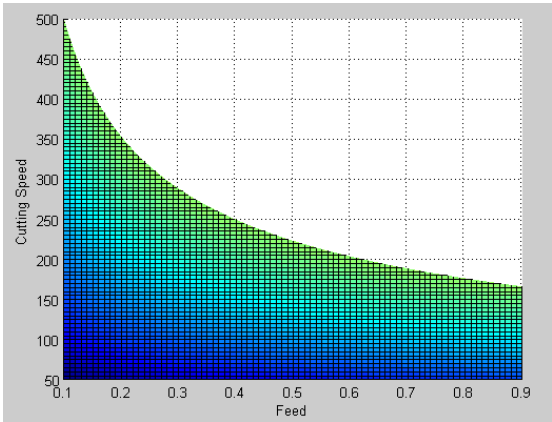
(a)



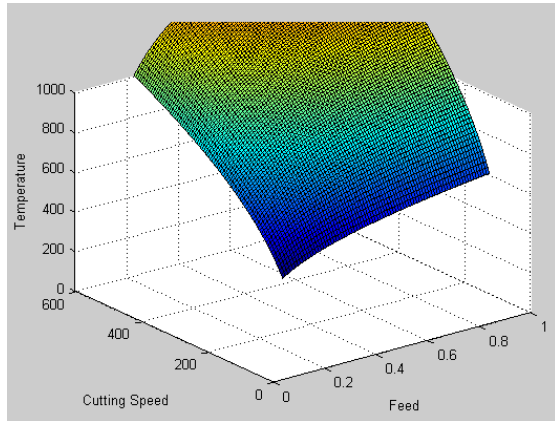
(b)



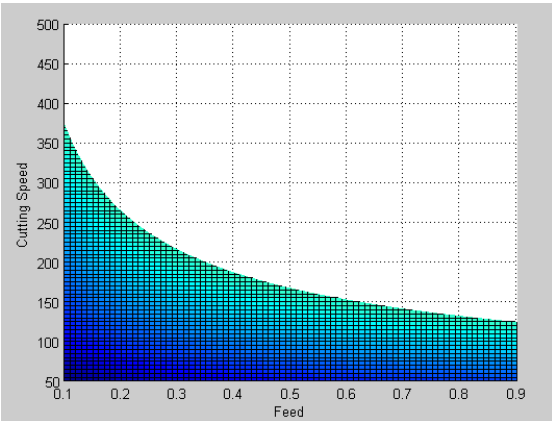
(c)



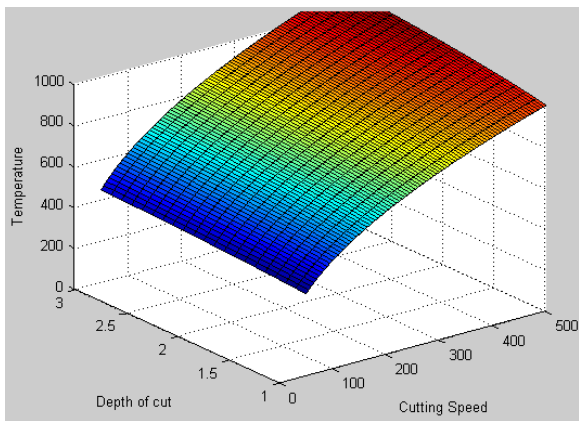
(d)



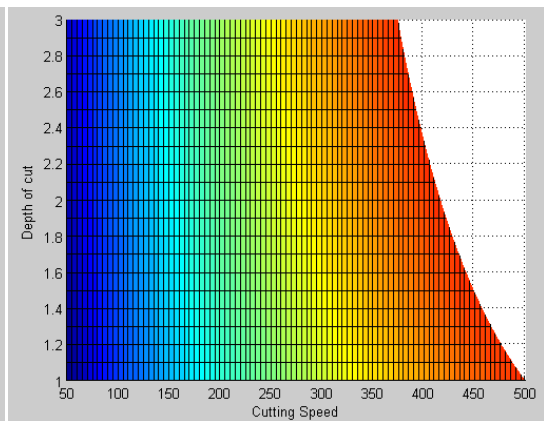
(e)



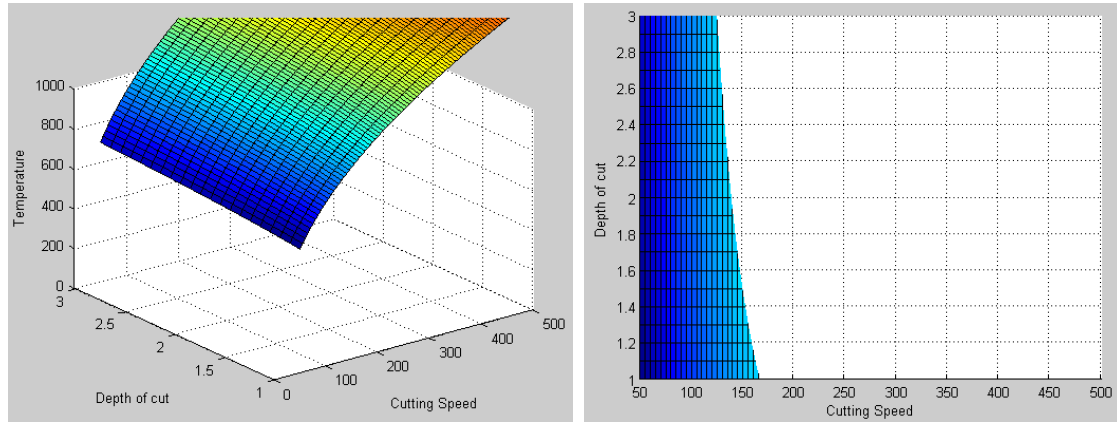
(f)



(g)



(h)



(i)

(j)

Figure 2.5 Effects of cutting speed, depth of cut and feed rate on chip – tool interface temperature (Constraints 8 and 16)

Due to the analysis, the most effective variable on chip – tool interface temperature is cutting speed. While all feed rate and depth of cut values are feasible for lower limit of cutting speed, feasible region cannot be found for the upper limit of cutting speed. It is also revealed that the effect of feed rate on temperature is more than the depth of cut. In order to reduce the temperature on chip – tool interface, cutting speed, feed rate, and depth of cut should also be decreased. It is revealed from these analyses that the most restrictive constraint is stable region constraint. Besides, power constraint is never terminated within the given range. The effects of decision variables change with respect to the constraint type.

#### 2.4.2 Parameter Analysis of Particle Swarm Optimization

Fine-tuning of algorithm parameter is an important task since the parameters affect the convergence of algorithm. The inertia weight adjusts the trade-off between the local and global exploration capability of the swarm. Large inertia weight is used to search wide areas while small inertia weight is used to search narrow areas. It is beneficial to select a

large inertia weight at the beginning of the algorithm in order to scatter particles in the feasible region. As the number of iteration increases, the inertia weight should be reduced to focus the search on a narrow area around the global best particle. Thus, inertia weight is selected as 0.99 initially. Then, it is gradually declined towards 0.05 for detailed search. The acceleration parameters  $c_1$  and  $c_2$  determine the speed of convergence. Kennedy (1998) proposed  $c_1 = c_2 = 2$  as default values. For  $c_1 = c_2 = 2$  and  $w = 0.99 - 0.05$  values, the impact of swarm size and iteration number for termination is investigated. The result obtained from the analysis is given in Table 2.2. Due to the results, the minimum unit cost obtained in this study is \$2.2938 and the result is achieved by most of the parameter sets. However, minimum cost with minimum CPU time is obtained with swarm size of 100 and iteration number of 500. Thus, swarm size and terminating iteration number for PSO is selected as 100 and 500 respectively. After determining the swarm size and termination criteria, the effect of change in acceleration parameters are investigated. In Table 2.3, the result of acceleration parameter is shown. According to the results, the values proposed by Kennedy (1998) are the best values for this optimization problem. Hence, acceleration coefficients are fixed to the value of 2, interval of inertia weight is determined as 0.99 – 0.05, population size is set to 100 and the algorithm is terminated after 500 iterations.

Table 2.2 Swarm size and iteration number analysis for PSO

Swarm size	Iteration #	CPU time (sec)	UC (\$)
100	250	25.298	2.2988
100	500	47.343	2.2938
100	1000	90.643	2.2938
200	250	40.057	2.2940
200	500	73.725	2.2938
200	1000	151.851	2.2938
300	250	53.267	2.2939
300	500	98.866	2.2940
300	1000	200.671	2.2938

Table 2.3 Acceleration parameter analysis for PSO

$c_1$	$c_2$	CPU Time (sec)	UC (\$)
0.5	2	49.091	2.3154
1	2	53.841	2.2941
1.5	2	51.887	2.2940
2	2	47.343	2.2938
2	1.5	50.322	2.2939
2	1	49.874	2.2938
2	0.5	47.702	2.2938
1	1	47.415	2.2938

### 2.4.3 Performance Evaluation of Particle Swarm Optimization

Macro-scale turning operation is one of the most frequently used operation type in machining processes. The model formulated by Chen and Tsai (1998) is solved by many researchers using different heuristic methods for the same parameter set. Table 2.4 summarizes the obtained results in the previous studies.

Table 2.4 Unit production cost values obtained in the literature

Study	Method	<i>UC</i>
Chen and Tsai (1996)	SA / HJPS	\$ 2.2959
Onwubolu, Kumalo (2001)	Genetic Algorithm	\$ 1.7610
Chen and Chen (2003)	FEGA	\$ 2.3065
Viyajakumar (2003)	ACO	\$ 1.6262
Chen (2004)	SS	\$ 2.0667
Wang (2007)	Correction to Viyajakumar	\$ 2.5429
Yıldız (2009)	HIHC	\$ 2.0468
Costa et al. (2011)	HPSO	\$ 1.9591

Chen and Tsai (1996) used SA / HJPS method. All of the constraints given in mathematical modeling section are considered in the constrained nonlinear model. The obtained unit production cost in this study is \$2.2959. Onwubolu and Kumalo (2001) introduced a new optimization technique based on GA. Although all constraints are taken into account in this study, number of rough cuts is not limited to an integer. Thus, unit production cost of \$1.761 is not a valid result. Chen and Chen (2003) revealed the mistake in Onwubolu and Kumalo (2001) and mentioned that the solution is infeasible due to the constraint violation. In addition, they applied FEGA method to solve the same model and reached the result of \$2.3065 per unit. Viyajakumar (2003) proposed ACO to

obtain near optimal values of multi-pass conventional turning machine parameters. In this study, achieved parameters are not provided. They stated that unit production cost per piece is \$1.6262. Chen (2004) proposed SS method in order to solve the benchmark problem. Constraints (1) – (21) are used in this study. The best result obtained in this study is \$2.0667. However, the values of the decision variables are not provided. Wang (2007) analyzed the cutting parameters that are found in Vijayakumar (2003) and stated that unit production cost cannot be gained with the provided decision variable values. With respect to Wang (2007), the minimum possible unit production cost is \$1.968 for one rough cut and \$2.5429 for two rough cuts. Yıldız (2009) solved multi-pass conventional turning optimization model in order to evaluate the performance of HIHC method. The whole constraint set given in mathematical modeling section is considered in the model. According to the gained result, minimum unit production cost is \$2.0468. The machining parameters are not provided in the study. Costa et al. (2011) used HPSO method and provided different benchmark models in order to compare the efficiency of HPSO with respect to other proposed studies. For different comparison models, various results are obtained. It is mentioned in the study that minimum unit productions cost obtained by HPSO is \$1.9591, but cutting parameters are not provided.

Mathematical model of the first case is solved for two different alternatives using PSO. The assumption in the first alternative is that, machining operation is done with a single rough cut and a single finish cut. Under this assumption, objective function value and its cutting conditions are given in Table 2.5.

Table 2.5 Obtained cutting parameters and *UC* for a single rough cut and a single finish cut

$d_r$	$d_s$	$V_r$	$V_s$	$f_r$	$f_s$	<i>UC</i> (\$)
3	3	109.6631	169.9785	0.5655	0.2262	2.0351

The assumption in the second alternative is that, machining is done with two rough cuts and a single finish cut. With respect to this assumption, unit production cost increases since machining time increases. Unit production cost and cutting parameters obtained by PSO algorithm are given in Table 2.6. Figure 2.6 shows the reduction of unit cost by the increase of iteration number using PSO algorithm. It is revealed from the figure that, objective function value decreases sharply at the beginning of algorithm. As the number of iteration increases, the algorithm focuses to a narrower region and searches for better solutions.

Table 2.6 Obtained cutting parameters and  $UC$  for two rough cuts and a single finish cut

$d_r$	$d_s$	$V_r$	$V_s$	$f_r$	$f_s$	$UC$ (\$)
2.0788	1.8424	98.4760	163.8091	0.9	0.3098	2.2938

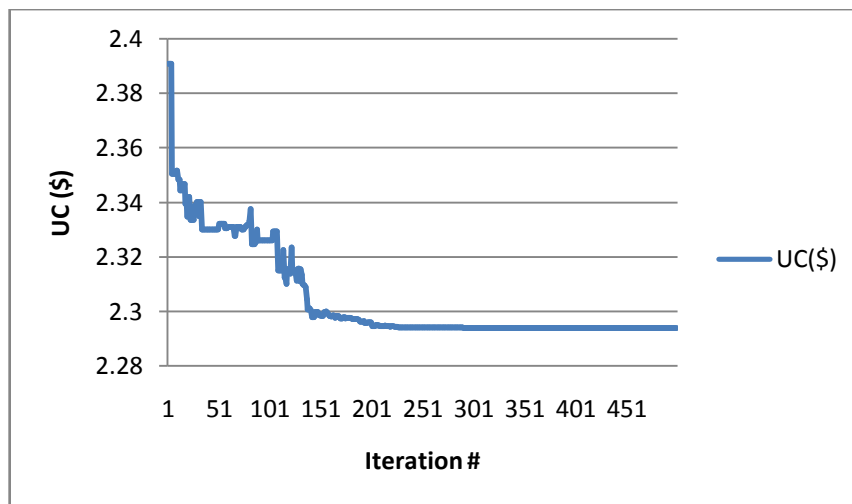


Figure 2.6 Unit production cost reduction with respect to the iteration number

A numerical example is also performed for the second case where the diameter is updated after each machining pass. Also for the second case, single rough cut and single

finish cut and multiple rough cuts and a single finish cut strategies are evaluated. In Table 2.7, the unit production cost and cutting parameters obtained using PSO for a single rough cut and a single finish cut are given.

Table 2.7 Obtained cutting parameters and  $UC$  for a single rough cut and a single finish cut

$d_r$	$d_s$	$V_r$	$V_s$	$f_r$	$f_s$	$UC$ (\$)
3	3	109.6631	169.9784	0.5655	0.2262	1.9499

When the result of case two alternative one is analyzed, it is clear that optimal cutting parameters are not changed when the reduction of workpiece diameter is taken into consideration. However, objective function value is decreased from \$2.0351 to \$1.9499 since the machining time decreases. In Table 2.8, the unit production cost and cutting parameters obtained using PSO for multiple rough cut and a single finish cut are given.

Table 2.8 Obtained cutting parameters and  $UC$  for two rough cuts and single finish cut

$d_r$	$d_s$	$V_r$	$V_s$	$f_r$	$f_s$	$UC$ (\$)
2.0788	1.8424	98.4761	163.8093	0.9	0.3098	2.1788

Due to the obtained results, consideration of workpiece diameter reduction does not affect the optimal cutting parameters, but reduces unit production cost. When the obtained results are compared with the previous studies, it can be stated that PSO achieves acceptable solutions. It is not possible to state whether proposed PSO algorithm significantly outperforms the earlier studies, since number of pass and optimal cutting conditions are not provided in the previous studies.

In order to evaluate the performance of PSO compared to conventional nonlinear optimization techniques, same problem is solved using Matlab Optimization Toolbox

(See Appendix for Matlab optimization toolbox algorithms). An initial feasible solution should be provided to the algorithm in order to solve the optimization problem. Different initial conditions may yield different solutions or in some cases no solutions were obtained. In Table 2.9, initial parameters given to the toolbox and obtained unit production cost values are shown. In addition to the unit production costs, CPU time for solution is also provided in the table.

Table 2.9 Obtained unit costs and CPU times for different initial solutions

$d_s$	$V_r$	$V_s$	$f_r$	$f_s$	$UC$ (\$)	CPU (sec)
3	98	163	0.85	0.3	2.2953	1.827
1	50	50	0.1	0.1	2.2967	1.747
2.99	499	499	0.89	0.89	No answer	-
2	250	250	0.6	0.6	No answer	-
3	100	100	0.5	0.5	2.2966	1.825

It is revealed from Table 2.9 that toolbox may not find any solution although a feasible initial solution is provided. Thus, it is useful to start with an initial point near the results obtained from PSO to see whether an improvement is obtained or not. The solutions obtained by Matlab Optimization Toolbox did not show any significant improvements.

## 2.5 Conclusion

In this chapter, a literature survey on the problem of multi-pass turning operation is given. It is shown that multi pass turning operation forms a nonlinear constrained optimization problem. Constraints of the model are analyzed in order to investigate the effects of decision variables on the constraints. Besides, parameters of PSO algorithm are determined. The optimization problem is solved by using PSO algorithm and the

results obtained are compared with those reported in the literature. It is revealed from the numerical examples that a single rough cut and a single finish cut is cost effective for a given total depth of cut in the numerical example. However, if the total depth of cut increases the results may change. Besides, consideration of workpiece diameter reduction provides in the objective function helped obtaining improved results.

The performance of PSO is found to be satisfactory although better results are reported in the literature. However, the details of some those studies were not given in detail which makes it difficult to compare. It must be noted that some improvements in objective function can be obtained by allowing process variables to have many digit points but it does not make sense in terms of the physics of the process.

# Chapter 3

## Experimental Investigation of Micro Milling

The output quality of fabricated micro product fundamentally depends on the strategies and parameters used in micro milling operation. For manufacturing high quality macro-scale products, computer aided design programs (CAD) and computer aided manufacturing programs (CAM) are available to determine near optimal parameters and cutting strategies for conventional milling operations. However, these programs are inadequate to produce good cutting strategies and parameters for micro milling operations since the relation between output quality and micro cutting parameters is still an unperceived issue due to the lack of studies on this subject. Besides, there are no reliable mathematical models which optimize manufacturing cost, tool life and surface roughness of micro products. Thus, experimental design approach is an effective method

to reveal the relation between the output quality and micro machining parameters and strategies.

This chapter mainly presents the procedure that followed to find the most appropriate process parameters of micro milling. Firstly, brief information about micro machining is presented. Secondly, previous experimental works in micro-milling are introduced. Then, frequently used experimental design methods are summarized. Finally, experimental investigation of micro-milling is performed.

### **3.1 Micro Machining**

Miniaturization has become more important in various industries to improve the life quality. Micro products are frequently used in medical, consumer technology and electronics industries. Dimensional accuracy and tolerance of the products is very important. In order to fabricate micro products with tight tolerances, various micro machining process types are provided. Mechanical micro machining, electrical discharge machining and grinding, and lithography are the samples of micro machining. Mechanical micro machining is one of the most preferable methods since it requires low setup and tool costs. Besides, it is possible to fabricate various materials with complex three dimensional geometries by this method.

While mechanical micromachining techniques provide advantages, there are challenges. One of the challenges is repeatability of process because of working material's microstructure, cutting tool geometry and its structure. In micromachining, working material can be assumed as non-homogenous because the chip size and grain size are similar. Another challenge in micromachining is the tool cutting edge radius. The cutting edge radius of micro tools is not sharp because of the limitations in micro tool manufacturing. The edge radius of cutting tool affects minimum chip thickness, chip

formation and cutting forces. If the edge radius is larger than the uncut chip thickness, tool cannot remove the useless part and elastic deformation occurs (a). Material recovers after the tool passed. If the edge radius of cutting tool is close to the uncut chip thickness, the tool both cuts and deforms the working part but the uncut part recovers after the tool past (b). In order to remove the useless part completely, the uncut chip thickness must be larger than the tool cutting edge radius (c). (Chae et al., 2006) In Figure 3.1, the effect of minimum chip thickness is given.

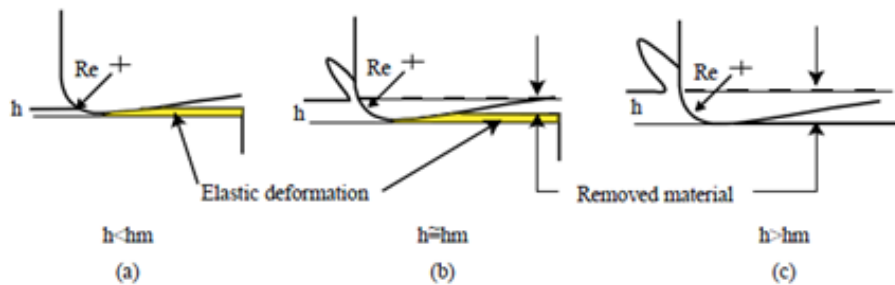


Figure 3.1 The effect of minimum chip thickness ( $R_e$  denotes the cutting edge radius,  $h_m$  denotes minimum chip thickness and  $h$  denotes undeformed chip thickness) (Chae et al., 2006)

When the tool edge radius increases, cutting forces also increase due to negative rake angle effect. As the forces increase, tool deflection and vibration occurs on the tool. Deflection and vibrations causes quality problems on fabricated products such as burr formation, high surface roughness and may cause tool breakage.

In mechanical micromachining, it is hard to detect tool defects during the manufacturing process. One of the reasons is that cutting edges are very small and it is not possible to detect damages by eyes. Another reason is that cutting forces may not be very reliable for the detection of tool wear. Since the cutting forces are small in micromachining, any noise signal may mislead us. Moreover, measurement of cutting forces at high rotational speeds may interfere with the dynamics of dynamometer and induce misinterpretations.

Tool run-out and shank length are important factors in micro machining. Tool run-out induces varying chip loads on cutting tool edges, so teeth may be broken during the operation or may not meet tight dimension tolerances. Tool shank length is important in terms of surface quality. The length should be selected cautiously in order to fabricate high quality products.

### **3.2 Literature Review**

The number of studies on micro milling is limited compared to macro scale milling operations in the literature since micro machining is a new area relative to the conventional machining. Although micro and conventional milling have similarities, micro milling operations differ from conventional milling operations in terms of physical structures of cutting tools, workpiece and dimensions of geometries to be cut. In order to clearly understand the structure of micro machining operations, various experimental studies are done by researchers.

An experimental investigation is done by Biermann et al. (2011) to analyze the machinability of hardened carbide-rich cold-work tool steel with coated carbide cutting tools. Three different types of coated tools are used in the experiments to find economical cutting parameter set by varying axial depth of cut, radial depth of cut and feed per tooth parameters with minimum quantity lubrication. The results are analyzed with respect to cutting forces, tool wear, surface quality, material removal rate and entire chip volume. It is revealed from the study that design of tool is important, low tool length and aspect ratio reduces tool deflections and vibrations, so increases surface quality. Filiz et al. (2007) conducted an experimental study on slot milling to investigate micro-machinability of pure copper 101 using tungsten carbide cutting tool. They monitored cutting forces, surface roughness, tool wear and burr formation under various cutting speeds and feed rates to analyze the effects of parameters on the control factors.

They realized that minimum chip thickness causes irregular variations in cutting force at low feed rates and similar cutting force structure to conventional milling at high feed rates. Tool wear formation increases as the feed rate and speed decreased and cutting forces increase as the tool wear increases. Lee et al. (2004) conducted an experimental study of slot milling for aluminium 6061 in order to find the parameters that are effective on surface roughness. The factors analyzed in this study are chip load, cutting speed and depth of cut. According to the study, chip load is the most dominant factor and interaction of cutting speed and chip load has a considerable effect on surface roughness. Tool run out also affects surface quality of machining. Natarajan et al. (2011) conducted a central composite experimental design (CCD) for aluminium workpieces that focused on the optimization of micro end milling process using response surface methodology to achieve maximum material removal rate (MRR) with minimum surface roughness. The parameters considered in the experimental design are spindle speed, feed rate and depth of cut. A model is developed to optimize machining parameters. Optimized parameters are experimented for confirmation and achieved convincing results. The result of study reveals that low feed rate yields better surface finish and spindle speed has not a dominant effect on surface roughness. Rahman et al. (2001) conducted an experimental study for micro milling of pure copper to investigate tool life. The parameters considered in the course of experiments are cutting speed, depth of cut, feed rate and tool helix angle. According to the results, formation of chips affects tool wear, tool wear and cutting force increases by the increase of machining time, increase of depth of cut increases tool life, tool life decreases as the cutting speed increases and helix angle has an important role on tool life. Uhlmann et al. (2005) studied the micro machinability of tungsten copper sintered composite materials. Coated and uncoated cemented carbide tools are used for cutting various characteristics' of tungsten copper sintered material in the experimental work. The effects of cutting speed and workpiece hardness on surface roughness, effect of feed per tooth on tool wear and effects of cutting speed and feed per tooth on cutting forces are investigated. They

revealed that increase of feed per tooth reduces dimensional inaccuracy, increases abrasive wear which leads to cutting edge roundness and increase of plastic deformation of material surface. In order to attain good surface quality, cutting speed is increased within the experiment parameter range. Vázquez et al. (2010) performed an experimental analysis to investigate surface finishing, shape and dimensional features of micro slot milling using conventional milling machine for aluminum and copper. Varying parameters in the experiments are spindle speed, depth of cut per pass, depth of cut, feed per tooth and coolant application. It can be concluded that quality of micro-channels in aluminum is better than copper in conventional milling machine, average micro-channel width in aluminum can be controlled in higher feed rates, coolant usage provides better surface quality and accurate channel dimensions and micro channels in copper are not in the required dimensions. Wang et al. (2005) studied the influence of cutting parameters on surface roughness. Brass is used for machining. The parameters studied in the experimental study are spindle speed, feed rate, depth of cut and tool diameter. They used analysis of variance (ANOVA) and response surface methodology (RSM) to develop optimization model and figure out the effects of main parameters and their interactions on surface roughness. Based on the results, the increase of spindle speed and tool diameter increases surface roughness, feed rate is important when the other of parameters are constant, cutter stiffness is the most dominant factor in micro milling. The best surface quality is obtained when the vibration is decreased and tool stiffness increased. Weinert and Petzoldt (2008) studied the machinability of NiTi using solid TiAlN-coated carbide end mill tool. In their study, slot milling experiments are conducted with  $\varnothing$  0.4 mm tool under dry conditions and minimum quantity lubrication. The evaluation criteria are tool wear, machining quality and cutting forces. The results in which minimum quantity lubrication used provided better surface quality and longer tool life. Besides, chip formation has an important effect on the extension of tool life and acquisition of better surface quality. Cutting with high feed rates and high width of cut provide better chip formation. Thepsonthi and Özel (2012) conducted research to

explore the performance of micro end milling of Ti-6Al-4V and machining parameters to improve surface quality and burr formation. The research consists of three main steps which are experimental step, modeling step and optimization step. Physical experiments are done at the first step. A predictive model is constructed using the results of experiments by response surface methodology (RSM) at the second step. Finally, the best parameters that satisfy multi-criteria quality requirements are found by multi objective particle swarm optimization (MOPSO). The parameters considered in the course of experiments are spindle speed, feed per tooth and axial depth of cut. With respect to the results of the research, it is revealed that axial depth of cut is the dominant factor for top burr formation, feed per tooth is the dominant factor for surface roughness and obtaining best surface roughness with minimum top burr formation is not possible. Li et al. (2008) performed an experimental study to figure out the influence of cutting parameters on the wear behavior of square micro end mills. Experiments are done based on CCD and ANOVA is used for the analysis of results. It is concluded that feed per tooth has a greater effect on the tool wear than cutting speed and depth of cut and there is an optimal feed per tooth value that minimizes tool wear when the cutting speed and depth of cut values are fixed. Aramcharoen et al. (2008) investigated the degradation of micro end mill while machining 45 HRC hardened mould and die tool steel. Slot milling experiment with a single parameter set under dry conditions is done in the study and tool diameter degradation is observed. It is revealed from the research that tool wear differs at each tooth, adhered material increases cutting forces and causes tool breakage and tool wear rapidly increases while milling hardened steel.

### **3.3 Design of Experiment (DOE) Methods**

There are various types of DOE methods. One of these methods is one-factor-at-a-time (OFAT) method. In this approach, experimenter selects a random starting point for each factor. Then, experimenter changes the level of only one factor while holding the other

factors constant and observes the changes in the response variables. Although OFAT is beneficial for observing the effect of single factors on response, it has two major disadvantages. First, it requires high number of experiments and second it cannot reveal the interactions between the parameters since it is not possible to change more than one variable at the same time and observe the response of the model (Frey et al., 2003, Montgomery, 2004). Taguchi approach is also commonly used in experimental design. The aim in this strategy is selecting the best combination of experiment parameters in order to construct a robust design, which means less sensitive to uncontrollable or noise parameters (Potvin and Roff, 1993, Ross, 1989). Taguchi method provides standard array tables for different number and levels of parameters. Prior to the selection of appropriate experimental design table, design parameters and minimum/maximum limits of the parameter levels need to be decided. If the gap between maximum and minimum values of one parameter is large, it is beneficial to select high number of levels. Otherwise, it is sufficient to select small number of levels in experimental design. Since the number of level affects required experiment number, decision of parameter levels is vital. After the selection of appropriate design table, experiments can be done and analyzed by using analysis tools.

An advantage of Taguchi method for experimental design is that it is easy to construct design table with respect to other design methods if the experiment parameters and its levels are chosen. Besides, this method provides a remarkable reduction in the required number of experiments, which means a great save in tooling costs and time. Besides the advantages of using Taguchi method, there are major disadvantages. One of the disadvantages of using Taguchi method is that it is difficult to reveal the main effects of parameters and interaction effects among all parameters in the design since the design does not include all possible combinations of parameters. Usage of Taguchi method is not efficient in dynamically changing process since it is not possible to change the design in the course of experiments according to the results and may lead to sub-optimal

solutions because of reduced number of experiments. Taguchi method is based on subjective knowledge of process in multi-objective optimization problems as shown by Phadke (1989). Besides, use of quadratic loss function may not be suitable in complex cutting processes. (Unal and Dean, 1991, Mukherjee and Ray, 2006)

Factorial experimental design is an alternative experimental design strategy. This method is efficient if the required design has two or more than two factors. In this strategy, all possible combinations of levels of factors are analyzed. Two major effects of factors can be analyzed by using this method. Main effect of a factor can be analyzed by changing only levels of one factor. When the level of same factors is changed, the variance in average response indicates the main effect of the factor. However, the variation in response between different levels of one factor may change at all levels of the other factors. If such a case occurs, it can be concluded that there is an interaction between factors.

Factorial designs have advantages in experimental studies. This strategy is more efficient than OFAT. The method provides more information according to OFAT although both methods require same number of experimental works. However, this method also requires high number of experiments. Thus, instead of using full factorial design, it is more convenient to use fractional factorial design or central composite design (CCD), which is a design method for fitting response surface methodology (RSM), to reduce the number of experiments.

The RSM is a dynamic tool of DOE which is used to model and analyze problems by using mathematical and statistical techniques. The aim in this methodology is to optimize the responses by analyzing the influential parameters on desired responses in the design. The relationship between responses and independent variables are mostly unknown in RSM problems. Hence, it is important to find an approximate relationship

between design parameters and responses. If the response is modeled as linear, the approximation will be first order model. However, first order model may not be sufficient to approximate the true relationship between parameters and responses. In this case, second order model can be used. After an approximate model is generated, several methods such as steepest ascent, hill climbing, stationary point approach and canonical analysis are used to solve the problem. In order to find a suitable approximation, response surface design parameters should be selected cautiously. Orthogonal first order design is used for fitting the first order model. In this design, parameters are designed with two levels ( $2^k$ ). CCD is used to construct experimental design for second order model. In general, CCD design has  $2^k$  factorial with  $n_f$  points, which are for fitting first order model,  $2k$  axial points, which are for adding quadratic terms to the first order model and  $n_c$  center points, which are for stabilizing the variance of response prediction. In CCD design, all factors have five levels. In Figure 3.2, schematic of CCD for 3 factors is given.

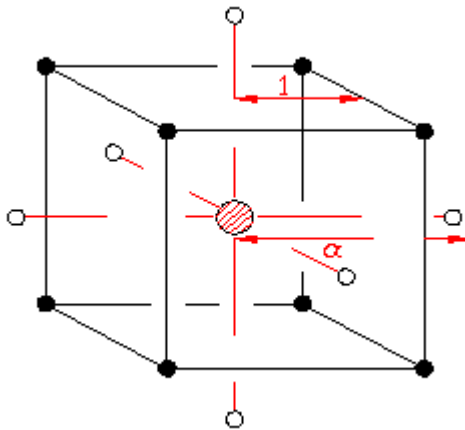


Figure 3.2 CCD for three factors

The distance ( $\alpha$ ) of axial points from the center and number of center points ( $n_c$ ) are given as parameter in CCD. Rotatability is an important issue in CCD in order to provide good predictions. Response surface design is rotatable if the variance of response is same at all design points which have the same the distance from the center. In order to provide rotatability, distance of axial points from the center should be selected as  $\alpha = (n_f)^{1/4}$ . For example, if we need to design a rotatable experiment with 3 parameters using CCD method,  $\alpha$  value should be selected as  $\alpha = (2^3)^{1/4} = 1.68179$ . In general  $n_c$  is selected three to five. As the number of center point increases, the model fits better. (Montgomery, 2004)

In order to fit a quadratic model using the generated experimental design, regression method can be used. Regression characterizes the relationship between dependent and independent variables. Statistical computer software is able to fit a regression model with respect to the provided data. Minitab, a statistical package, fits a regression model consists of linear, interaction and square effects. The software also provides information about the goodness of fit. Hence, the reliability of model is determined.

### **3.4 Experimental Investigation**

Although the physical effects of micro milling differ from conventional, influential controllable factors in micro milling operations are the same as in conventional milling operations. Thus, the same parameters can be used for the experiments in micro milling operations. The testing factors differ according to the required cutting geometry. In experimental design, slot milling and pocket milling methods, which are mostly used in micro milling, are used. While tool entrance into the workpiece strategy, cutting speed ( $V$ ), feed per tooth ( $f_z$ ), axial depth of cut ( $a_p$ ) and tool diameter ( $\phi$ ) are tested parameters for cutting a linear channel, cutting strategy,  $V$ ,  $f_z$ ,  $a_p$ , radial depth of cut

$(a_e)$  and  $\emptyset$  parameters are tested for pocket milling. The controllable factors investigated in milling experiments are summarized in Table 3.1.

Table 3.1 Controllable factors in experimental studies

Controllable Factors	Slot Milling	Pocket Milling
Cutting strategy		✓
Tool entrance into the workpiece	✓	
Cutting speed ( $V$ )	✓	✓
Feed per tooth ( $f_z$ )	✓	✓
Axial depth of cut ( $a_p$ )	✓	✓
Radial depth of cut ( $a_e$ )		✓
Tool diameter ( $\emptyset$ )	✓	✓

After the determination of controllable factors in micro milling operations, a sequence of experimental designs are generated and performed. In the experiments, NS Tools are used for milling stainless steel 304 work-pieces, which is hard material for processing. Since the tools and workpiece materials are expensive, experiments are done in two stages in order to decrease experimentation costs. In the first part, influential factors in slot milling are studied. Afterwards, pocket milling experiments are done by using the obtained results from the first part.

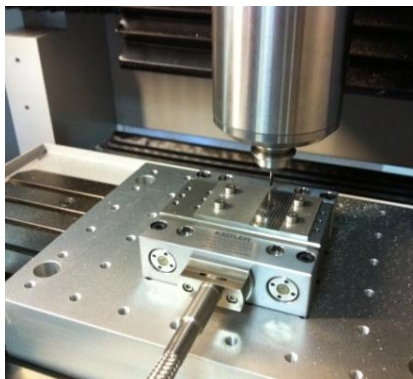
### 3.4.1 Experimental Setup

The micro milling experiments were done on a hybrid micro machining center, Micro Tools DT-110, which has the capabilities of micro milling, micro turning, micro EDM, micro wire EDM and micro wire EDG (See Figure 3.3a). High speed spindle (Fischer Precise SC 3062, 1.3 kW maximum power, 25 Ncm maximum torque) with speed

between 10000 – 60000 rpm was used in the experiments. The position accuracy of machining center on the workpiece is  $\pm 1 \mu\text{m} / 100 \text{mm}$ . Collet type precise tool holders are used in the experiments. Since the machining center does not contain touch probe for workpiece coordinate setting, cutting force monitoring method is used to set the workpiece coordinates. Cutting force data are also used for tool life determination experiments. Kistler MiniDyn 9256C1 is used for cutting force monitoring. (See Figure 3.3b) The dynamometer consists of four 3-component force sensors and can measure forces up to 250 N. Dry cutting method is used in the experiments. NI PXI-7854R data acquisition card is used in order to transfer the data to the PC. (See Figure 3.3c)



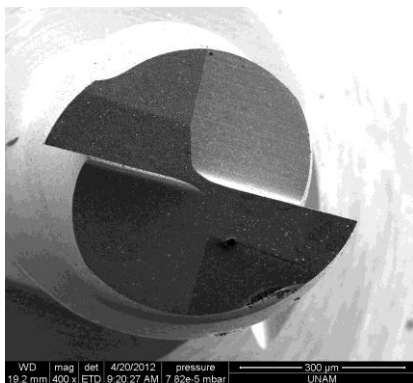
(a)



(b)



(c)



(d)

Figure 3.3 (a) Micro Tools DT-110 (b) Kistler 9256 C1 dynamometer (c) NI PXI-7854R data acquisition card and PC (d) SEM image of micro cutting tool

In order to gather force data, dynamometer is fixed on an aluminum plate and the workpiece is fixed on the dynamometer. Four holes are drilled for fixing the workpiece on the dynamometer and the piece is screwed on the dynamometer. After fixing the workpiece on the machining center, the surfaces of the workpiece is face milled to provide a good flatness. 100  $\mu\text{m}$   $a_p$  face milling is done by using  $\varnothing$  2 mm end mill to flatten the surface of the part according to the machining center. Observation of channels in terms of dimension measurement, burr formation and surface quality are done by Vision Engineering Hawk non-contact measuring microscope, Keyence VHX 1000 digital microscope and Zygo NewView 7200 white light interferometer.

NS cutting tools are used in the experiments. The diameter of cutting tools used in the experiments are  $\varnothing$  0.4 and  $\varnothing$  0.8 mm. Both tools have 2 cutting edges,  $30^\circ$  helix angle and 55 HRC surface hardness. The diameters of cutting tools are smaller than the given nominal diameter values since run-out issue is considered by tool manufacturers. Scanning Electron Microscope (SEM) image of cutting tool is given in Figure 3.3d.

The workpiece material is stainless steel 304 with the dimensions of 305 $\times$ 305 $\times$ 3 mm (L $\times$ W $\times$ H). However, the plate is cut into pieces with the dimensions of 37 $\times$ 55 $\times$ 3 to prevent vibration on the workpiece and simplify the experiment processes. In order to minimize the effect of workpiece material in micro milling processes, the same plate is used in all experiments. Tool shank length is fixed around  $\pm$  50  $\mu\text{m}$  while changing the cutting tools during the experiments. All experiments are conducted under dry conditions.

### 3.4.2 Slot Milling Experiments

Experimental works are started with slot milling for  $\varnothing 0.8$  and  $\varnothing 0.4$  mm cutting tools since the cutting geometry is simpler. In the first step, the effect of tool entrance strategy into the workpiece is investigated. Two types of entrance strategy are tested. First strategy is plunging the cutting tool out of the workpiece and giving the feed in the required direction. (See Figure 3.4a – b) The second strategy is plunging the cutting tool directly into the workpiece with smaller feed rate and giving the feed in the required direction. (See Figure 3.4c – d)

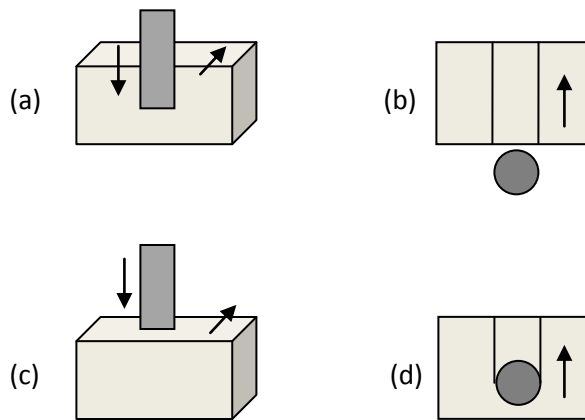


Figure 3.4 Cutting tool is plunged out of the workpiece and feed direction is given in (a) and (b). Cutting tool is plunged into the workpiece with small feed rate and feed direction is given in (c) and (d)

For both strategies, channels with same length and axial depth of cut are cut and tool cutting edges are examined by using microscope. According to the analysis, it is decided that the second tool entrance method is more conservative since hitting impact is decreased by this strategy.

After the decision of tool entrance strategy, channel experiments are done to find the effects of  $V$ ,  $f_z$  and  $a_p$  on tool life. Since the radial depth of cut value is equal to the cutting tool diameter, the effect of  $a_e$  cannot be measured in channel cut experiments. The experiments are done for two different tool diameters  $\emptyset 0.8$  and  $\emptyset 0.4$  mm. First experiment is done for  $\emptyset 0.8$  mm cutting tool. 11 workpieces are used for channel experiments. At each workpiece, 20 slots with 30 mm length are cut. Fresh cutting tool is used for each workpiece. In the course of experiments, cutting forces are gathered. After the channels are cut, they are observed by the microscope and measurement of axial depth of cut and radial depth of cut are done.

Axial depth of cut and width of channel are important factors in micro channel in terms of fluid transportation in various areas, especially biomedical and biochemical devices. Width of channel only depends on the tool wear. As the channels are cut, width of the channels decreases as the diameter of tool. However, axial depth of cut depends on elongation of tool due to heat increase and zero point setting of milling machine. Elongation of tool cannot be controlled in dry cutting method. In order to cut channels with small  $a_p$  tolerances, zero point of the machining center should be set precisely. For cutting tools with large diameters such as  $\emptyset 1.5$  and  $\emptyset 2$  mm, contact of tool edge with workpiece can be visually realized. However, it is not possible for small diameter cutting tools. Thus, dynamometer is used to realize the surface coordinate of workpiece and setting it as the zero point of the machining center. In order to detect the touch point, real time cutting forces are followed while the tool is brought closer to the workpiece. As the real time cutting force reaches 0.1 N, it is assumed that the tool touches to the surface of workpiece and that coordinate is set as the zero point of machining center. After the detection of zero point, the experiments are done. Slot milling experiment parameters for  $\emptyset 0.8$  mm cutting tool are given in Table 3.2.

Table 3.2 Slot milling experiment parameters

<i>Exp #</i>	<i>N (rev/min)</i>	<i>a<sub>p</sub> (μm)</i>	<i>f (μm/tooth)</i>	<i>feed rate (mm/min)</i>
1	24000	80	1.145	55
2	30000	80	1.145	68
3	18000	80	1.145	42
4	36000	80	1.145	82
5	24000	80	1.5	72
6	30000	80	1.5	90
7	24000	80	1.965	94
8	30000	100	1.5	90
9	30000	120	1.5	90
10	24000	80	1.145	55
11	30000	80	1.145	68

Parameters of the experiments are based on the catalogue values of cutting tool. They are determined between  $\pm 30\%$  of catalogue parameters. The effect of spindle speed, depth of cut and feed on tool wear are investigated in the experiments. The  $a_p$  and  $a_e$  measurements of the experiments are given in Table 3.3.

Table 3.3 Measurements of slot milling experiments for  $\varnothing$  0.8 mm cutting tool

<i>Exp #</i>	$a_p$ ( $\mu\text{m}$ )	Max $a_e$ ( $\mu\text{m}$ )	Min $a_e$ ( $\mu\text{m}$ )	1 <sup>st</sup> Channel $a_e$ ( $\mu\text{m}$ )	20 <sup>th</sup> Channel $a_e$ ( $\mu\text{m}$ )
1	89	787	771	786	776
2	87	792	779	790	789
3	88	801	780	801	783
4	83	805	778	802	778
5	89	796	784	796	785
6	93	800	791	800	791
7	91	792	785	785	789
8	103	797	789	796	791
9	125	794	783	790	784
10	90	790	784	790	789
11	85	800	789	798	789

Axial depths of channels are measured by optical microscope. Five measurements are done in each channel and average of the measurements is given in the table. When the actual depths of cuts and required depths of cuts are investigated, it can be seen that they are different. The possible reasons of difference are machine zero point setting problems and elongation of tool due to the heat increase. Since the burrs on both sides of the channel cannot be avoided, measurement of  $a_e$  may mislead the original width. However, it can be revealed from the results that channel width reduces as the diameter of cutting tool reduces due to wear.

Figure 3.5 shows the surface roughness of experiment 2. Due to the obtained results, it can be mentioned that surface quality reduces by the increase of tool wear. However, it is not possible to measure the exact surface quality difference because white light

interferometer measures a small region on the channel and surface roughness may change within the channel due to the burr adhesion on the surface.

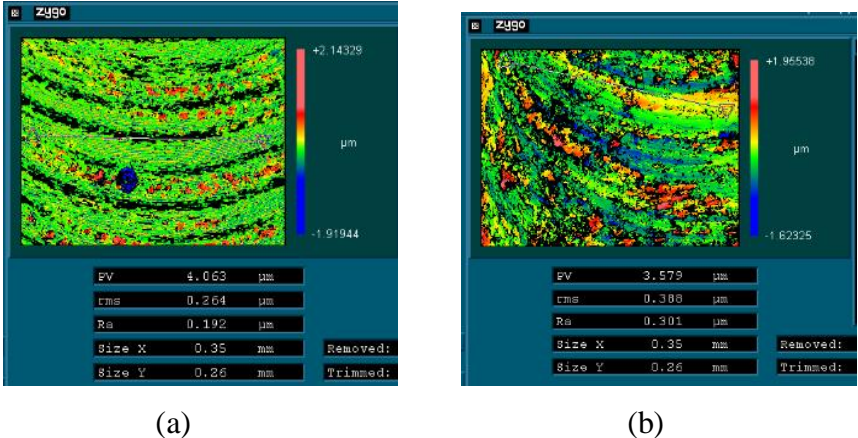
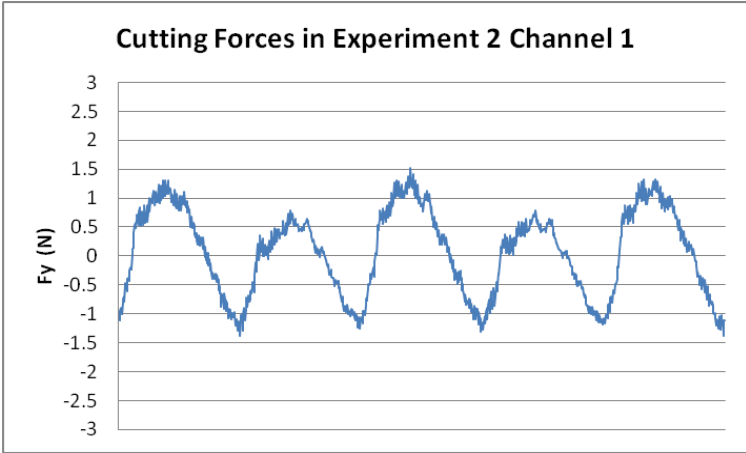
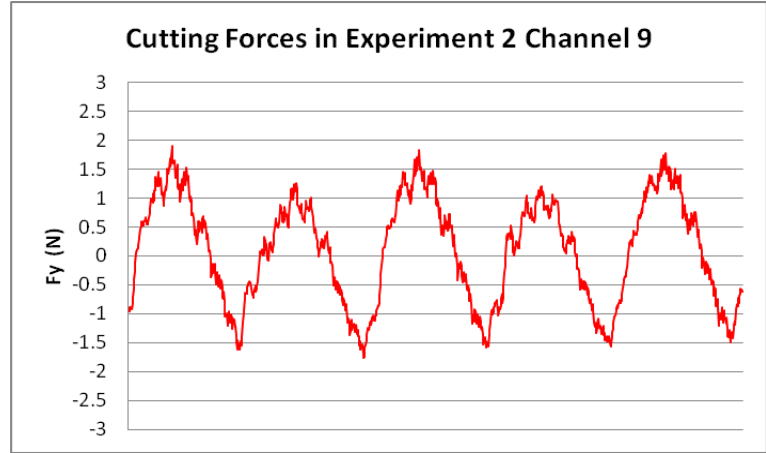


Figure 3.5 Surface roughness measurement of experiment #2: (a) Channel #1 (b) Channel #19

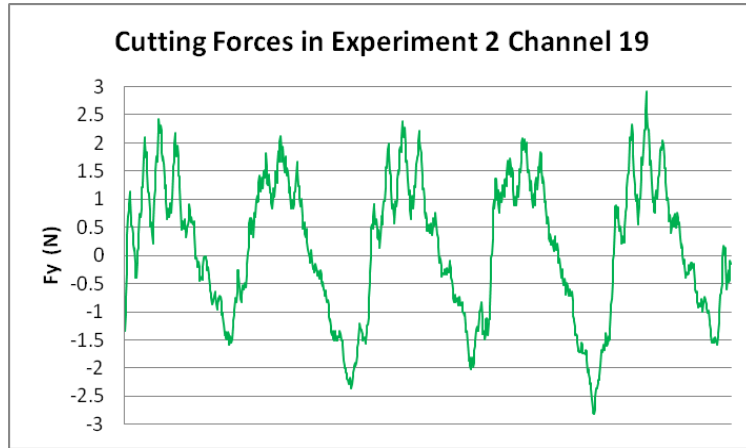
Cutting forces are also analyzed in order to monitor the tool wear. Figure X. shows the cutting forces occurred in y-axis during the machining operation of experiment 2. Tool run out and tool wear on each cutting edges can be realized by monitoring the forces. Cutting forces increase as the number of cut channels increase. The increase in cutting forces can be clearly seen in Figure 3.6.



(a)



(b)

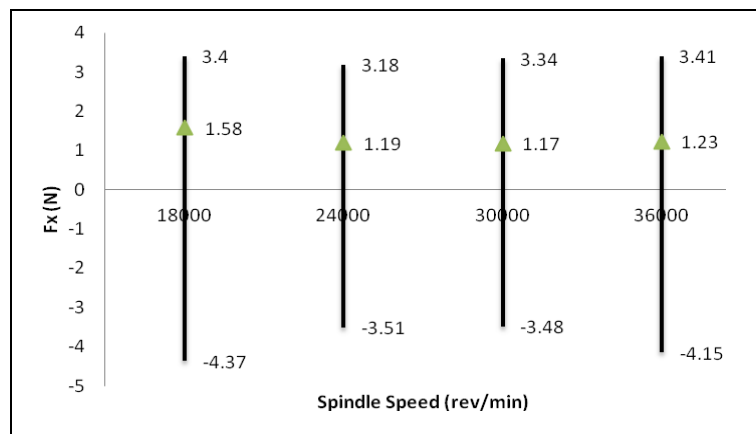


(c)

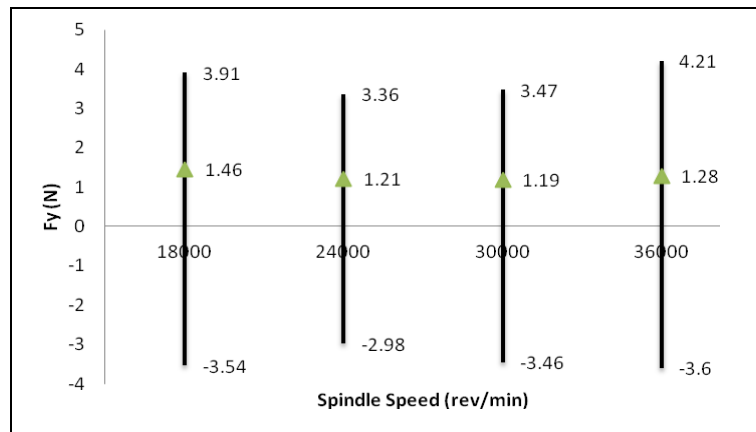
Figure 3.6 Micro channel milling force measurements in Exp #2: (a) Channel #1, (b) Channel #9, (c) Channel #19

The root mean square (RMS) values of cutting forces in x and y axis also increases as the number of cut channels increases.

In experiments 1-4, the effect of spindle speed on tool wear is investigated. Figure 3.7 shows the percentage change in resultant cutting force with respect to the number of machined channel in experiments 1-4.



(a)



(b)

Figure 3.7 Change in cutting forces

It is revealed from the cutting force analysis that spindle speed between 24000 – 30000 rev/min is fairly good for  $\varnothing$  0.8 mm tool.

When the cutting force increase, channel width and channel burr formation criteria are considered together, the results in Table 3.4 are achieved.

Table 3.4 Tool life values of experiments 1,2,3 and 4

Spindle Speed (rev / min)	18000	24000	30000	36000
Tool Life (# of channel )	9	15	15	11
Total Cutting Length (mm)	270	450	450	330
Material Removal Rate ( $mm^3/min$ )	2.688	3.52	4.352	5.248
Tool Life (min)	6.43	8.18	6.62	4.02

It can be stated that tool life in terms of total cutting length increases between 24000 – 30000 rev/min. It can be stated that, as the spindle speed increases, chip – tool interface temperature increases and induces tool wear. Besides, required ductility may not be met in low spindle speeds. Thus, tool life decreases.

Due to the obtained results, range of cutting speed for AISI 304 is 60 – 70 m/min. With respect to this analysis, it can be revealed that spindle speed of 48000 – 50000 rev/min is convenient for  $\varnothing$  0.4 mm cutting tool.

After analyzing the parameters for  $\varnothing$  0.8 mm cutting tool, the channel experiments for  $\varnothing$  0.4 mm cutting tool are done. A single workpiece is used for channel experiments. For each parameter set, one slot with 10 mm length is cut. For each slot, fresh cutting tools are used. Slot milling experiment parameters for  $\varnothing$  0.4 mm cutting tool are given in Table 3.5.

Table 3.5 Slot milling parameters for  $\varnothing$  0.4 mm cutting tool

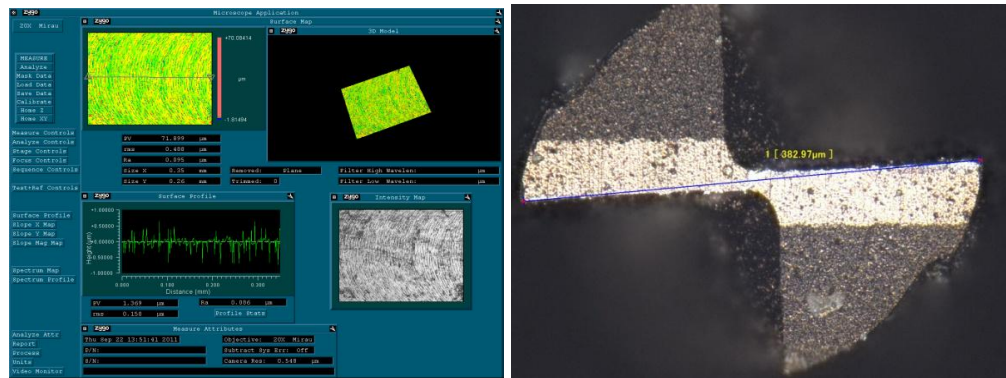
<i>Exp #</i>	<i>N (rev/min)</i>	<i>a<sub>p</sub> (μm)</i>	<i>f (μm/tooth)</i>	<i>feed rate (mm/min)</i>
1	47700	20	0.52	50
2	47700	20	0.52	50
3	47700	20	0.62	60
4	47700	20	0.73	70
5	40000	20	0.62	50
6	47700	30	0.62	60
7	50000	20	0.62	62

Parameters of the experiments are based on the catalogue values of the tool. After the channels are cut, they are observed using microscope in terms of actual depth of cut, tool wear, burr formation and surface roughness. The measured data are given in Table 3.6.

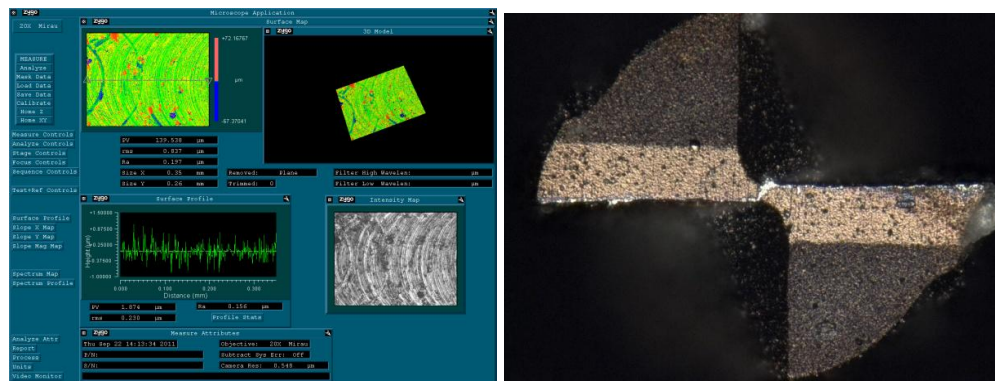
Table 3.6 Measurements of slot milling experiments for  $\varnothing$  0.4 mm cutting tool

<i>Exp #</i>	Measured <i>a<sub>p</sub> (μm)</i>	Tool wear (μm)	Burr Height (μm)		Surface Roughness (nm)
			Up	Down	
1	25	3	44	26	66.75
2	30	4	40	25	42.25
3	30	3	45	8	76.75
4	29	2.5	35	52	51
5	31	5	66	42	85.25
6	41	5.5	50	28	32.75
7	35	5.5	60	63	181.5

In order to achieve surface roughness value, measurement is done in four different regions within the channel and the average value of each parameter set is found. Figure 3.8 presents the surface roughness values and corresponding tool wears of experiment 3 and 7. It is possible to state that increase in cutting speed also increases tool wear formation and decreases surface quality since run-out increases by the increase cutting speed. High run-out induces imbalanced chip load distribution on edges. Thus, edges are worn out faster than expected.



(a)



(b)

Figure 3.8 Relationship between tool wear and surface roughness

In small feed rates, formed chips sticks between cutting tool and workpiece and this situation causes surface roughness on the machined surface. In order to increase the machined surface quality, minimum quantity lubrication can be used.

### **3.4.3 Pocket Milling Experiments**

Micro mold manufacturing has become important by the increase of demand micro medical and electronics products. Micro milling is one of the most convenient manufacturing methods for micro mold fabrication since complex 3D geometries can be cut with high precision, high speed and low cost with respect to other methods. First step of micro mold milling is cutting a pocket on the workpiece. It is done by roughing cut and finishing cut respectively. Roughing cut is used to remove the material with less precision but in high volumes. Then, finishing cut is done in order to provide good surface quality. Finishing cut is used to reach the final dimension of the required geometry with good surface quality and tolerances.

In the course of cutting processes, cutting strategy and parameters should be selected carefully in order not to wear out the tool before the completion of process because changing the tool during the machining leads time loss and defective parts, which causes decrease in production. An experimental study for pocket milling is performed to investigate the effect of radial and axial depth of cut on tool life, so tool change/failure during the machining process can be prevented using tool life knowledge. The experiments are done for two different tool diameters  $\emptyset$  0.8 and  $\emptyset$  0.4 mm.

Before designing an experimental study on the cutting parameters, a preliminary analysis is done to determine the direction and tool path strategies in pocket milling. For direction strategy determination, up milling and down milling methods are experimented. According to the observations, down milling is a better strategy in terms

of burr formation and tool wear. For tool path strategy determination, linear cutting and spiral cutting strategies are experimented. In linear cutting strategy, the tool starts cutting from left bottom corner of the pocket and follows the path as shown in Figure 3.9a. In spiral cutting strategy, the tool enters to the workpiece at the center of pocket and follows an outward spiral path shown in Figure 3.9b.

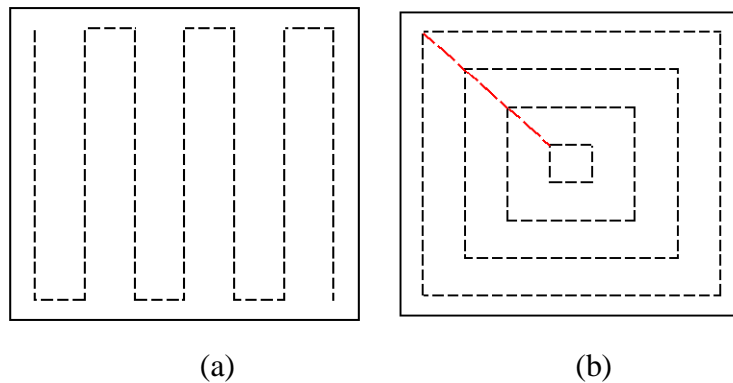


Figure 3.9 (a) Linear cutting strategy (b) Spiral cutting strategy

According to the observations, spiral tool path strategy is better since the chip load on the tool is smaller than the linear path.

As a result of preliminary analysis, it is decided to make pocket milling experiments using down milling with spiral tool path strategy.

First experimental study for pocket milling is done for 10 different parameter sets with  $\varnothing$  0.8 mm cutting tool. 10 workpieces are used in the study. At each workpiece, 10 square pockets are cut. The dimensions of the pockets are  $6.4 \times 6.4 \times 0.8$  mm (L $\times$ W $\times$ H). The length and width of the pockets are selected as 8 times tool diameter ( $8 \times \varnothing$ ) and axial depth of cut is the same as tool diameter. The pockets are cut in multi-pass since it is not possible to cut 0.8 mm depth in one pass. Depth of cut for each pass varies with respect to the axial depth of cut parameter in the experimental design. Radial depths of cuts are given as the percentage of tool diameter in pocket milling experiments.

After making the decision of cutting strategies, pocket dimensions and cutting parameters, G-codes are generated using Cimatron E10 Computer Aided Manufacturing (CAM) software. The tool path generated by Cimatron and actual tool path observed after machining are given in Figure 3.10 a and b.

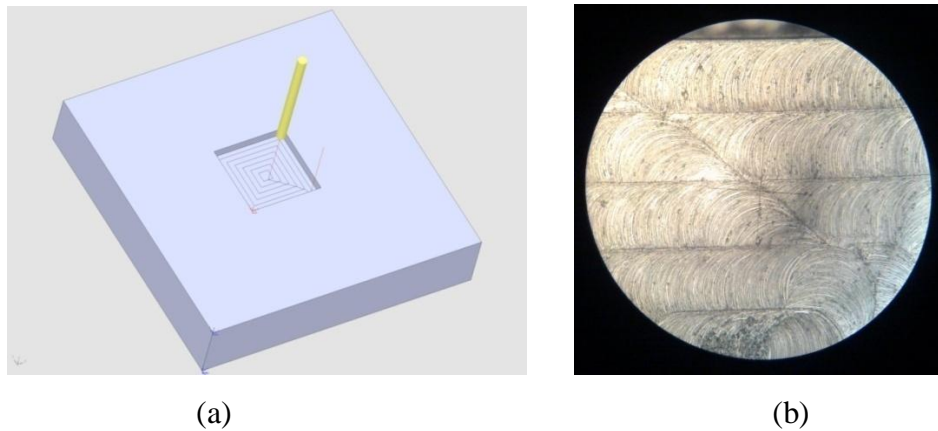


Figure 3.10 (a) Tool path generated by Cimatron, (b) Actual tool path after machining

Cutting tools with larger diameters, such as  $\varnothing$  1.5 or 2.0 mm, can be used for cutting large pockets but spindle speed should be slow. However, high speed spindle cannot provide the required torque below spindle speed 15000 rev/min. In order not to enforce the high speed spindle, cutting tools with large diameters are not selected in experimental studies.

After the pockets in each parameter set are cut, they are observed by the microscope to analyze surface quality and burr formation of pockets. Besides, tool edges are analyzed with the microscope.

Spindle speed ( $N$ ) and feed ( $f_z$ ) parameters are selected according to the results of channel experiments and fixed. Spindle speed and feed parameters used in pocket milling experiments are given in Table 3.7.

Table 3.7 Spindle speed and feed parameters used in  $\varnothing$  0.8 mm cutting tool pocket milling experiments

Parameters	
$N$ (rev / min)	25000
$f_z$ ( $\mu\text{m}$ / tooth)	1.1

Radial depth of cut and axial depth of cut for each pass in pocket milling experiments are given in Table 3.8.

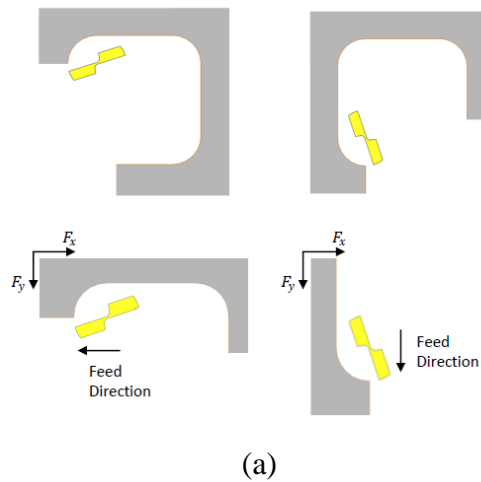
Table 3.8 Axial and radial depth of cut parameters used in  $\varnothing$  0.8 mm cutting tool pocket milling experiments

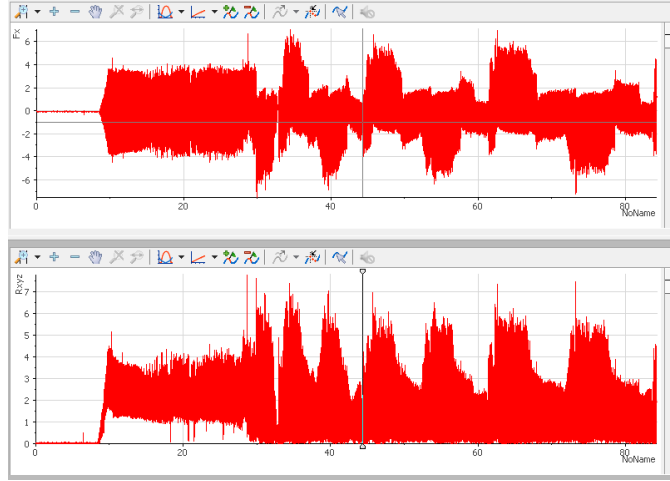
Exp #	Axial Depth of Cut (mm)	Radial Depth of Cut
1	0.080	$0.25 \times \varnothing$
2	0.080	$0.50 \times \varnothing$
3	0.080	$0.75 \times \varnothing$
4	0.080	$0.90 \times \varnothing$
5	0.114	$0.50 \times \varnothing$
6	0.114	$0.75 \times \varnothing$
7	0.114	$0.90 \times \varnothing$
8	0.160	$0.50 \times \varnothing$
9	0.160	$0.75 \times \varnothing$
10	0.160	$0.90 \times \varnothing$

In order to cut 0.8 mm total depth of cut, 10 passes are done for  $80 \mu\text{m } a_p$ , 7 passes are done for  $114 \mu\text{m } a_p$  and 5 passes are done for  $160 \mu\text{m } a_p$  at each pocket. Upper limit of axial depth of cut is determined as  $160 \mu\text{m}$  in order not to enforce the spindle.

After the first experiment is done, the pockets' surface qualities and tool edges are analyzed by the microscope. It is realized that 25% radial depth of cut is not a feasible axial depths of cuts for 25% radial depth of cut are not tested.

In order to evaluate tool wear with respect to cutting force, data are gathered using dynamometer by data acquisition card at fixed intervals to observe the increase at forces. The dynamometer measures 3 component forces  $F_x$ ,  $F_y$  and  $F_z$ . During the cutting process, cutting forces in  $x$  and  $y$  directions are changing due to the spiral cutting path. Figure 3.11a. Change in cutting forces is shown in Figure 3.11b.





(b)

Figure 3.11 As the feed direction changes (a), direction of cutting forces changes (b)

In order to analyze the increase in cutting force, data must be gathered within the same cutting intervals. Thus, the simulation of tool path in Cimatron and real time tool path are compared and the interval is determined for cutting force data gathering. The data are not gathered for each pass in one pocket because of data storage problem, so it is done periodically. For  $80 \mu\text{m}$   $a_p$ , cutting forces are gathered at 1<sup>st</sup>, 4<sup>th</sup>, 7<sup>th</sup> and 10<sup>th</sup> passes of each pocket. For  $114 \mu\text{m}$   $a_p$ , cutting forces are gathered at 1<sup>st</sup>, 4<sup>th</sup> and 7<sup>th</sup> passes of each pocket. For  $160 \mu\text{m}$   $a_p$ , cutting forces are gathered at 1<sup>st</sup>, 3<sup>rd</sup> and 5<sup>th</sup> passes of each pocket. Then, the resultant force  $R_{xyz}$  of  $F_x$ ,  $F_y$  and  $F_z$  is calculated using DIAdem software according to the following equation:

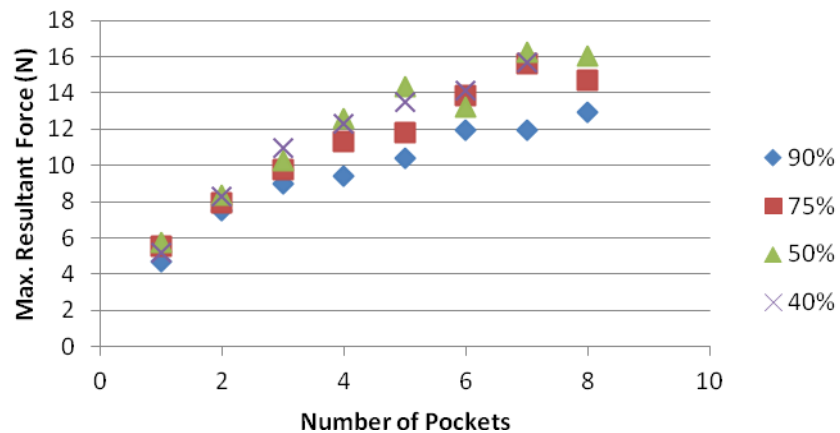
$$R_{xyz} = \sqrt{(F_x)^2 + (F_y)^2 + (F_z)^2} \quad (42)$$

After the resultant force calculation, root mean square (RMS) of the signal values is calculated using DIAdem with respect to the following equation:

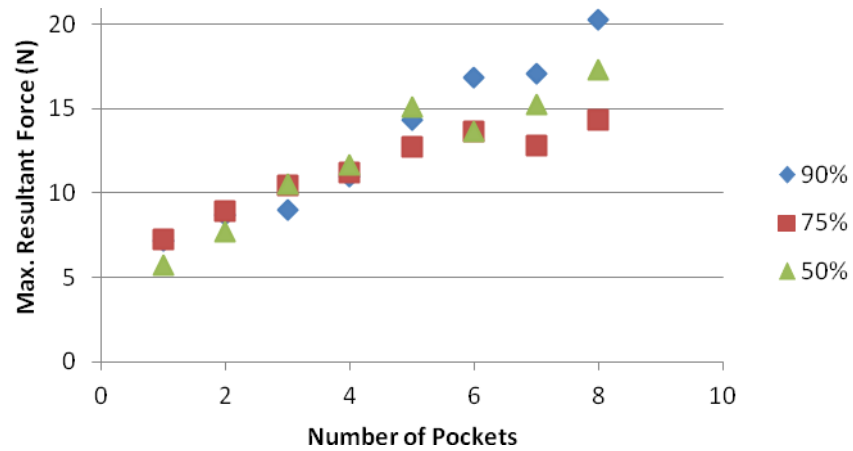
$$\text{Rms} = \sqrt{\frac{1}{N} \sum_{i=j}^{j+N-1} (R_{xyz})_i^2} \quad (43)$$

where N is the number of gathered data, and j is the start time of data.

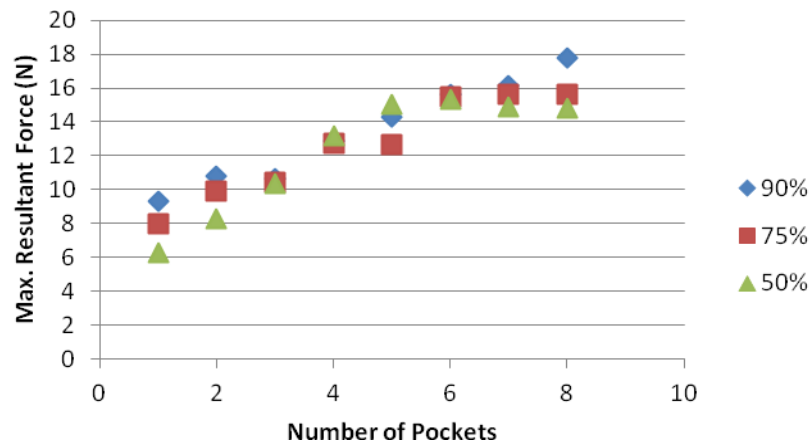
Figure 3.12 shows the change in maximum resultant force with respect to the number of machined pockets. Maximum resultant forces increase as the number of machined pockets increase. Besides, increase in the burr formation in the pockets can be visually observed. By combining two results, it is revealed that cutting force and the tool wear are dependent factors.



(a)



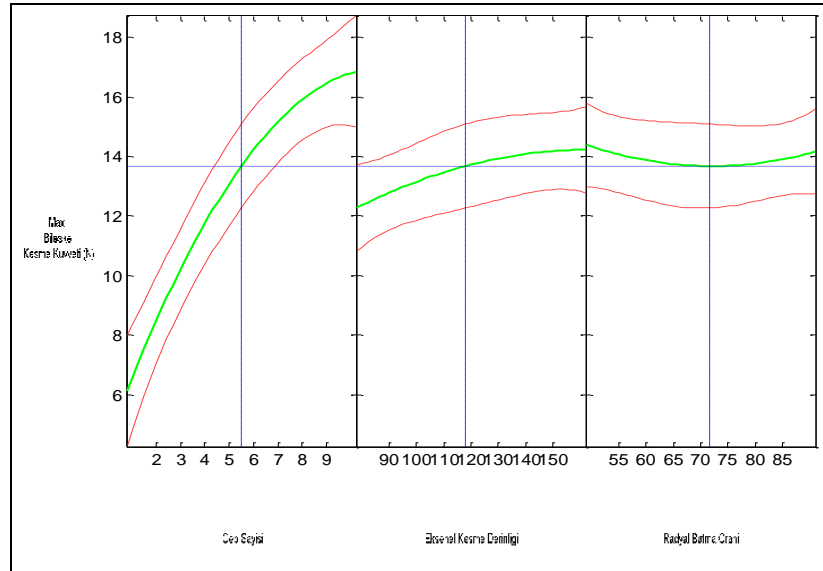
(b)



(c)

Figure 3.12 Cutting Forces with respect to axial depth of cuts (a) 80, (b) 114, (c)160 micron

The change in cutting forces are analyzed by using ANOVA and the relationship between tool life, radial depth of cut and axial depth of cut is found. ANOVA analysis is given in Figure 3.13.



(a)

Analysis of Variance					
Source	Sum Sq.	d. f.	Mean Sq.	F	Prob>F
X1	1006.8	9	111.867	117.65	0
X2	53.81	2	26.905	28.3	0
X3	6.29	2	3.146	3.31	0.048
X1*X2	18.48	18	1.027	1.08	0.4078
X1*X3	31.27	18	1.737	1.83	0.0609
X2*X3	41.05	4	10.262	10.79	0
Error	34.23	36	0.951		
Total	1191.93	89			

(b)

Figure 3.13 ANOVA result of  $\emptyset$  0.8 mm pocket milling experiments

According to the analysis, cutting forces increase as the number of machined pocket (X1) and the axial depth of cut (X2) increase. Cutting forces are relatively small near 70% radial depth of cut. Besides, radial and axial depth of cuts has a correlation. The relationship between resultant force and experiment parameters can be mathematically explained by the following equation:

$$\begin{aligned}
\text{Max Resultant Force} = & 10.6337 + 2.4037C + 0.0279a_p - 0.272a_e + \\
& (3.4725e - 4)C^2 - 0.0032a_p^2 + (8.1953e - 4)a_e^2 - 0.0982Ca_p - (2.1781e - \\
& 4)Ca_e + 0.0013a_p a_e
\end{aligned} \tag{44}$$

where  $C$  denotes number of pockets,  $a_p$  denoted axial depth of cut and  $a_e$  denotes radial depth of cut. The equation can be used as a constraint in micro-milling process optimization problems.

It is previously mentioned that tool wear affects cutting forces. The type of wear changes measured cutting force values. In order to analyze the impact of tool wear type on cutting forces, tool edges and surface of machined workpieces are investigated by digital microscope. In Figure 3.14, wear regions on cutting tools are shown. As the radial depth of cut decreases, area of wear increases around the cutting edge and as the axial depth of cut is increased, wear on tool edge reduces. It is revealed from the Figure that cutting edges become blunt and tool diameter decreases by the increase of wear. Reduction in tool diameter can be determined as wear criteria. However, irregular wear formation complicates the measurement and evaluation.

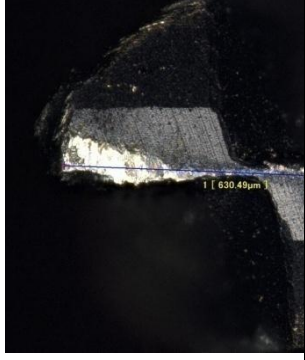
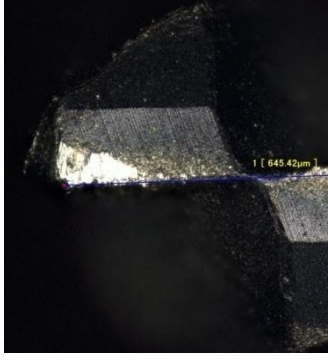
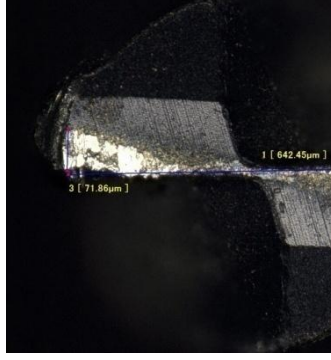
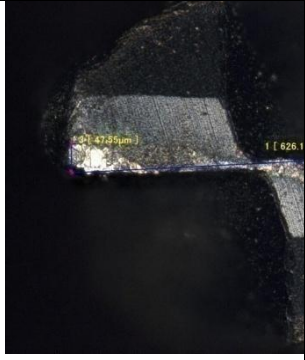
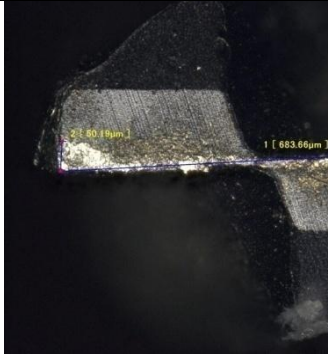
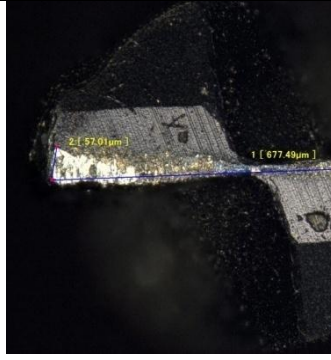
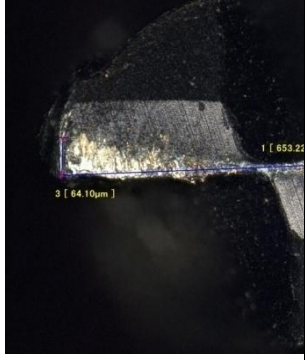
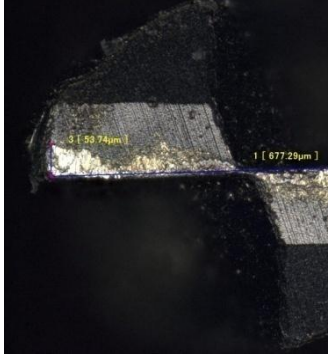
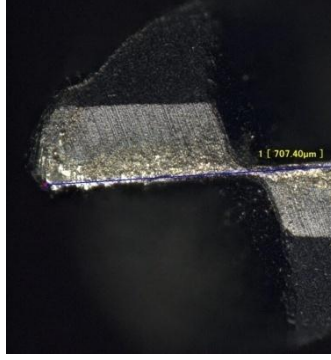
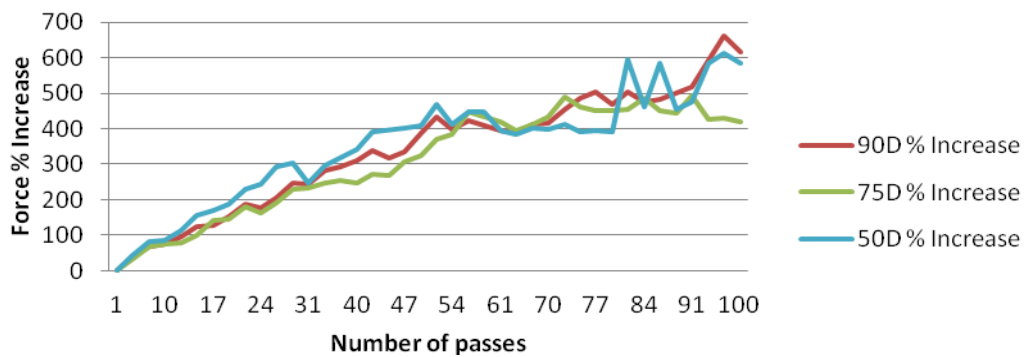
	50%	75%	90%
80 micron			
114 micron			
160 micron			

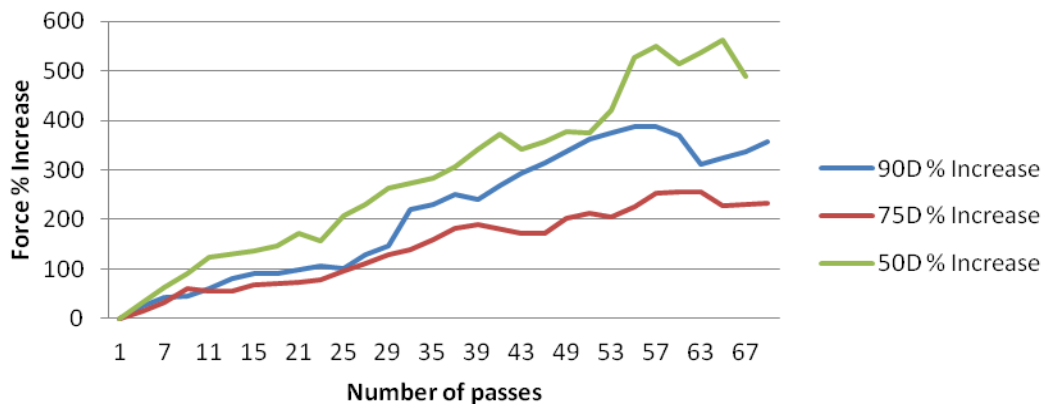
Figure 3.14 Tool wears of different cutting conditions

Due to the observed wears on cutting tools, 90%  $a_e$  with 160  $\mu\text{m}$   $a_p$  is the best condition in terms of tool wear minimization criteria. Besides, radial depth of cut has to be increased as the axial depth of increases.

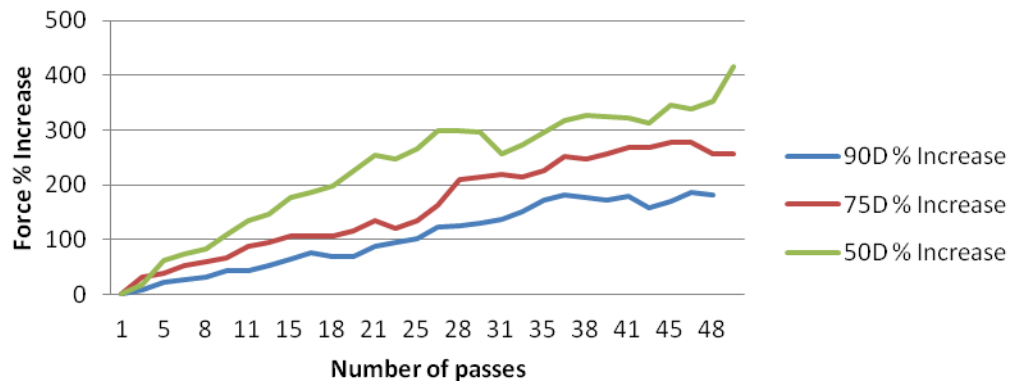
In the pocket milling study, various axial depths of cuts are tested in order to find the influential factors on tool wear. It is not possible to compare the observed forces for different axial depth of cuts. Thus, cutting force in the first pass for each parameter is set as base and incremental force with respect to the base is investigated. Figure 3.15 shows the percentage increase in cutting forces with respect to the first pass.



(a)



(b)



(c)

Figure 3.15 Resultant force increase due to tool wear for axial depth of cuts (a) 80  $\mu\text{m}$ , (b) 114  $\mu\text{m}$  and (c) 160  $\mu\text{m}$

When the each cutting force curves are fit to a line and normalized with respect to the axial depth of cut, following tool wear rates are obtained. (See Table 3.9)

Table 3.9 Tool wear rates of experiment parameters

	<b>50%</b>	<b>75%</b>	<b>90%</b>
<b>80 <math>\mu\text{m}</math></b>	2,4	1,912	2,075
<b>114 <math>\mu\text{m}</math></b>	1,97	1,15	1,97
<b>160 <math>\mu\text{m}</math></b>	1,4	1	0,95

According to Table 3.9, tool wear rate decreases as the axial depth of cut increases by contrast with conventional milling operations.

In order to evaluate the performance of cutting conditions in terms of tool life, total machining time is taken into consideration. Initially, cutting time of a single pass is

estimated. Then, total machining time for machining 10 pockets with dimension of 6.4×6.4×0.8 mm is calculated with respect to the following equation:

$$\text{Total Machining Time} = (\text{cutting time of a single pass}).(\text{total \# of passes})$$

Cutting time of a single pass and total machining time for 10 pockets are given in Table 3.10.

Table 3.10 Cutting times of experimented parameters

	<b>50%</b>	<b>75%</b>	<b>90%</b>
<b>Single pass</b>	1.71 min	1.39 min	1.13 min
<b>80 μm</b>	171 min	139 min	113 min
<b>114 μm</b>	119 min	97 min	79 min
<b>160 μm</b>	85 min	69 min	56 min

It is revealed from the study that, machining time decreases as the the radial depth of cut increases. The tool can be used at least 171 min without breakage. However, good surface quality cannot be assured.

The cutting conditions of experimental design are also evaluated with respect to the surface quality. Figure 3.16 and 3.17 show the surface of first and last pockets of each parameter set respectively. It can be revealed from the investigated surfaces that reduction in tool diameters induce uncut material in the surface. The maximum uncut material is observed in the cutting condition of 80 μm  $a_p$  and 90%  $a_e$ . For roughing operations, uncut material in the surface is not substantial. However, smaller radial depths of cuts are recommended in finishing operations with respect to this analysis.

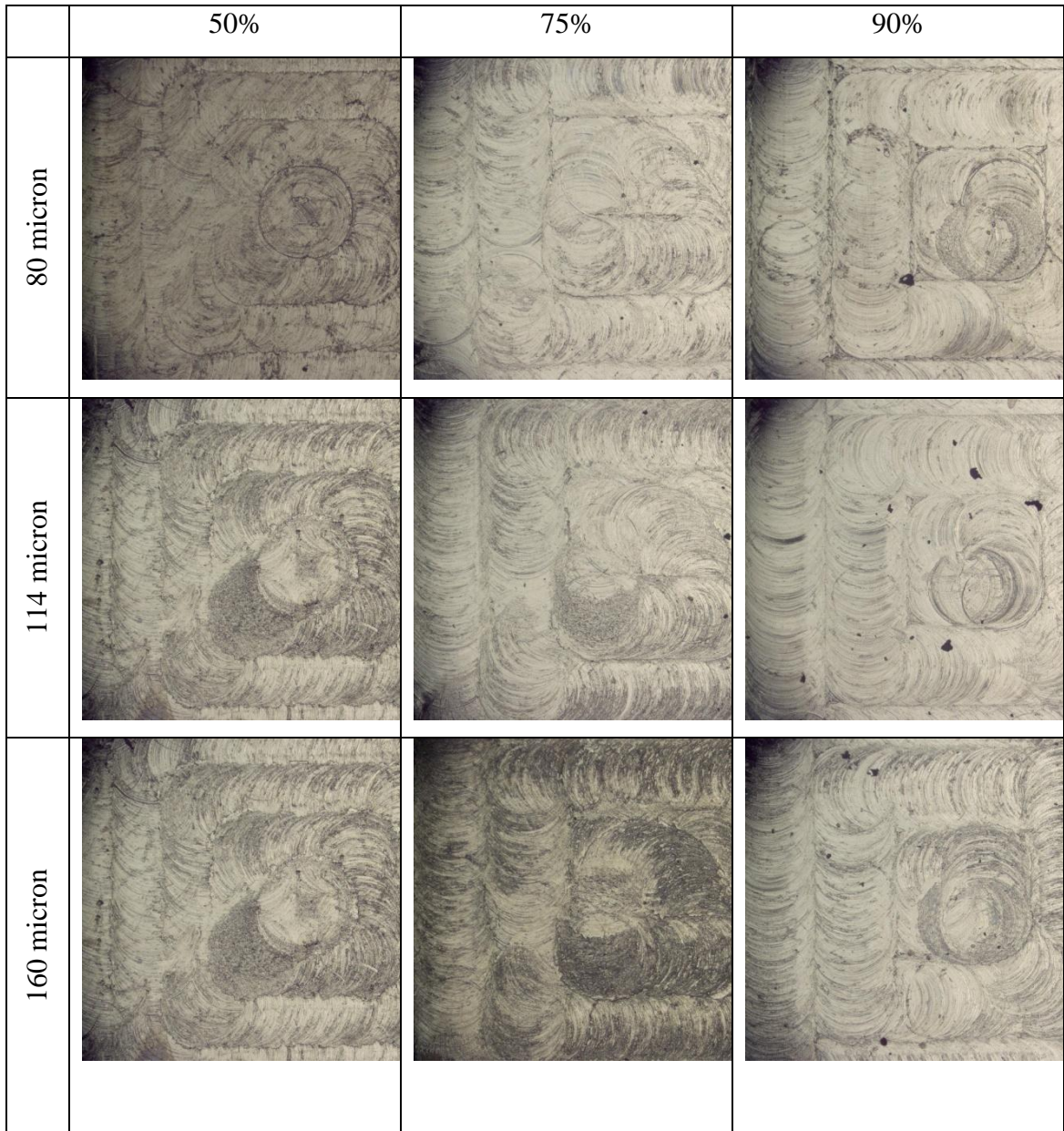


Figure 3.16 Surface images of first pockets

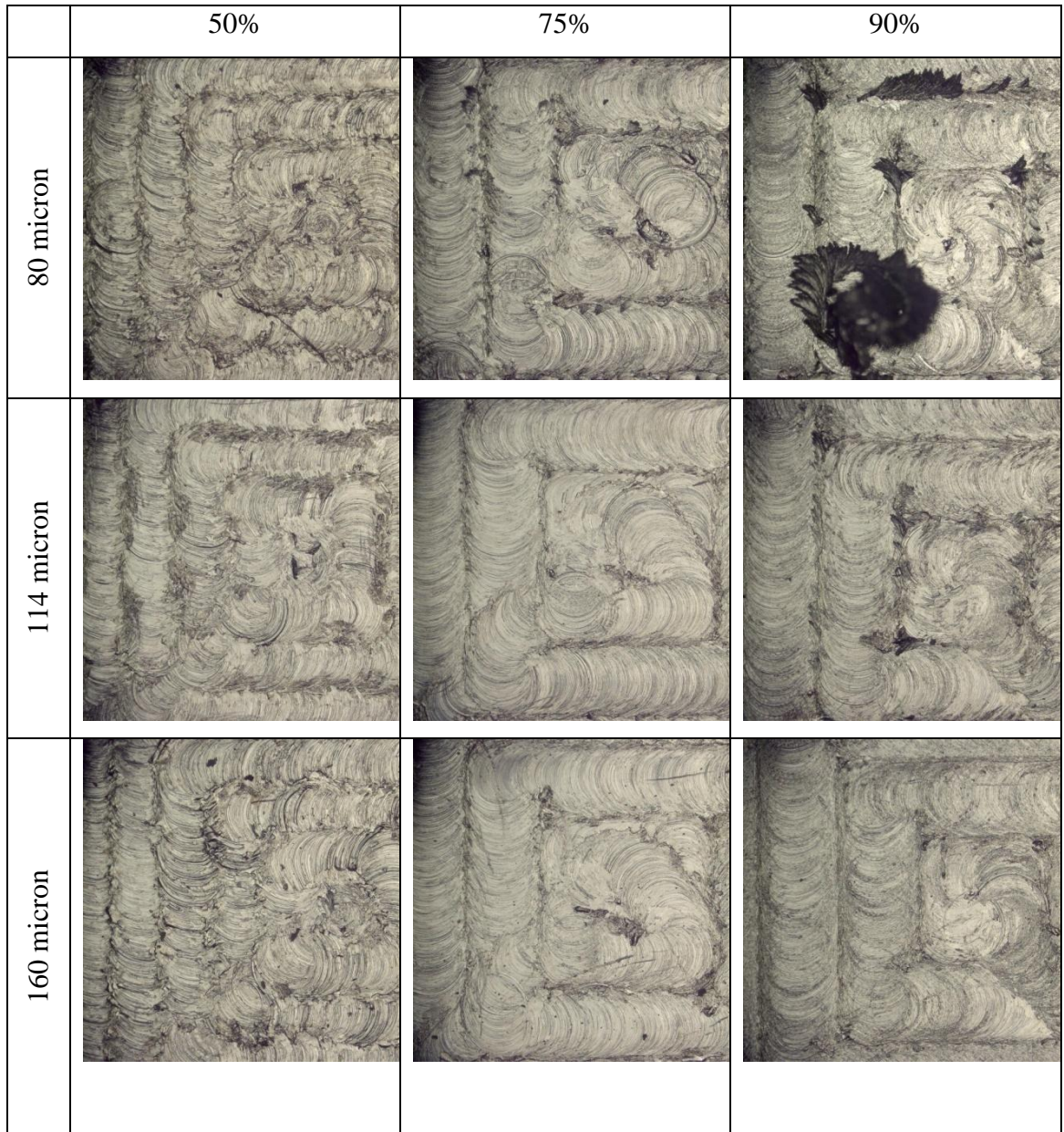


Figure 3.17 Surface images of tenth pockets

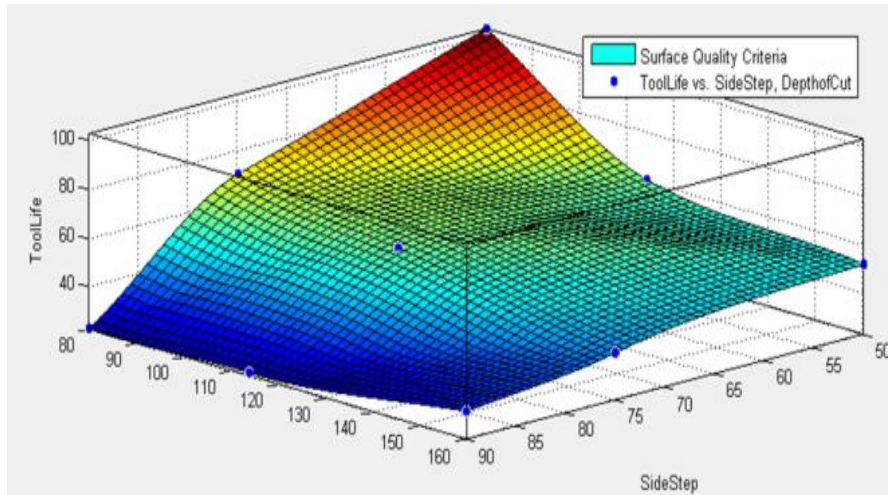
Finally, burr formations in the pocket walls are analyzed and tool life for each parameter are determined with respect to the burr formation criteria. By considering the cutting

time of single pass and total number of passes cut until reaching the maximum allowable burr formation, tool lives of parameter set is calculated and given in Table 3.11.

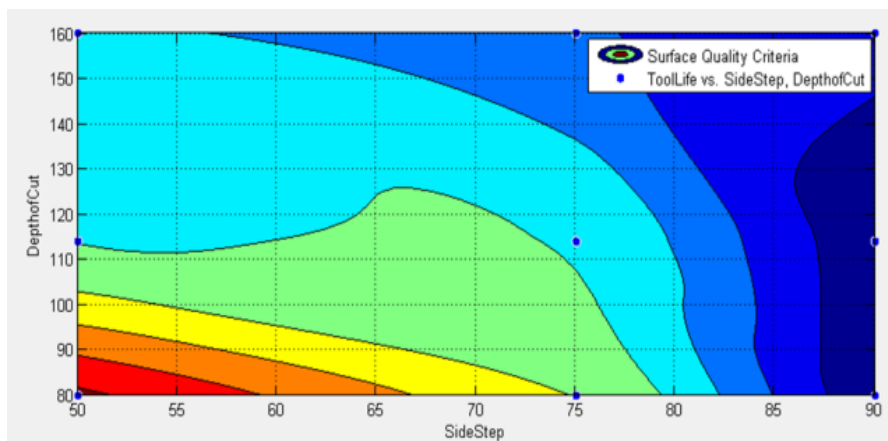
Table 3.11 Determined tool lives for burr formation criteria

$a_p$ ( $\mu\text{m}$ )	$a_e$ (D%)	Tool Life (min)
80	50	102.32
80	75	69.63
80	90	22.58
114	50	59.69
114	75	58.49
114	90	23.71
160	50	51.16
160	75	41.78
160	90	33.87

Obtained tool life values are used to fit a surface in order to estimate the tool life in different cutting conditions. Matlab software is used to fit a surface. The interpolant model is used for surface fitting. The fitted surface is given in Figure 3.18. According to the fitted surface, burr formation decreases as the radial and axial depth of cut values decrease. For finishing operations, burr formation is an important criterion. However, it is not essential in roughing operations.



(a)



(b)

Figure 3.18 The effect of cutting conditions in terms of burr formation

It is revealed from the analysis that, roughing operation, with large axial and radial depth of cut, is required in order to remove the material fast and economically. Finishing operation, with small radial and axial depth of cuts, is required in order to achieve a good surface quality. The obtained results are similar to the conventional milling operations.

Pocket milling experiments are preceded with  $\emptyset$  0.4 mm cutting tools. CCD method is used to prepare an experimental design in order to minimize required experiment number and analyze both main and interaction effects of parameters on tool life. A preliminary work is done to determine the upper and lower limits of parameters. The parameters considered in  $\emptyset$  0.4 mm pocket milling experiments are spindle speed ( $N$ ), feed per tooth ( $f_z$ ) and axial depth of cut ( $a_p$ ). Effect of radial depth of cut is not investigated in order to decrease the required number of experiments, so tooling cost and time consumption is minimized. Radial depth of cut is assumed to be  $0.7 \times \emptyset$  which provided favorable tool life for  $\emptyset$  0.8 mm cutting tool. Dimensions of pockets in the preliminary analysis are  $3.2 \times 3.2 \times 0.4$  mm and three pockets are milled for each parameter set unless tool is broken. Investigated parameters in the preliminary study and measured tool lives after milling process are given in Table 3.12.

Table 3.12 Measured cutting tool diameter after the preliminary study

<i>Exp #</i>	<i>N</i> ( <i>rev/min</i> )	<i>f</i> ( $\mu\text{m}/\text{tooth}$ )	$a_p$ ( $\mu\text{m}$ )	<i>feed rate</i> ( <i>mm/min</i> )	Volume ( $\text{mm}^3$ )	Measured $\emptyset$ ( $\mu\text{m}$ )
1	50000	0.5	20	50	12.288	$\approx 308$
2	50000	0.5	80	50	12.288	$\approx 314$
3	50000	0.5	100	50	12.288	$\approx 345$
4	50000	0.625	100	62.5	12.288	$\approx 371$
5	50000	0.8	100	80	12.288	$\approx 326$
6	50000	0.625	133	62.5	12.288	$\approx 385$
7	50000	0.8	133	80	2.724	* Broken
8	50000	0.625	150	62.5	12.288	$\approx 387.5$
9	50000	0.625	180	62.5	9.216	* Broken
10	50000	0.5	200	50	0	* Broken

Based on the preliminary analysis, range of axial depth of cut and feed per tooth are determined as 100 - 150  $\mu\text{m}$  and 0.5 – 0.72  $\mu\text{m}$  / tooth respectively. Table 3.13 summarizes the parameters to be used in the experiments and pocket dimensions.

Table 3.13 Parameter ranges used in  $\varnothing$  0.4 mm cutting tool pocket milling experiments

<i>Parameters</i>	
<i>N (rev/min)</i>	40000 – 50000
<i>f (<math>\mu\text{m}/\text{tooth}</math>)</i>	0.52 – 0.72
Radial depth of cut (%)	$0.7 \times \varnothing$
<i>a<sub>p</sub> (<math>\mu\text{m}</math>)</i>	100 – 150
Pocket Dimensions ( <i>mm</i> × <i>mm</i> × <i>mm</i> )	$8\varnothing \times 8\varnothing \times 2a_p$

Using CCD method and given parameter range, an experimental design with 20 experiments is prepared using Minitab software. The design consists of six center points, six axial points and eight corner points. Figure 3.19 illustrates the relationships among the varieties and Table 3.14 summarizes the parameters of the experimental design. For each parameter, five levels are set.

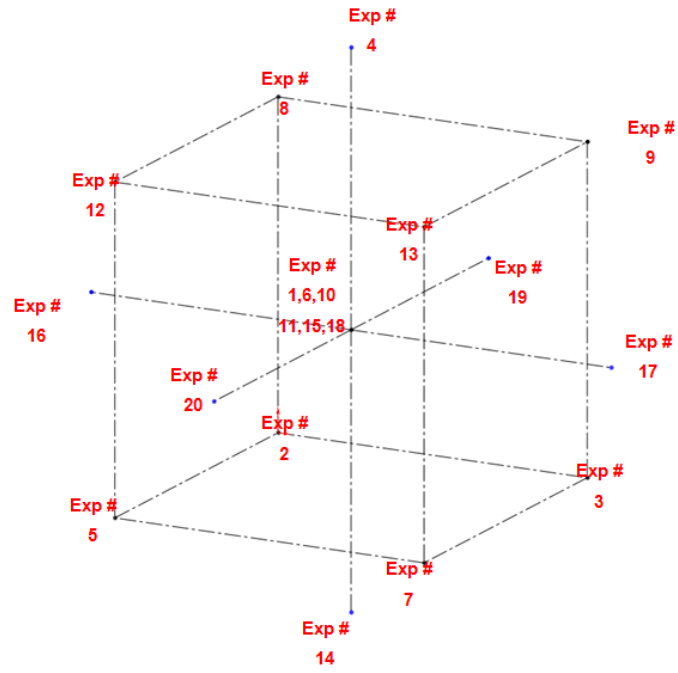


Figure 3.19 Experimental design of  $\varnothing 0.4$  mm cutting tool pocket milling experiments

Table 3.14 Experiment parameters

<i>Exp #</i>	<i>N (rev/min)</i>	<i>f (μm/tooth)</i>	<i>a<sub>p</sub> (μm)</i>	<i>feed rate (mm/min)</i>
<b>1</b>	45000	0,623	125	56,07
<b>2</b>	40000	0,526	100	42,08
<b>3</b>	50000	0,526	100	52,60
<b>4</b>	45000	0,623	167	56,07
<b>5</b>	40000	0,720	100	57,60
<b>6</b>	45000	0,623	125	56,07
<b>7</b>	50000	0,720	100	72,00
<b>8</b>	40000	0,526	150	42,08
<b>9</b>	50000	0,526	150	52,60
<b>10</b>	45000	0,623	125	56,07
<b>11</b>	45000	0,623	125	56,07
<b>12</b>	40000	0,720	150	57,60
<b>13</b>	50000	0,720	150	72,00
<b>14</b>	45000	0,623	83	56,07
<b>15</b>	45000	0,623	125	56,07
<b>16</b>	36591	0,623	125	45,59
<b>17</b>	53409	0,623	125	66,55
<b>18</b>	45000	0,623	125	56,07
<b>19</b>	45000	0,460	125	41,40
<b>20</b>	45000	0,786	125	70,74

The increase in spindle speed may cause interference between natural frequency of dynamometer and spindle speed frequency and distort the exact results. Hence, tool life is evaluated based on tool diameter reduction instead of changes in cutting forces. Two passes are done at each pocket. After cutting each pocket, diameter of cutting tool is

measured by microscope. Critical tool life diameter is set as 375  $\mu\text{m}$ . Pockets are machined until the diameter reaches critical value.

In order to evaluate the performance of cutting conditions, the surfaces of cutting tools and pockets are investigated. Burr formations in the pocket walls are also considered. In Figure 3.20 images of fresh and worn tools are shown.

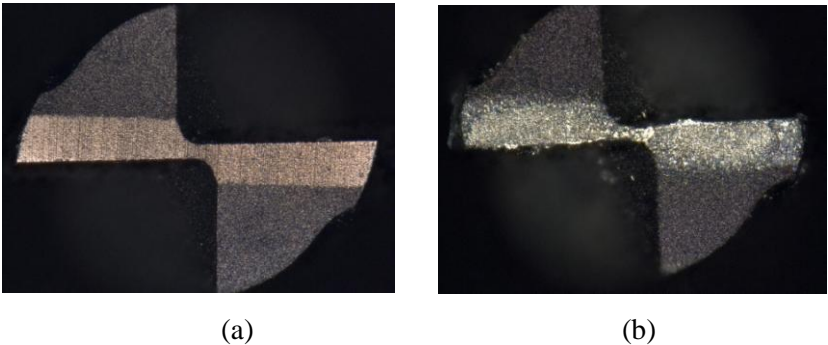


Figure 3.20 Images of (a) fresh and (b) worn tools

In Figure 3.21, measured tool diameter values with respect to the number of pass for the first three experiments are given. The reduction in tool diameter can be observed clearly.

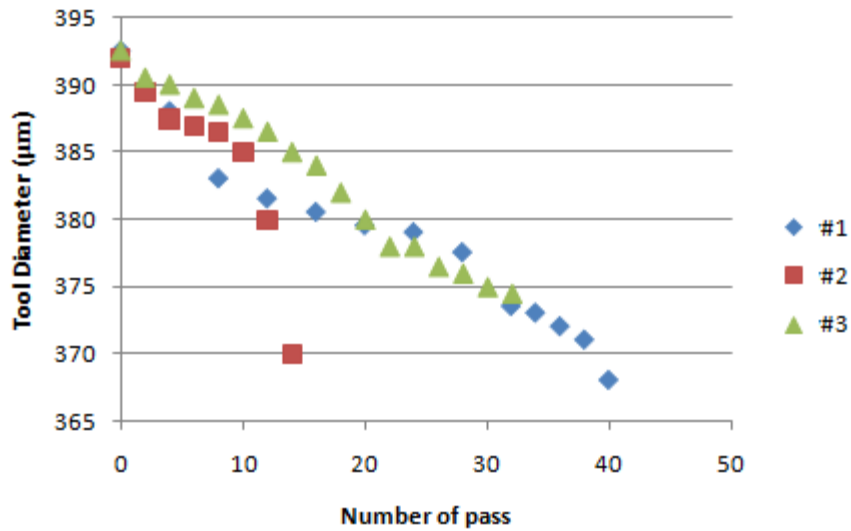


Figure 3.21 Measured tool diameters values with respect to the number of passes for experiments # 1, #2 and #3

In experiments 4, 9, 10, 12, 13, 16 and 20, the tools are broken before achieving the critical tool diameter value. The cutting time of each pass is estimated using a formulation. Total machining time until reaching the critical value is calculated by using number of pass and single pass cutting time values. The tool lives in each experiment with respect to the minimum allowable tool diameter criteria is given in Table 3.15.

Table 3.15 Tool life values obtained in the experiments

Exp #	Tool Life	Exp #	Tool Life
1	19,12	11	16,57
2	20,5	12	4,34
3	20,39	13	2,48
4	1,91	14	17,22
5	14,27	15	16,57
6	15,30	16	10,98
7	12,91	17	16,11
8	15,29	18	17,21
9	6,12	19	16,40
10	14,66	20	1,52

In order to find the relationship between tool life and cutting parameters, regression analysis and ANOVA are performed. In Figure 3.22, the results of the analysis are given. Based on the experimental analysis, the second order RMS model for tool life is formulated. The tool life equation is as follows:

$$Tool\ Life = -152.103 + 204245f_z + 1113.81DoC + 2.16514V - 248075399f_z^2 - 3391.78DoC^2 - 0.0179843V^2 - 45237.6f_zDoC + 1242.21f_z - 7.60179DoCV \quad (45)$$

where  $f_z$  denotes feed per tooth,  $DoC$  denotes axial depth of cut and  $V$  denotes cutting speed. To measure model adequacy,  $R^2$  and adjusted  $R^2$  are calculated and found 91.10% and 83.10% respectively. Since both models obtained satisfactory  $R^2$  results, it is possible to state that the models are well fitted to the real data.

Estimated Regression Coefficients for ToolLife(min)

Term	Coef	SE Coef	T	P
Constant	16.5230	1.045	15.817	0.000
fz (mm/tooth)	-6.5636	1.165	-5.634	0.000
DoC (mm)	-8.0692	1.165	-6.925	0.000
V (m/min)	-0.4747	1.166	-0.407	0.692
fz (mm/tooth) * fz (mm/tooth)	-6.5911	1.908	-3.455	0.006
DoC (mm) * DoC (mm)	-5.9895	1.908	-3.139	0.011
V (m/min) * V (m/min)	-2.0081	1.908	-1.052	0.317
fz (mm/tooth) * DoC (mm)	-0.3099	2.558	-0.121	0.906
fz (mm/tooth) * V (m/min)	2.1396	2.559	0.836	0.423
DoC (mm) * V (m/min)	-3.3755	2.560	-1.319	0.217

S = 2.56135 PRESS = 437.487  
R-Sq = 91.10% R-Sq(pred) = 40.68% R-Sq(adj) = 83.10%

Analysis of Variance for ToolLife(min)

Source	DF	Seq SS	Adj SS	Adj MS	F	P
Regression	9	671.840	671.840	74.649	11.38	0.000
Linear	3	524.158	523.889	174.630	26.62	0.000
fz (mm/tooth)	1	208.225	208.214	208.214	31.74	0.000
DoC (mm)	1	314.836	314.587	314.587	47.95	0.000
V (m/min)	1	1.097	1.088	1.088	0.17	0.692
Square	3	131.595	131.595	43.865	6.69	0.009
fz (mm/tooth) * fz (mm/tooth)	1	63.295	78.316	78.316	11.94	0.006
DoC (mm) * DoC (mm)	1	61.035	64.657	64.657	9.86	0.011
V (m/min) * V (m/min)	1	7.265	7.265	7.265	1.11	0.317
Interaction	3	16.088	16.088	5.363	0.82	0.513
fz (mm/tooth) * DoC (mm)	1	0.096	0.096	0.096	0.01	0.906
fz (mm/tooth) * V (m/min)	1	4.585	4.585	4.585	0.70	0.423
DoC (mm) * V (m/min)	1	11.406	11.406	11.406	1.74	0.217
Residual Error	10	65.605	65.605	6.561		
Lack-of-Fit	5	53.413	53.413	10.683	4.38	0.065
Pure Error	5	12.192	12.192	2.438		
Total	19	737.445				

Estimated Regression Coefficients for ToolLife(min) using data in uncoded units

Term	Coef
Constant	-152.103
fz (mm/tooth)	204245
DoC (mm)	1113.81
V (m/min)	2.16514
fz (mm/tooth) * fz (mm/tooth)	-248075399
DoC (mm) * DoC (mm)	-3391.78
V (m/min) * V (m/min)	-0.0179843
fz (mm/tooth) * DoC (mm)	-45237.6
fz (mm/tooth) * V (m/min)	1242.21
DoC (mm) * V (m/min)	-7.60179

Figure 3.22 ANOVA and regression analysis

Due to the performed analysis, the range of axial depth of cut, which is convenient for 70% radial depth of cut, is 80 – 100  $\mu\text{m}$ . The ratio of axial depth of cut to the tool diameter is approximately 20 – 25%. If the ratio is applied to the cutting tools with diameter of 0.8 mm, it is possible to state that, 200  $\mu\text{m}$  axial depth of cut is applicable. In

terms of spindle speed, the best range for  $\varnothing$  0.4 mm is 40000 – 45000 rpm. The range of feed per tooth is determined as 0.5 – 0.6  $\mu\text{m}/\text{tooth}$ . The estimated regression coefficients for tool life using data in uncoded units are used in the tool life equation for optimization problem.

### **3.5 Conclusion**

In this chapter an experimental investigation of the micro machinability of AISI 304 is performed. Tungsten carbide tools are used for the experiments. Prior to the experiments, controllable machining factors are determined. The controllable factors are cutting strategy, tool entrance strategy into the workpiece, cutting speed, feed per tooth, axial and radial depths of cut and tool diameter. In order to search the effects of factors, an experimental setup is prepared.

Firstly, slot milling experiments are performed for  $\varnothing$  0.4 and  $\varnothing$  0.8 mm cutting tools. In these experiments, workable cutting parameter intervals for AISI 304 with tungsten carbide micro end mills are determined for pocket milling by considering surface roughness, chip formation and cutting forces.

Next, pocket milling experiments are performed for  $\varnothing$  0.4 and  $\varnothing$  0.8 mm cutting tools in order to reveal the optimal cutting parameters that maximize cutting tool life. In  $\varnothing$  0.8 mm pocket milling experiments, tool lives of parameter sets are found for different criteria. Besides, the relationship between resultant cutting force and experiment parameters are revealed by ANOVA and explained with an equation. In  $\varnothing$  0.4 mm pocket milling experiments, a central composite design is formed. Then, experiments are performed and obtained results are analyzed using regression and ANOVA. Tool life equation is acquired and used in the next chapter.

# Chapter 4

## Modeling and Optimization of Square Pocket Milling

Mathematical formulations of micro milling operations are the same as macro milling operations. Cutting speed ( $V$ ), feed rate ( $f_r$ ) and machining time ( $t_m$ ) are calculated according to the following equations:

$$V = \pi \cdot D \cdot N \quad (46)$$

$$f_r = f_z \cdot z \cdot N \quad (47)$$

$$t_m = \frac{\pi \cdot L \cdot D}{f_z \cdot z \cdot V} \quad (48)$$

where  $D$  denotes the diameter of cutting tool,  $N$  denotes the spindle speed,  $f_z$  denotes the feed per tooth,  $z$  denotes the number of tooth on the cutting tool and  $L$  is cutting length. When  $V$  is replaced with  $\pi \cdot D \cdot N$ , new formulation of machining time is:

$$t_m = \frac{L}{f_r} \quad (49)$$

In slot milling, it is simple to calculate the cutting length. However, tool follows a complicated path in pocket milling with regard to slot milling. The tool path in pocket milling is shown in Figure 4.1.

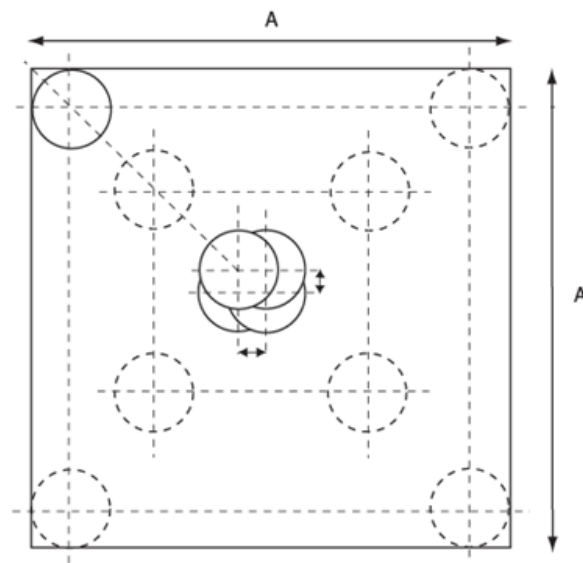


Figure 4.1 Tool path from center to outwards

The cutting tool moves on counter clockwise direction because of down milling process. The tool is plunged into the workpiece at the center of pocket and follows a square path. (See Figure 4.2a) Then, cutting tool moves diagonally with the distance of  $a_e \cdot D$ , where  $a_e < 1$ , and degree of 45 and completes the square path. (See Figure 4.2b) This procedure continues until reaching the required dimensions. (See Figure 4.2c)

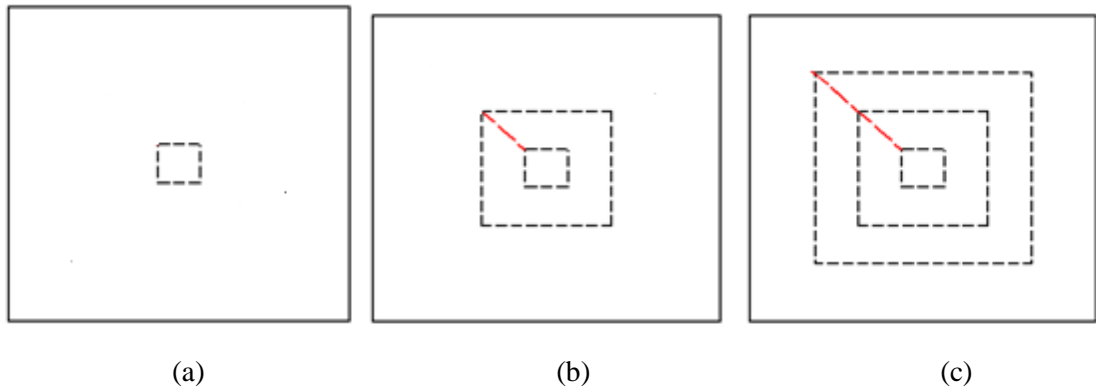


Figure 4.2 Pocket milling procedures cutting path

Cutting length at each square path in pocket milling is calculated according to the following formulation:

$$\begin{aligned}
 L_0 &= 2. (a_e D) \\
 L_1 &= 4. (2a_e D) \\
 L_2 &= 4. (4a_e D) \\
 L_3 &= 4. (6a_e D) \\
 &\dots \\
 L_k &= 4. [(2k)a_e D]
 \end{aligned}$$

where  $k$  is the square cycle's number in the course of milling and  $L$  is the cutting length at that cycle. For each diagonal movement, cutting length is calculated with respect to the following equation:

$$L_d = \sqrt{2}. a_e D \quad (50)$$

Total number of square cycles has to be integer. If the pocket is square with the dimension of length  $A$ , it can be written as following:

$$A = \frac{D}{2} + 2ka_e D + \frac{D}{2} \quad (51)$$

The formulation can be rewritten as following equation in order to find the total number of cycles in the pocket:

$$k = \frac{A-D}{2a_e D} \quad (52)$$

Total cutting length of cycles at one pass can be calculated by the following equation:

$$\sum L = 4k(k+1)a_e D + 2a_e D \quad (53)$$

In addition to the total cycle length, total diagonal cutting length ( $L'$ ) at one pass can be calculated by the following equation:

$$\sum L' = (k-1)\sqrt{2}a_e D \quad (54)$$

Total material removing length ( $L_c$ ) can be formulated as following:

$$L_c = \sum L + \sum L' = [4k(k+1)a_e D + 2a_e D] + [(k-1)\sqrt{2}a_e D] \quad (55)$$

If the pocket requires multi-pass milling, the tool has to get back to the center of pocket from the left top corner for the next pass without removing material. The length of tool return ( $L_r$ ) is given in the following equation:

$$L_r = \frac{\sqrt{2}(A-D)}{2} \quad (56)$$

In multi-pass milling terminology,  $d_r$  denotes axial depth of roughing cut in one pass,  $w$  denotes the required total axial depth of cut and  $d_f$  denotes the axial depth of finishing cut. If finishing cut is not required in pocket milling, required number of passes ( $n$ ) is calculated as following:

$$n = \frac{w}{d_r} \quad (57)$$

If finishing cut is required after roughing cut in milling process,  $n$  is calculated as

$$n = \frac{w-d_f}{d_r} \quad (58)$$

where  $n$  has to be an integer. Total machining time of pocket milling ( $t_{total}$ ) consists of three main components which are tool plunge time ( $t_{plunge}$ ), material removal time ( $t_{cutting}$ ) and tool return time ( $t_{return}$ ). The equation of total machining time is given following:

$$t_{total} = t_{plunge} + t_{cutting} + t_{return} \quad (59)$$

It is possible to use different feed rates for plunging, cutting and tool returning processes. Total machining time for single pass pocket milling is

$$t_{total} = \left[ \frac{a_p}{f_{plunge}} + \frac{L_c}{f_{cut}} \right] \quad (60)$$

Total machining time for multi pass milling with only roughing cut is

$$t_{total} = \left[ \frac{d_r}{f_{r\_plunge}} + \frac{L_c}{f_{r\_cut}} + \frac{L_r}{f_{r\_return}} \right] \cdot \frac{w}{d_r} \quad (61)$$

where  $f_{r\_plunge}$  is plunging feed,  $f_{r\_cut}$  is cutting feed and  $f_{r\_return}$  is tool return feed for roughing cut. Plunging and tool return feeds are commonly selected with respect to the properties of workpiece material and machining center and fixed to a constant value. However, cutting feed changes with respect to the values of feed per tooth and cutting speed.

Total machining time for multi pass roughing cut and a single finishing cut is

$$t_{total} = \left[ \frac{d_r}{f_{r\_plunge}} + \frac{L_c}{f_{r\_cut}} + \frac{L_r}{f_{r\_return}} \right] \cdot \frac{w-d_f}{d_r} + \left[ \frac{d_f}{f_{f\_plunge}} + \frac{L_c}{f_{f\_cut}} \right] \quad (62)$$

where  $f_{f\_plunge}$  is plunging feed and  $f_{f\_cut}$  is cutting feed for finishing cut.

In previous studies for multi-pass milling optimization problems, two different objective functions are used. The first alternative is minimization of unit production cost. The second alternative is maximum production.

In this problem, minimization of unit production cost is selected as objective function. Unit production cost ( $UC$ ) consists of three different elements which are tool replacement cost, tool cost and machining cost. The objective function of the problem is as follows:

$$UC = c_0 t_{total} + (c_0 t_c + c_t) \frac{t_k}{T} \quad \text{where } t_k = \left[ \frac{a_p}{f_{plunge}} + \frac{L_c}{f_{cut}} \right] \cdot n \quad (63)$$

where  $c_0$  denotes the labor overhead cost (\$/unit),  $c_t$  denotes tool cost (\$),  $t_{total}$  denotes the total machining time (min),  $t_c$  denotes tool change time (min),  $t_k$  denotes the actual

machining time (min) and  $T$  denotes the tool life (min) with respect to the given parameters.

The constraint set is determined with respect to the performed experiments. The constraint set is as follows:

$$12.5 \text{ m/min} < V < 75 \text{ m/min} \quad (64)$$

$$0.46 \mu\text{m} < f_z < 0.786 \mu\text{m} \quad (65)$$

$$0.08 \text{ mm} < d_r < 0.16 \text{ mm} \quad (66)$$

$$10000 \text{ rpm} < N < 60000 \text{ rpm} \quad (67)$$

$$0 \text{ min} < \text{Tool Life} < 20.5 \text{ min} \quad (68)$$

#### 4.1 Numerical Example for Square Pocket Milling

In this section, two numerical studies are presented for pocket milling with dimensions  $8.8 \times 8.8 \times 0.7$  mm using  $\varnothing 0.4$  mm cutting tool. In the first study, machining costs of cutting conditions achieved by PSO and proposed cutting conditions by tool manufacturer are compared. In the second study, cutting parameters which minimize unit production cost are investigated. In both of the numerical studies, tool return feed rate and plunging feed rate values are fixed. The values are given in Table 4.1.

Table 4.1 Tool return and plunge feed rates

	Tool Return	Plunging
Feed Rate (mm / min)	10	1

### 4.1.1 Comparison of Machining Costs

In the first study, Equation (61) is used to calculate total machining time and unit labor cost is determined as \$60 per hour. The tool life equation is not taken into consideration in the calculation of machining cost for tool manufacturer catalogue values since the value of axial depth of cut proposed by the manufacturer is out of the experiment range. The cutting parameters proposed by tool manufacturer and its total machining cost ( $C_M$ ) are given in Table 4.2.

Table 4.2 Obtained results due to tool manufacturer catalogue values

V(m / min)	$f_z$ ( $\mu\text{m}$ / tooth)	$d_r$ ( $\mu\text{m}$ )	$C_M$ (\$)
50	0.68	20	199.2962

Then, PSO algorithm is used to find the cutting parameters that minimizes total machining cost. The reason of using PSO algorithm instead of exact methods is that it is not possible solve the nonlinear constrained problems using exact methods. In machine cost minimization problem, the objective function is nonlinear since  $f_{f\_cut}$  is calculated with respect to the following equation:

$$f_{r\_cut} = f_z \cdot z \cdot N = (f_z \cdot z \cdot V \cdot 1000) / (\pi \cdot D) \quad (69)$$

where  $f_z$  and  $V$  are the decision variables. Besides, tool life constraint obtained from pocket milling experiments is also nonlinear. In Table 4.3, the results achieved by PSO for different number of passes are given. Due to the results, total machining cost is reduced by the increase of depth of cut in each pass.

When the total machining cost obtained from PSO parameters and tool manufacturer catalogue parameters are compared, it can be clearly stated that large volumes of material can be removed in shorter time with smaller costs by optimizing cutting parameters. Besides, cutting tools are able to work in harder conditions than tool manufacturers' suggestions. For surface finishing processes, it may be beneficial to base the catalogue values of cutting tools. However, experimental analysis and optimization for machining conditions provide large amount of gains for roughing processes.

Table 4.3 Obtained cutting parameters obtained by PSO

#of Pass	V (m/min)	$f_z$ ( $\mu\text{m}$ / tooth)	$d_r$ ( $\mu\text{m}$ )	$C_M$ (\$)
5	65.099	0.67	140	23.54
6	70.713	0.70	116.7	25.16
7	72.478	0.69	100	29.03
8	73.836	0.73	87,5	31.26

#### 4.1.2 Unit Production Cost Minimization

In the second study, previously formulated mathematical model is solved using PSO method. The model is implemented in Matlab. In the algorithm, remaining tool life is tracked during the cutting operation and the cutting tool is changed if the remaining tool life is smaller than the required cutting pass time. The drawback of this strategy is that cutting tool may not be utilized 100 % since the tool is changed earlier than the end of its life. However, the part quality is very important in micro products. Thus, less utilization of the tool is can be acceptable.

Tool change time is set as 5 minutes in the problem by considering the knowledge achieved from experiments. Unit tool cost and labor cost are \$100 and \$60 per hour respectively. Equation (63) is used as the objective function and equations (64) – (68) are used as constraints. The obtained results for this study are presented in Table 4.4.

Table 4.4 Obtained cutting parameters for unit production cost minimization problem

#of Pass	V (m/min)	$f_z$ ( $\mu\text{m} / \text{tooth}$ )	d (mm)	Total # of required cutting tool	UC (\$)	Tool Change Pass #
5	67.930	0.64	0.14	3	338.6514	2
6	74.538	0.67	0.1167	2	234.9884	3
7	70.380	0.70	0.1	2	239.3378	4
8	74.721	0.69	0.0875	2	242.3476	4

It is revealed with respect to the achieved results that large axial depth of cut and slow cutting speed may increase the total number of required cutting tools, so the unit production cost increases. Minimum unit production cost is obtained for six numbers of passes. It can also be stated that tool cost is the biggest cost item in micro machining. Thus, optimization of machining parameters is very important.

## 4.2 Summary

Modeling of pocketing operation is developed and optimization problem is solved for two example cases. In the first case, the cutting parameters determined by tool manufacturer is evaluated and compared with the machining parameters obtained from particle swarm algorithm. It is revealed from the comparison that tool manufacturers

propose very conservative cutting parameters. It is possible to extend the offered limits by conducting experiments. In the second case, unit cost minimization problem is solved using particle swarm optimization method and demonstrated that it may induce significant cost increase if the cutting conditions are not selected carefully.

# Chapter 5

## Conclusion and Future Work

In this thesis, multi pass turning and micro milling processes have been investigated in the framework of process parameter optimization.

In multi-pass turning operation, a well known nonlinear constrained optimization problem is considered. Two different mathematical models are implemented and solved in Matlab software using particle swarm optimization and Matlab Optimization Toolbox. It is shown that particle swarm optimization technique can produce good results in short time also insensitive to the initial guess. Besides, the optimal machining conditions results obtained from the optimization algorithm is similar those reported in the literature.

In multi-pass micro milling operation, first an experimental study is performed to reveal the significant machining parameters during pocket milling for AISI 304 stainless steel. Firstly, slot milling experiments were conducted and acceptable range of machining

parameters for both  $\varnothing$  0.4 and  $\varnothing$  0.8 mm cutting tools were identified. Pocket milling experimental parameters were determined based on the results of slot milling studies. For  $\varnothing$  0.8 mm cutting tools, surface quality and increase in cutting forces due to tool wear were considered as tool life criteria. For each parameter set, tool conditions were observed. The relationship between cutting parameters and resultant cutting force are represented with an equation obtained through surface fit in Matlab. For  $\varnothing$  0.4 mm cutting tools, a central composite design (CCD) was designed including 20 experiments. The results of experiments are analyzed using ANOVA technique and a tool life equation was obtained using regression analysis. Analytical model square pocket milling was derived which allows calculation of machining time for given machining conditions. Then, an objective function was formulated to minimize unit production cost. Finally, the results were discussed with a numerical study. It is shown that developed model can help in the process of machining parameter selection.

As a future work, square pocket milling operation can be generalized to other shapes of pockets (rectangle, circle etc.) and optimization studies can be performed for combined shapes. During experimental studies, it was observed that as cutting tool diameter decreases process outputs become increasingly hard to model due to non linear and stochastic nature of the process. The use of probabilistic techniques is recommended especially when tool diameter is less than 0.5 mm because the obtained results changes drastically due to the physical properties of micro cutting tools. It is left as a future study. Finally, introducing physics based process models (machining forces, tool vibration models) into the machining optimization problems help selecting machining parameters with less experimentation.

# Bibliography

Aramcharoen, A., Mativenga, P. T., Yang, S., Cooke, K. E., & Teer, D. G. (2008). Evaluation and selection of hard coatings for micro milling of hardened tool steel. *International Journal of Machine Tools and Manufacture* , 48 (14), 1578-1584.

Biermann, D., Baschin, A., Krebs, E., & Schlenker, J. (2011). Manufacturing of dies from hardened tool steels by 3-axis micromilling. *Production Engineering Research and Development* , 5, 209-217.

Chae, J., Park, S., & Freiheit, T. (2006). Investigation of micro-cutting operations. *International Journal of Machine Tools and Manufacture* , 46 (3-4), 313-332.

Chen, M. C. (2004). Optimizing machining economics models of turning operations using the scatter search approach. *International Journal of Production Research* , 42 (13), 2611–2625.

Chen, M. C., & Chen, K. Y. (2003). Optimization of multi-pass turning operations with genetic algorithms: a note. *International Journal of Production Research* , 41 (14), 3385-3388.

Chen, M. C., & Tsai, D. M. (1996). A simulated annealing approach for optimization of multi-pass turning operations. *International Journal of Production Research* , 34 (10), 2803-2825.

Costa, A., Celano, G., & Fichera, S. (2011). Optimization of multi-pass turning economies through a hybrid particle swarm optimization technique. *International Journal of Advanced Manufacturing Technology* , 53 (5-8), 412-433.

Ermer, D. S. (1971). Optimization of constrained machining economics problem by geometric programming. *ASME Journal of Engineering for Industry* , 93, 1067-1072.

- Filiz, S., Conley, C. M., Wasserman, M. B., & Ozdoganlar, O. B. (2007). An experimental investigation of micro-machinability of copper 101 using tungsten carbide micro-endmills. *International Journal of Machine Tools and Manufacture* , 1088-1100.
- Frey, D. D., Engelhardt, F., & Greitzer, E. M. (2003). A role for "one-factor-at-a-time" experimentation in parameter design. *Research in Engineering Design* , 14, 65-74.
- Gilbert, W. W. (1950). Economics of Machining. *Machining Theory and Practice* (pp. 465-485). American Society of Metals .
- Groover, M. P. (2012). *Introduction to Manufacturing Processes*. John Wiley and Sons Inc.
- Hunter, J. (2010, June 28). Retrieved from Curious Cat Investing and Economics Blog: <http://investing.curiouscatblog.net/2010/06/28/manufacturing-output-as-a-percent-of-gdp-by-country/>
- Kappmeyer, G., Hubig, C., Hardy, M., Witty, Wittey, M., & Busch, M. (2012). Modern machining of advanced aerospace alloys - Enabler for quality and performance. *CIRP Conference on High Performance Cutting* (pp. 28-43). Zurich: CIRP.
- Karpat, Y., & Özel, T. (2007). Multi-objective optimization for turning processes using neural network modeling and dynamic-neighborhood particle swarm optimization. *International Journal of Advanced Manufacturing Technology* , 234-247.
- Karpat, Y., & Özel, T. (2006). Swarm-intelligent neural network system (SINNS) based multi-objective optimization of hard turning. *Transactions of NAMRI/SME* , 179-186.
- Kennedy, J. (1998). The behavior of particles. *Lecture Notes in Computer Science* , 1447, 579-589.
- Kennedy, J., & Eberhart, R. (1995). Particle Swarm Optimization. *IEEE International Conference on Neural Networks*, (pp. 1942-1948). Washington, DC.
- Lee, K., & Dornfeld, D. A. (2004). A study of Surface Roughness in th Micro-End-Milling Process. *UC Berkeley: Laboratory for Manufacturing and Sustainability* .
- Masuzawa, T. (2000). State of the Art of Micromachining. *Annals of The CIRP*, (pp. 473-488).

- Moavenzadeh, J., Philip, R., Giffi, C. A., & Thakker, A. (2012). *The Future of Manufacturing: Opportunities to drive economic growth* . World Economic Forum .
- Montgomery, D. C. (2004). *Design and Analysis of Experiments* (6 ed.). New York, USA: John Wiley and Sons Inc.
- Mukherjee, I., & Ray, P. K. (2006). A review optimization techniques in metal cutting processes. *Computer and Industrial Engineering* , 50, 15-34.
- Natarajan, U., Periyanan , P., & Yang, S. (2011). Multiple-response optimization for micro-endmilling process using response surface methodology. *International Journal of Advanced Manufacturing Technology* , 56, 177-185.
- Onwubolu, G. C., & Kumalo, T. (2001). Optimization of multi-pass turning operations with genetic algorithms. *International Journal of Production Research* , 39 (16), 3727-3745.
- Phadke, M. S. (1989). *Quality engineering using robust design*. New Jersey: AT&T Bells Laboratory / Prentice Hall.
- Potvin, C., & Roff, D. A. (1993). Distribution-Free and Robust Statistical Methods: Viable Alternatives to Parametric Statistics. *Ecological Society of America* , 74 (6), 1617-1628.
- Rahman, M., Kumar, A., & Prakash, J. (2001). Micro milling of pure copper. *Journal of Materials Processing Technology* , 116 (1), 39-43.
- Ross, P. J. (1989). *Taguchi techniques for quality engineering* . New York: McGraw-Hill.
- Shin, Y. C., & Joo, Y. S. (1992). Optimization of machining conditions with practical constraints. *International Journal of Production Research* , 30 (12), 2907-2919.
- Thepsonthi, T., & Özel, T. (2012). Multi-objective process optimization for micro-end milling of Ti-6Al-4V titanium alloy . *International Journal of Advanced Manufacturing Technology* .
- Uhlmann, E., Piltz, S., & Schauer, K. (2005). Micro milling of sintered tungsten-copper composite materials. *Journal of Materials Processing Technology* , 167 (2-3), 402-407.

- Unal, R., & Dean, E. B. (1991). Taguchi Approach to Design Optimization for Quality and Cost: An Overview. *Annual Conference of the International Society of Parametric Analysis* , (pp. 1-9).
- Vazquez, E., Rodriguez, C. A., Elias-Zuniga, A., & Ciurana, J. (2010). An experimental analysis of process parameters to manufacture metallic micro-channels by micro-milling. *International Journal of Advanced Manufacturing Technology* , 51, 945-955.
- Vijayakumar, K., Prabhakaran, G., & Asokan, P. (2003). Optimization of multi-pass turning operations using ant colony. *International Journal of Machine Tools & Manufacture* , 43, 1633–1639.
- Wang, W., Kweon, S., & Yang, S. H. (2005). A study on roughness of the micro-end-milled surface produced by a miniaturized machine tool. *Journal of Materials Processing Technology* , 162-163, 702-708.
- Wang, Y. C. (2007). A note on 'optimization of multi-pass turning operations'. *International Journal of Machine Tools & Manufacture* , 47, 2057–2059.
- Weinert , K., & Petzoldt, V. (2008). Machining NiTi micro-parts by micro-milling. *Materials Science and Engineering A* , 672-675.
- Yıldız, A. R. (2009). An effective hybrid immune-hill climbing optimization approach for solving design and manufacturing optimization problems in industry. *Journal of Materials Processing Technology* , 2773–2780.

# Appendix

Matlab Optimization Toolbox uses various optimization algorithms according to the problems' objective functions and constraints. The problem in this thesis is a minimization problem which has a nonlinear objective function with both linear and nonlinear constraints. Available algorithms to be used in Matlab for this study are trust region reflective, active set and interior point algorithms.

## **Trust Region Reflective Algorithm**

The trust-region reflective algorithm is used to solve large scale bound constrained problems or linear equalities. In the default configuration of Matlab, optimization toolbox uses trust region reflective algorithm. This algorithm is efficient in use but requires special conditions. Trust region reflective algorithm can be applicable if the gradient of the objective function is provided and constraints are in a single type, whether only bound constraint type or linear equality constraint type but not both of them.

The method in this algorithm is to build a simpler function  $q$  which approximates the objective function  $f$  in a trust region radius  $\Delta$  around an initial point  $x$ . Initial point  $x$  and trust region radius  $\Delta > 0$  are selected randomly. Then, a trial step  $s$  is calculated and  $f$  value is updated. Trial step is  $s$  used to determine search direction. If the new objective function value  $f(x + s)$  is smaller than the current objective function's value  $f(x)$ , the current point  $x$  is updated as  $x + s$  and  $\Delta$  value is updated according to the reduction ratio. The ratio is calculated as following:

$$r_k = \frac{\text{Actual reduction}}{\text{Predicted reduction}}$$

where

$$\begin{aligned} \text{Actual reduction} &= f(x_k) - f(x_k + s_k) \\ \text{Predicted reduction} &= -(g_k^T s_k + s_k^T H_k s_k) \end{aligned}$$

As the predicted reduction value becomes closer to the actual reduction value (e.g.,  $r_k > 0.75$ ), the steps will lead to better objective function values. Thus,  $\Delta$  value is increased. As the reduction value becomes smaller (e.g.,  $r_k < 0.25$ ),  $\Delta$  is decreased to find a point with a better smaller objective value. If neither of these conditions are occurred,  $\Delta$  is not changed and continued with the new point  $x + s$ .

However, if the new objective function value  $f(x + s)$  is smaller than the current objective function value  $f(x)$ , the current point is not changed,  $\Delta$  value is reduced and a new  $s$  is calculated by using reduced trust region radius. In order to calculate  $s$ , the following constrained minimization problem is solved:

$$\begin{aligned} \min f &\approx g_k^T s + \frac{1}{2} s^T H_k s \\ &\text{subject to } \|s\| \leq \Delta \end{aligned}$$

where  $\Delta$  is the trust region radius,  $H$  is the Hessian matrix and  $g$  is the gradient of  $f$  current point  $x$ . As seen in the mathematical formulation,  $s$  is restricted by  $\Delta$  in order to be stayed in the trust region in a given direction.

The inequality constraint  $\|s\| \leq \Delta$  reveals two possible step size value calculation methods

If  $\|s\| < \Delta$ , then the step size is calculated as  $s_k = H_k g_k$  if  $\|H_k g_k\| < \Delta$  where  $k$  is the iteration number

If  $\|s\| = \Delta$ , then the step size is calculated as  $s_k = -(H_k + \mu I) g_k$ ,  $\mu > 0$ , and  $\|s\| = \Delta$  where  $\mu$  is a quantity related with the trust region constraint.

Until the termination criteria are satisfied, these procedures are applied iteratively.

Trust Region Algorithm (Papalambros and Wilde, 2000)

1. Begin with random point  $x_1$  and a trust region radius  $\Delta_1 > 0$ . Iteration counter  $k$  is set as 1.
2. Calculate the gradient  $g_k$  and Hessian  $H_k$  at  $x_k$ .
3. Calculate the step  $s_k$  by solving constrained minimization problem.
4. Calculate the value of  $f(x_k + s_k)$  along with the predicted reduction, actual reduction and ratio  $r_k$ .
5. (Unacceptable Step) If  $(x_k + s_k) \geq f(x_k)$ , then do not accept the new point. Set  $\Delta_{k+1} = \Delta_k/2$ ,  $x_{k+1} = x_k$ ,  $k = k + 1$  and go to step 3.
6. (Altering the Trust Region) Set  $x_{k+1} = x_k + s_k$ . If  $r_k < 0.25$ , then set  $\Delta_{k+1} = \Delta_k/2$ ; if  $r_k > 0.75$ , then set  $\Delta_{k+1} = 2 \Delta_k$ ; otherwise set  $\Delta_{k+1} = \Delta_k$ . Set  $k = k + 1$  and go to step 2.

### Active Set Algorithm

The active set algorithm is used to solve general nonlinear optimization problems. The method used in active set algorithm is to achieve optimal point  $x_*$  from a starting point  $x_k$  by activating or deactivating constraints in the course of iterations in the problem. The constraint is called active if the optimum solution changes when it removed from the constraint set.

All equality constraints and active inequality constraints are included in the active set. The working set includes the equality and active inequality constraints at the current iteration and the candidate set contains candidate constraints that can be added to the working set during iterations. The algorithm starts with an initial feasible point  $x_k$ , which is not necessarily to be optimal. Initially, starting feasible point  $x_k$  and a working set is generated. Then, Karush-Kuhn-Tucker (KKT) conditions are checked for the current point. If  $x_k$  is not optimal, there are two alternative steps. First alternative is to continue with the same working set and follow subsequent steps. Second alternative is to change the working set by deleting a constraint, update all computations according to the newly generated working set and check KKT conditions. Afterwards, a feasible search vector  $s_k$  can be calculated as

$$s_k = -g_k \text{ or } s_k = -H_k^{-1}g_k.$$

Then, the step length  $\alpha_k$  along  $s_k$  is computed as following:

$$\alpha_k = \text{arg} \min_{0 < \alpha < \infty} f(x_k + \alpha s_k)$$

If the step length violates any constraint, the violated constraint is added to the working set, step length value is reduced to the maximum possible value that provides feasibility. If  $\alpha_k$  does not violate the constraints, new point  $x_{k+1}$  is calculated as  $x_{k+1} = x_k + \alpha_k s_k$ . Adding constraint continues until no further progress is possible without violating constraint. In order to explain adding constraint procedure clearly, the following figure is given:

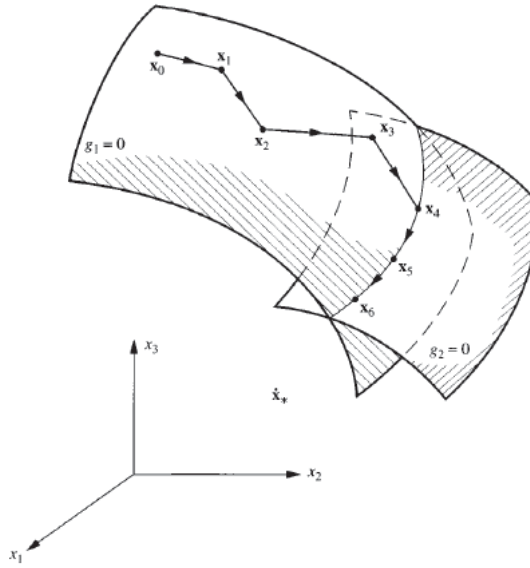


Figure. Active set algorithm

Initial point  $x_0$  and constraint  $g_1$  are generated. Then, objective function value is improved according to the constraint  $g_1$  until no further progress is possible without violating a constraint in the model. Then, a new constraint  $g_2$  is added from the candidate set to the working set and the algorithm continues searching better feasible points at the intersection of constraints  $g_1$  and  $g_2$ .

If no further constraint left in the candidate set to be added, KKT conditions are re-checked at the last founded feasible point  $x_F$  according to the following equation:

$$\nabla f(x_F) + \sum_i \mu_i \nabla g_i(x_F) = 0^T, \quad i \in \mathcal{A}$$

where  $g$  is the constraint,  $\mu$  is the coefficient of constraint and  $\mathcal{A}$  is the index working set of active constraints at  $x_F$ . If  $x_F$  is a KKT point and  $\mu$  is nonnegative, the point is

optimal. However, if  $\mu$  is a negative value, then the algorithm continues with deleting constraints from the working set since negative coefficient means that it is possible to find a better objective value. Only one constraint can be deleted at each iteration. Constraint with the most negative coefficient is deleted first and KKT conditions are checked until no negative  $\mu$  value left.

In the course of KKT equations' calculation, Lagrange multipliers are solved. In order to solve the Lagrange multipliers, Sequential Quadratic Programming (SQP) method is used. SQP method solves nonlinear problems at three basic steps. In the first step, Hessian Matrix of Lagrangian function is updated by using Quasi-Newton method. Then, the problem is divided into sub-problems, named Quadratic Programming (QP). At the final step, Line Search (LS) is done to form a new iteration. (Papalambros and Wilde, 2000)

### **Interior Point Algorithm**

Interior Point Algorithm is used to solve general nonlinear optimization problems. The algorithm is based on barrier function. It is also possible to provide feasibility according to the bounds at all iterations as an option. The method of the algorithm is to construct approximate minimization sub-problems and solve iteratively. Since approximate problem has equality constraints, solving the problem is easier than solving an inequality constrained problem.

The mathematical formulation of approximate problem is that, for each  $\mu > 0$

$$\min_{x,s} f_{\mu}(x, s) = \min_{x,s} f(x) - \mu \sum_i \ln(s_i)$$

*Subject to,  $h(x) = 0$  and  $g(x) + s = 0$*

where  $s$  is the slack variables,  $g$  is the inequality constraints and  $\mu \sum_i \ln(s_i)$  is the barrier function. In order to keep  $\ln(s_i)$  bounded, the slack variables are restricted to be positive. By the decrease of  $\mu$  value to zero, objective function  $f_\mu$  approaches original objective function  $f$ . At each iteration, the algorithm uses two types of steps. First type is direct step (Newton step), which solves KKT equations via linear approximation and used by default. Second type is conjugate gradient step, which uses trust region algorithm. Unless the algorithm cannot solve by direct step, tries conjugate gradient step. (Papalambros and Wilde, 2000)